NEW ASPECTS OF POLYPHASE INDUCTION MOTOR DESIGN

By

RUSSELL LLOYD RIESE

Bachelor of Science in Electrical Engineering
University of Washington
Seattle, Washington
1946

Master of Science
Oklahoma Agricultural and Mechanical College
Stillwater, Oklahoma
1950

Submitted to the faculty of the Graduate School of
the Oklahoma Agricultural and Mechanical College
in partial fulfillment of the requirements
for the degree of
DOCTOR OF PHILOSOPHY
August, 1955

NEW ASPECTS OF POLYPHASE

INDUCTION MOTOR DESIGN

Thesis Approved:

Chas. F. Cameron
Thesis Adviser

W. S. Thuesen

A. Nasten

N. L. Jones

L. Wayne Johnson

Robert Nordin
Dean of the Graduate School

PREFACE

Every branch of science has made remarkable advances during the last several decades. However, in my opinion, the advancement of electrical machine design methods has not kept pace. The present schemes for design of electrical machinery are based upon intelligent comparison of empirical data. The advances made in electrical machine design methods are mostly refinements in the empirical relations. Unfortunately, most of the people whose experience and knowledge would entitle them to speak with authority on this subject are deterred from publishing by commercial reasons. While it is true that a comparatively small group of engineers may be concerned with such design work, the philosophy and technique of approach could be of interest to an entire profession which is so profoundly influenced by the designer's work.

For several years, I have been greatly interested in the art and science of polyphase induction motor design. This interest was intensified when my adviser, Professor C. F. Cameron, suggested the separation of the components of the D^2L equation of polyphase induction motor design as a possible topic for a thesis. This thesis is a result of an investigation of the separation of the components and a study of the influence of the air gap on the operating power factor.

I wish to express my appreciation for the friendly advice, encouragement, and discerning criticism of Professor Cameron

in all of my activities leading up to and the preparation of this thesis. In addition, I am indebted to him for the use of many technical papers and notes he has collected on design procedures and the subject of leakage reactance.

To mention all of the people that have helped me in my program at Oklahoma A. and M. College would be an endless task. I, therefore, wish only to mention a few. I would like to take this opportunity to thank you, the American taxpayer, for the financial assistance given me through the G. I. Bill of Rights. Also, I wish to thank the administration of New Mexico College of A. and M. A. for granting me a sabbatical leave during the 1954-55 academic year.

In addition, I wish to express my appreciation to Professor A. Naeter, Dr. H. L. Jones, Dr. L. Wayne Johnson, and Professor H. G. Thuesen for their comments and assistance; to Miss M. M. Graves and her library staff for their assistance; to Mr. A. P. Juhlin for obtaining articles not in the Oklahoma A. and M. College Library; and to Mrs. Sara Preston for her excellent job of typing this thesis in its final form. I also wish to express my sincere appreciation to Professor David L. Johnson for his detailed reading of this material and suggestions on style and arrangement. Last but not least, I wish to thank my wife, Helen, for arranging my household duties so that they would not interfere with my work and for her assistance in preparing the manuscript. Her assistance has been invaluable.

TABLE OF CONTENTS

LIST OF TABLES

LIST OF ILLUSTRATIONS

CHAPTER I

THE D^2L EQUATION

Nearly all of the present-day design procedures for the design of polyphase induction motors require, as one of the first steps, the determination of D^2L, where D is the outside diameter of the armature in inches and L is the gross axial length of the armature core in inches.

DERIVATION OF THE D^2L EQUATION

The output of a polyphase induction motor, expressed in horsepower, is

$$hp = V_1 I_1 \frac{n \eta}{746} \cos \theta \qquad (1)$$

where

hp = output in horsepower

V_1 = motor phase voltage in volts

I_1 = motor phase current in amperes

$\cos \theta$ = power factor

n = number of phases

η = efficiency

In order to make this formula useful in determining the leading dimensions of a machine, certain substitutions must be made.

A sine-wave flux distribution is generally assumed for an induction motor, because the distributed stator winding produces an air-gap flux wave which is very nearly sinusoidal.

On this assumption, the phase voltage, V_1, in the expression for the horsepower output can be expressed as

$$V_1 = 2.22\ k_w\ f\ \phi\ Z\ 10^{-8} \text{ volts} \qquad (2)$$

where

k_w = the winding factor

f = the frequency in cycles per second

ϕ = the total flux per pole in lines

Z = the total number of inductors in series per phase

For an induction motor,

$$f = \frac{p\ N_s}{120} \qquad (3)$$

in which

p = the number of poles

N_s = the synchronous speed in rpm

Also

$$\phi = B''_g\ \frac{\pi D\ L}{p} \qquad (4)$$

where

B''_g = the average value of the flux density over a pole pitch

Substituting Equations (3) and (4) into Equation (2), one obtains

$$V_1 = 2.22\ \left(\frac{p\ N_s}{120}\right)\ \left(B''_g\ \frac{D\ L}{p}\ k_w\ Z\ 10^{-8}\right)$$

$$= 5.81\ N_s\ B''_g\ D\ L\ k_w\ Z\ 10^{-10} \qquad (5)$$

A quantity q is generally used in dynamo design. It is defined as the ampere-conductors per inch of air-gap periphery. Thus

$$q = \frac{n\ Z\ I_1}{\pi D} \tag{6}$$

Solving for I_1,

$$I_1 = \frac{q\ \pi\ D}{n\ Z} \tag{7}$$

The substitution of Equations (5) and (7) into the expression for the horsepower output yields

$$hp = (5.81\ N_s\ B''_g\ D\ L\ k_w\ Z\ 10^{-10})\ (\frac{q\pi D}{n\ Z})\ \ \frac{n\ \eta}{746}\ \cos\ \theta$$

Hence

$$D^2L = \frac{4.07\ hp\ 10^{11}}{B''_g\ q\ N_s\ k_w\ \eta\ \cos\ \theta} \tag{8}$$

This expression is commonly known as the D^2L equation and as the output equation. It is the basic equation of polyphase induction motor design.

USE OF THE D^2L EQUATION

The output equation is actually a <u>measure</u> of the physical volume of the machine. By methods which will be discussed later, it can be separated into its two components D and L.

In order to use this equation in the beginning design of a polyphase induction motor, the various factors on the right-hand side of the equation must first be approximated before D^2L can be evaluated. These factors will be considered one at a time to show how they are generally determined.

Horsepower. The term hp, the horsepower output of the motor, will, of course, be the desired horsepower output of the machine at full load.

Synchronous Speed. The synchronous speed, N_s, will be slightly higher numerically than the full-load speed of the motor. The actual value is determined by the frequency of the supply voltage and the number of poles. [See Equation (3)].

Winding Factor. The winding factor, k_w, is known only after a suitable number of slots and the type of winding have been chosen. In America, double-layer windings are used for all but the very small sizes. All remarks will refer to the double-layer winding. By definition, the winding factor is equal to the product of the distribution factor, k_d, and the pitch factor, k_p.

The value of the distribution factor at fundamental frequency for any arrangement of slots and windings can be determined from

$$k_d = \frac{\sin (n_s \alpha/2)}{n_s \sin (\alpha/2)} \qquad (9)$$

in which

n_s = the number of slots per pole per phase

α = the number of electrical degrees between adjacent slots

With full-pitch, three-phase windings the distribution factor will have one of the values shown in Table I.

TABLE I[1]

DISTRIBUTION FACTORS

FOR THREE-PHASE WINDINGS

Slots per pole	n_s	α^o	k_d
3	1	60	1.000
6	2	30	0.966
9	3	20	0.960
12	4	15	0.958
15	5	12	0.956
18	6	10	0.955

If the coil span, in electrical degrees, is symbolized by β, then the pitch factor at the fundamental frequency can be found from

$$k_p = \sin \frac{\beta}{2} \qquad (10)$$

Table II lists pitch factors for three-phase stator windings having 3 to 15 slots per pole and coil spans of 180 to 120 electrical degrees.

Power Factor. The curves of Figure 1 can be used to estimate the probable full-load power factor of a three-phase induction motor. The usual full-load power factors lie between the limits indicated by the dotted lines. In general, the higher power factors apply to high-speed motors

[1]Alfred Still and Charles S. Siskind, Elements of Electrical Machine Design (New York, 1954), p. 172.

TABLE II[2]

PITCH FACTORS FOR

THREE-PHASE WINDINGS

Slots per pole	Coil span, β										
	180°	168°	165°	160°	156°	150°	144°	140°	135°	132°	120°
3	1.0										0.866
6	1.0					0.966					0.866
9	1.0			0.985				0.940			0.866
12	1.0		0.991			0.966			0.924		0.866
15	1.0	0.995			0.978		0.951			0.914	0.866

[2]Ibid., p. 173.

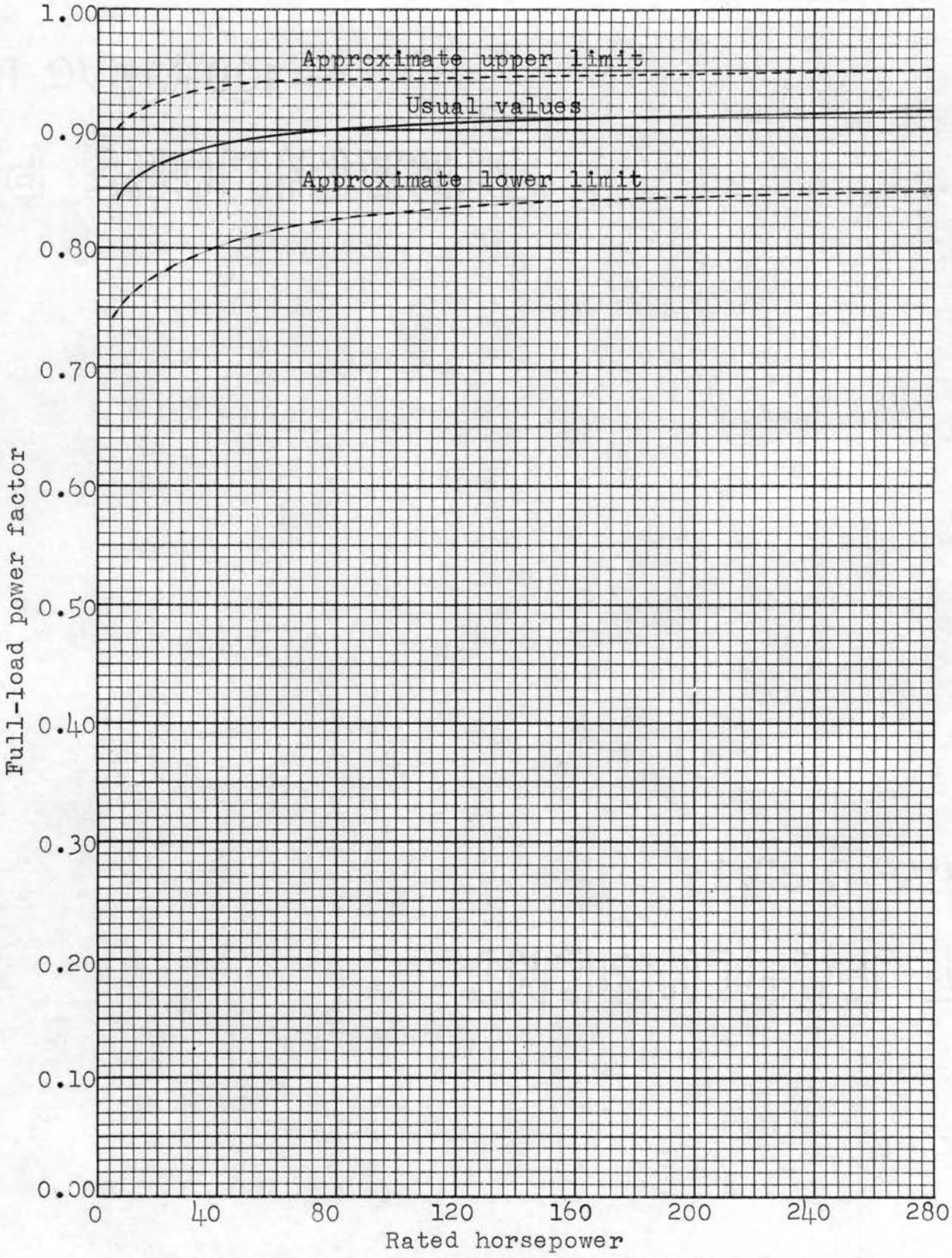

Figure 1. Full-load power factors of three-phase induction motors.

while the lower power factors apply to slow-speed machines.

Efficiency. Figure 2 may be used to estimate the usual full-load efficiencies of three-phase induction motors. The higher efficiencies, indicated by the upper dotted curve, are characteristic of high-speed machines, while the lower efficiencies are generally obtained with slow-speed machines.

Both Still and Siskind[3] and Kuhlmann[4] give tables of typical performance data for three-phase, 60-cycle, general-purpose squirrel-cage and wound-rotor induction motors for voltages up to 600 volts. Rated horsepowers from 1/2 to 200 are tabulated for various full-load speeds. The values given are typical of the efficiency and power factor to expect at full load and provide the necessary data for plotting the curves of Figures 1 and 2.

Flux Density. The value of B''_g, the apparent average gap flux density over a pole pitch, is defined as

$$B''_g = \frac{\phi}{\tau L} \tag{11}$$

where

τ = the pole pitch in inches

As stated previously, a sine-wave distribution of flux is generally assumed. On this assumption, the apparent maximum value of the air-gap flux density is

$$B_g = (\pi/2)B''_g \tag{12}$$

---

[3] Ibid., pp. 268-271.

[4] John H. Kuhlmann, Design of Electrical Apparatus (New York, 1950), pp. 299-302.

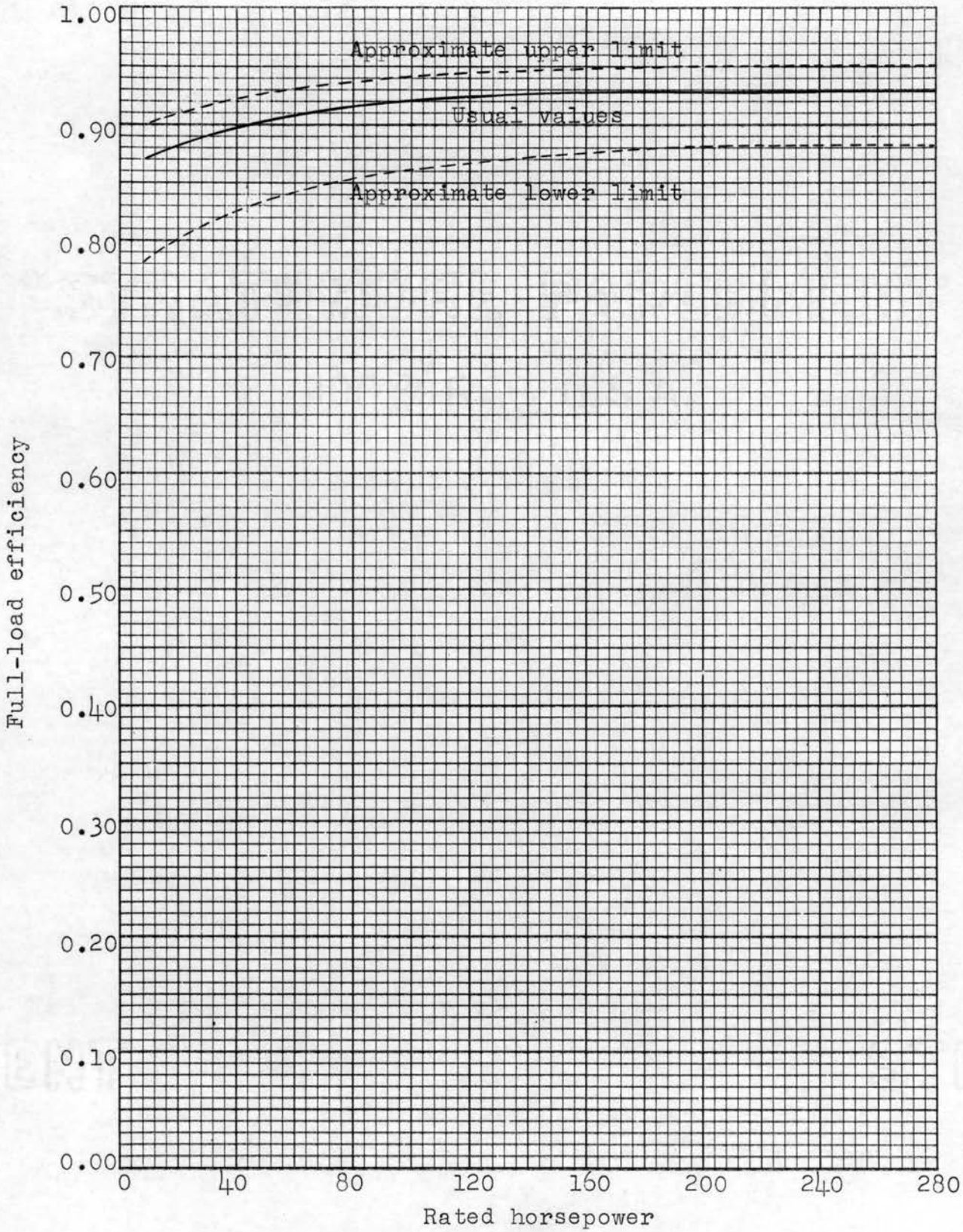

Figure 2. Full-load efficiencies of three-phase induction motors.

and the maximum tooth density over a tooth pitch is

$$B_t = (\pi/2)\, B''_g \frac{\lambda L}{t L_n} \qquad (13)$$

wherein

λ = the tooth pitch

t = the equivalent tooth width

L_n = the net length of iron in the armature core

all measured in inches. The ratio L/L_n is sometimes referred to as the iron insulation factor. The value of B''_g is limited by the permissible value of B_t; B_t should not be so high that magnetic saturation takes place in the teeth. High tooth densities result in high core losses and a large magnetizing current. Since the magnetizing current lags the supply voltage by 90°, it must be kept small if one is to obtain reasonable operating characteristics. Usual values for B''_g lie between the limits of 25,000 and 45,000 lines per square inch. The higher values are for large-capacity, high-speed motors. For general-purpose motors, densities from 30,000 to 40,000 lines per square inch are very common.

Ampere-Conductors. The value of the ampere-conductors per inch of air-gap periphery, q, is a function of the number of phases, the number of conductors per phase, the air-gap diameter, the leakage reactance, and the type of ventilation. Average values of q are given in Figure 3 for general-purpose, 40°C, three-phase induction motors having rated

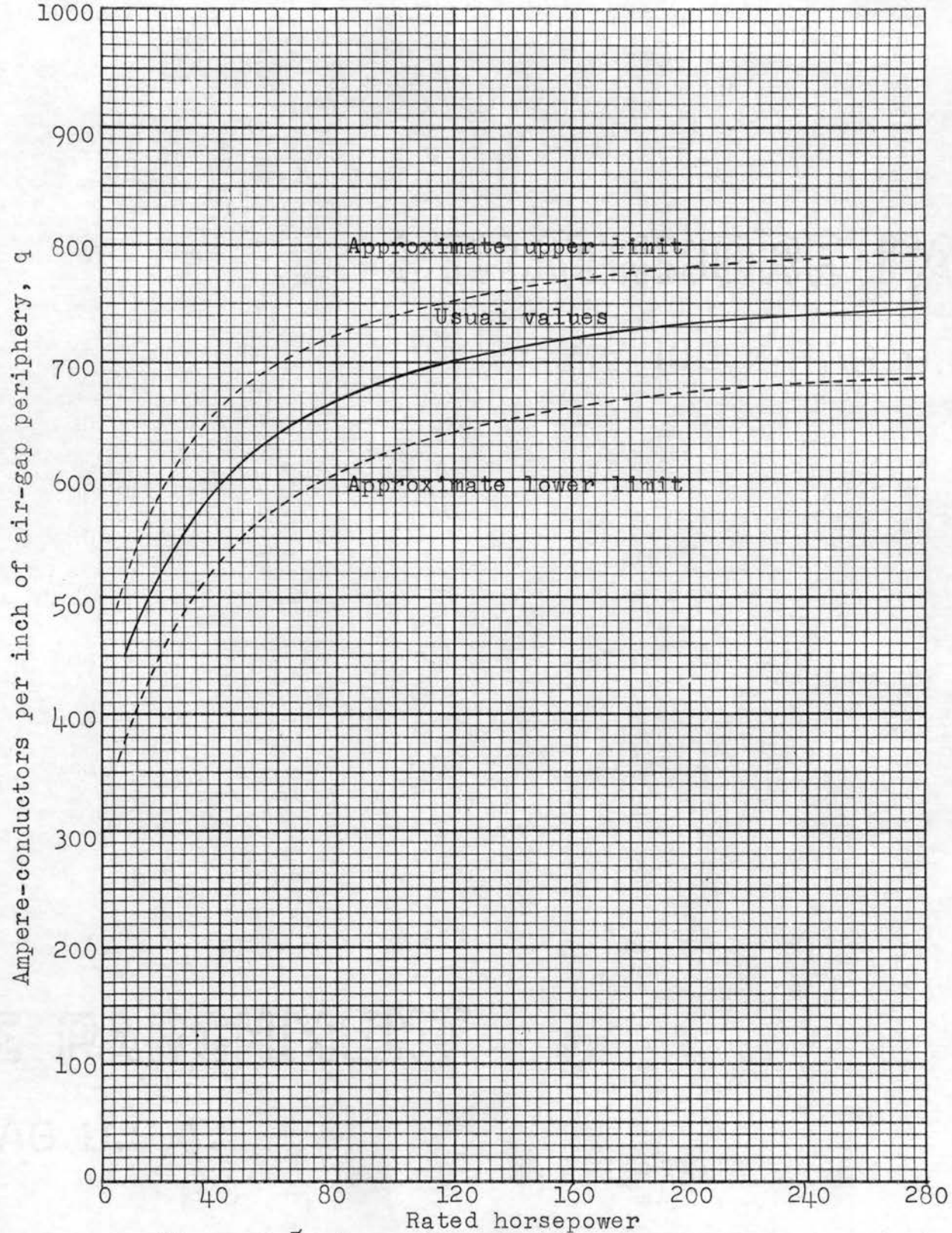

Figure 3.5 Approximate values for the ampere-conductors per inch of air-gap periphery of induction motors.

[5]Still and Siskind, p. 272.

voltages up to 2500 volts. The solid curve asymptotically approaches a value of 850 for motors of 1000 horsepower and larger.

ILLUSTRATIVE EXAMPLE

To illustrate the application of the D^2L equation and the accompanying curves and tables, suppose one wishes to determine, as an initial design step, the value of D^2L, for a 50-hp, 440-volt, 60-cycle, 900-srpm, general-purpose three-phase induction motor.

From the specifications, the rated horsepower is 50, and the synchronous speed is 900 rpm.

Something must be known about the winding before the winding factor can be determined. The winding factor is the product of the distribution factor and the pitch factor. For a machine with the ratings given, a winding having four slots per pole per phase is about right. Assuming a standard double-layer frictional-pitch winding and arbitrarily choosing a coil pitch one slot short of full pitch, that is, a coil span of 165 electrical degrees, one finds from Tables I and II that k_d = 0.958 and k_p = 0.991, or k_w = 0.95.

Using Figures 1, 2, and 3, one finds the usual values of power factor, efficiency, and ampere-conductors per inch for this size motor to be 0.84, 88%, and 600, respectively.

A typical value of flux density, B''_g, for this size of motor is 30,000 lines per square inch.

Applying Equation (8), the value of D^2L is

$$D^2L = \frac{4.07\ hp\ 10^{11}}{B_g''\ q\ N_s\ K_w\ \eta\ \cos\theta}$$

$$= \frac{(4.07)\ (50)\ 10^{11}}{(30{,}000)(600)(900)(0.950)(0.88)(0.84)}$$

$$= 1790\ in.^3$$

CHAPTER II

COMMON METHODS OF SEPARATING THE COMPONENTS OF THE D^2L EQUATION

Once the value of D^2L has been determined, a person is then faced with one of the most difficult problems of polyphase induction motor design, namely, the separation of D^2L into its two components, D and L.

Three of the most widely used books on the subject of electrical machine design are those written by Gray,[1] Still and Siskind,[2] and Kuhlmann.[3] The methods these authors propose for determining the components of the D^2L equation will be referred to as Gray's Method, Still's Method, and Kuhlmann's Method, respectively.

GRAY'S METHOD

Gray states:[4]

> There is no simple method whereby D^2L can be separated into its two components in such a way as to give the best machine. The only satisfactory method is to assume different sets of values, work out the design roughly for each case, and pick out that which will give good operation at a reasonable cost.

This book contains several examples pointing out the application of this method. In one example,[5] a preliminary

---

[1] Alexander Gray, Electrical Machine Design (New York, 1926).

[2] Alfred Still and Charles S. Siskind, Elements of Electrical Machine Design (New York, 1954).

[3] John H. Kuhlmann, Design of Electrical Apparatus (New York, 1950).

[4] Gray, p. 393.

[5] Ibid., p. 396.

design sheet is worked out for a three-phase, 75-hp, 900-srpm, squirrel-cage induction motor having a value of D^2L of 2180 cubic inches. The tabulated figures indicate that a value of length approximately equal to the pole pitch was used as a center point in separating the components. That is,

$$L \cong \tau = \frac{\pi D}{p} \tag{14}$$

Substitution of this value of L into the D^2L equation results in an expression involving D only. Gray's Method is to determine D and L under this condition and then roughly design several machines on each side of this value, i.e., by choosing several values of L greater than τ and several values of L less than τ. For each of these sets of values, he roughly determines the operating characteristics and the possible costs. In this particular example, air-gap diameters of 15, 17, 19, 21, and 23 inches are used with corresponding lengths of 9.5, 7.5, 6.0, 5.0, and 4.0 inches. Calculations show the 15-inch machine has the largest magnetizing current and, therefore, the lowest power factor, while the 23-inch machine has the smallest circle diagram diameter (see Chapter III) and, therefore, the smallest overload capacity. Since shop conditions are not known, the costs of the machines cannot be intelligently compared although they will not vary appreciably over the range given. Gray concludes that as far as operation is concerned the 19-inch diameter will probably give the best all-around machine.

Numerous other examples appear using the same line of approach, namely, working out the performance of a group of

machines and the final selection of one of these on the basis of characteristics and cost.

STILL'S METHOD

In agreement with Gray, Still states:[6]

> It is not possible to lay down hard-and-fast rules regarding the relation of the diameter of the rotor (or stator) to the length measured parallel to the shaft. The number of poles is an important consideration and, for a definite relation between pole pitch and axial length, we would have $L \propto D/p$, the condition for a square polar area being $L = \tau = \pi D/p$; but large variations are permissible. It is obvious that, if we can decide upon a suitable value for either τ or L, the other dimension is obtained from the output equation.

Still's Method of separating the components is dependent on the fact that the pole pitch, τ, depends upon the horsepower per pole. If machines are considered on the basis of the same horsepower output per pole, it is evident that the area of the air gap, (τ times L), would have to be larger for a low-frequency machine than for a high-frequency machine, because of the slower rate at which the conductors cut the flux. The peripheral velocity of the outer edge of the rotor must be kept within reasonable limits and must also be considered; however, the diameter is rarely determined on this basis.

Typical values of τ and peripheral velocity, v', in feet per minute, found in commercial machines are given in Table III. This table is to be used only as a guide in deciding on dimensions. In the sample designs worked out in the

---

[6] Still and Siskind, p. 274.

book, either L or D is rounded off to a whole number somewhere near the values obtained by using Table III.

TABLE III[7]

APPROXIMATE USUAL VALUES OF POLE PITCH AND PERIPHERAL VELOCITY

Hp per pole	f = 60 cps		f = 25 cps	
	τ, in.	v', ft/min	τ, in.	v', ft/min
1	4	2,400	5	1,250
2	5	3,000	6 1/4	1,560
4 1/2	6	3,600	7 1/2	1,875
8	7	4,200	8 3/4	2,190
15	8	4,800	10	2,500
25	9	5,400	11 1/4	2,810
40	10	6,000	12 1/2	3,130
60	11	6,600	13 3/4	3,440
85	12	7,200	15	3,750
120	13	7,800	16	4,000

KUHLMANN'S METHOD

The D^2L equation can be rearranged, giving

$$\frac{D^2 L N_s}{hp} = \frac{4.07\ 10^{11}}{B_g'' q k_w \eta \cos \theta} \qquad (15)$$

Expressed in this form, it is easily seen from observing the right-hand side of the equation that a series of constants

[7] Ibid., p. 275.

can be derived for various ratings and speeds which can be used to calculate D^2L. Kuhlmann prefers to rewrite the output equation in terms of the outside diameter of the stator rather than the gap diameter and the total stator length instead of the length of the air-gap section. The output equation is written as

$$\frac{D_o^{\,2}\, L_s\, N_s}{hp} = C \qquad (16)$$

where

D_o = outside diameter of the stator in inches

L_s = total stator length in inches

C = the output constant

This particular form of the output equation serves as an aid in selecting the standard frame size for a given motor rating.

Typical sets of curves from which the output constant, C, can be determined are shown in Figures 4 and 5.

The use of these curves results in the determination of $D_o^{\,2} L_s$. The gap diameter, D, is found from D_o with the aid of Table IV, which gives the ratio, r, of the stator outside diameter to the gap diameter for various numbers of poles.

Kuhlmann states:[8]

> For motors with large pole pitch the diameter and length are selected to give minimum cost, and for motors with small pole pitch the diameter and length are proportioned to give good power factor at reasonable cost.

---

[8]Kuhlmann, p. 304.

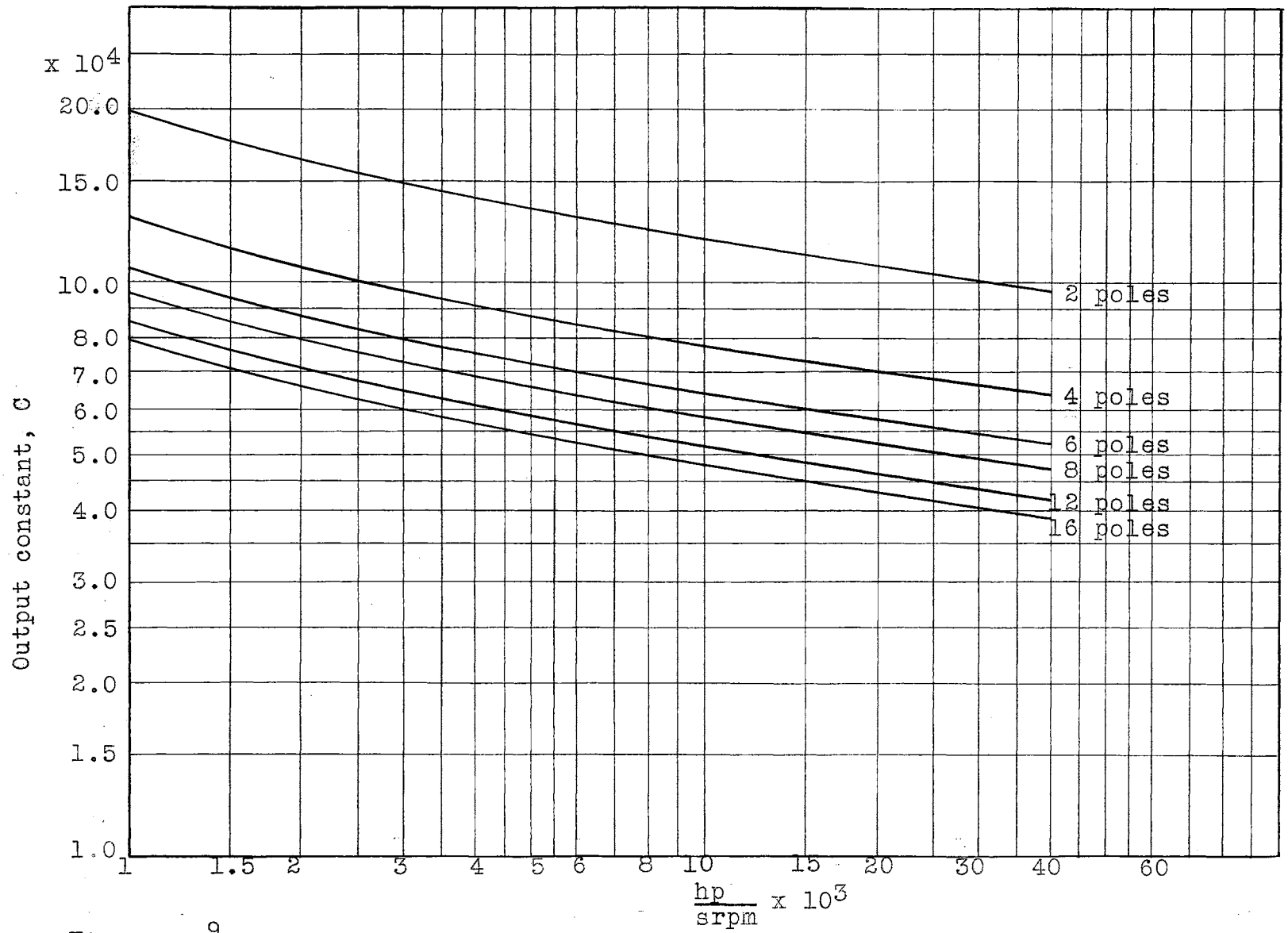

Figure 4.[9] Output constants for 60-cycle polyphase induction motors up to 600 volts with partly closed stator slots.

[9] Ibid., p. 303.

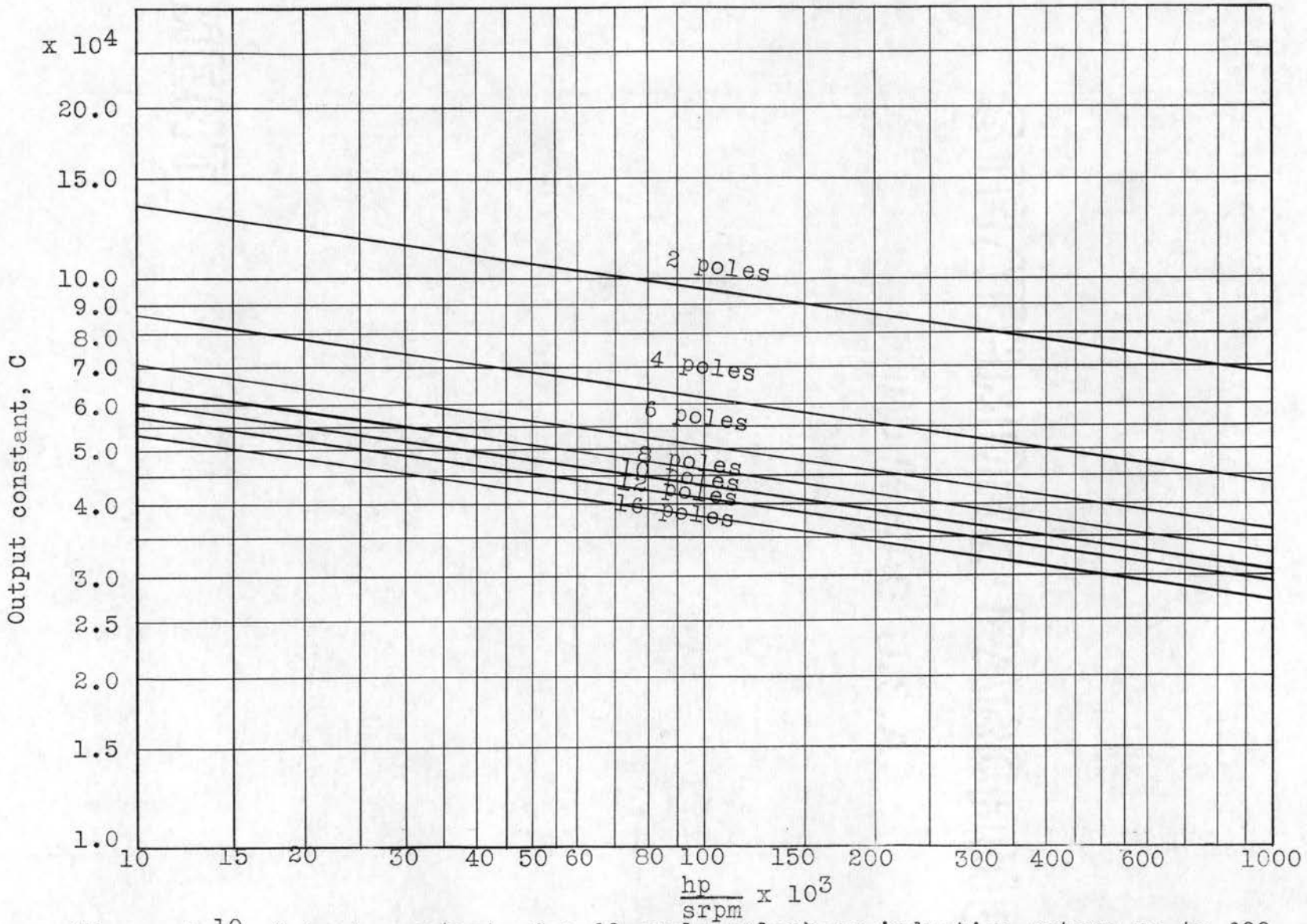

Figure 5.[10] Output constants for 60-cycle polyphase induction motors up to 600 volts with open stator slots.

[10] Ibid., p. 303.

TABLE IV[11]

RATIO OF STATOR OUTSIDE DIAMETER TO GAP DIAMETER

Poles	$r = D_o/D$	Poles	$r = D_o/D$
2	1.85 to 1.95	10	1.23 to 1.27
4	1.45 to 1.55	12	1.22
6	1.35 to 1.43	14	1.20
8	1.28 to 1.33	16	1.18

According to Kuhlmann's Method, the ratio of stator core length to pole pitch, L_s/τ, should be in the range from 0.60 to 2.0. Since the pole pitch is equal to $\pi D/p$,

$$L_s = (\pi D/p)(0.60 \text{ to } 2.0) \tag{17}$$

The output constants in Figures 4 and 5 are for Equation (16), which is in terms of the stator outside diameter, D_o. Using the values of r from Table IV, the stator core length in terms of the stator outside diameter is

$$L_s = (\pi D_o/r\ p)(0.60 \text{ to } 2.0) \tag{18}$$

Substituting Equation (18) into the modified output equation, Equation (16), one obtains

$$D_o = \sqrt[3]{\frac{p\ C\ hp\ r}{\pi(0.60 \text{ to } 2.0)\ N_s}} \tag{19}$$

Once D_o has been determined, L_s can be found from

$$L_s = \frac{C\ hp}{D_o^2\ N_s} \tag{20}$$

Kuhlmann's Method then consists of using Equation (19) to determine D_o. This value of D_o is then substituted into

---

[11] Ibid., p. 304.

Equation (20) to obtain the length, L_s. Thus, the D^2L equation is easily separated into its components. The greatest difficulty is the selection of a suitable value for the ratio of stator core length to pole pitch within the range from 0.60 to 2.0.

GENERALIZED STATEMENT OF PROBLEM

With this brief background, a generalized statement can now be made of the purpose of this thesis.

From the relations presented, the first point to be kept in mind is that the product of the square of the outside diameter of the rotor and the gross axial length is a constant for certain factors on the right-hand side of Equation (8). This is based on the supposition that the flux density, the ampere-conductors, the winding constant, the efficiency, and the power factor are independent of the diameter of the rotor. Usual values for these quantities are assumed in a rather arbitrary manner, leaving one "totally in the dark" as to how these quantities are obtained or how they are related to the performance of the machine. An experienced designer can decide on suitable values. These decisions are based on judgment and past experience; however, it <u>does not follow</u> that his values are the best for best performance.

It is obvious that in designing a polyphase induction motor it may be built with a large diameter and short length or a small diameter and great length, and the output equation may still be satisfied. Undoubtedly there will be a great

difference in performance between two such machines in which the diameters and lengths are selected at these two extremes. The selection of the most appropriate dimensions is of great importance; however, this is not indicated in the output equation.

From the discussion of the common methods of separating the components of the D^2L equation, it is easily noted that the procedures are rather vague and indefinite, involving cut-and-try processes.

This certainly points up the statement that is commonly made in regard to electrical machine design, namely, that electrical machine design is both an art and a science. The many decisions involved that rely on judgment and past experience make it an art.

Present polyphase induction motor design methods are best summarized by Lloyd. He lists the steps as:[12]

1. Select the proportions of the machine by more or less empirical methods.
2. Calculate the constants and determine the performance.
3. Incorrect performance results in the need for readjustment by proportions, or, in some cases, complete redesign of the motor.

This thesis will put the separation of the components on a sound engineering basis, where a general-purpose machine is to be designed when given the type of slots, as is very often the case. Certainly no single mathematical relation can be

---

[12] T. C. Lloyd, "Machine Synthesis," Electrical Engineering, LXIX (November, 1950), 1001.

derived, nor can absolutely definite relations for each of the various factors be given, but influences can be shown in many cases which will aid in the preliminary design. In addition, the effect of the length of the air gap will be investigated.

Before presenting these items, a review of the equivalent circuits and vector diagrams of polyphase induction motors (Chapter III) and the subject of machine reactances (Chapter IV) will be necessary.

CHAPTER III

VECTOR DIAGRAMS AND EQUIVALENT CIRCUITS OF THE POLYPHASE INDUCTION MOTOR

When an induction motor is running, losses occur in it which can be represented by in-phase currents, such as would be demanded by resistances, and magnetic effects represented by quadrature currents, such as would be demanded by reactances. It is thus possible to represent the machine by a network of resistances and reactances and to determine the performance of the machine from this network. Such a network is termed the "equivalent circuit" of the machine.

Some of these losses and effects are practically constant and nearly independent of the load on the machine. These are represented by shunt circuits, and are most conspicuous when the machine is running light without any load. Other losses and effects depend almost entirely upon the load and should be represented by components in series. These are most important in a standstill test.

The complete motor can be represented by very simple equivalent circuits. These circuits are similar to those of a transformer since an induction motor is simply an electric transformer whose magnetic circuit is separated by an air gap into two relatively movable portions, one carrying the primary and the other the secondary windings. Relative motion between the two structures is produced by the electromagnetic forces corresponding to the power transferred across

the air gap by induction. In an induction motor, the flux is produced by the stator, or primary winding, which is located on the outer stationary part of the machine and to which the supply is connected, while the rotating inner part of the machine, the rotor, has spread on it a rotor or secondary winding. The rotor winding usually (1) is of a squirrel-cage type or (2) consists of a winding, the ends of which are brought out to an external circuit by means of slip rings. Machines having the first type of rotor are called squirrel-cage induction motors, and those of the second type are called wound-rotor induction motors. It is possible to design a motor so that the supply is connected to a winding on the rotating member; then the squirrel-cage or secondary winding would be constructed on the stator. The action would be the same. To avoid confusion in the discussion which follows, the assumption will be that the stator winding is connected to the supply, and hence is the primary.

EMF AND CURRENT RELATIONS, GENERAL VECTOR DIAGRAM

In the analysis of induction motors, it is assumed that the voltage, V_1, impressed upon each phase of the primary winding, is purely sinusoidal and that the flux per pole, ϕ, is sinusoidally distributed in space around the air gap. Actually the impressed voltage may include time harmonics, and the flux may be distorted by the presence of space harmonics, but their presence and effects are neglected.

When the frequency of the voltage applied to the stator winding of p poles is f cycles per second, the magnetic field produced travels at the synchronous speed of N_s revolutions per minute in accordance with Equation (3). When the rotor of the motor is rotating, the rotor frequency is less than the supply frequency due to the fact that both the rotating magnetic field and the rotor are revolving in the same direction, and hence the rate of cutting is less. For example, if the rotor is running at 95 per cent of its synchronous speed, the rate of cutting will obviously be only 5 per cent of the value it would have if the rotor were at rest. Likewise, the frequency will be only 5 per cent of the primary frequency.

The frequency of the rotor emf is

$$f_2 = \left(\frac{N_s - N}{N_s}\right) f \quad \text{cycles per second} \tag{21}$$

in which N is the rotor speed in rpm. The quantity, $(N_s - N)/N_s$, defines the slip, s, so

$$f_2 = sf \tag{22}$$

Also, the rotor emf while running, E_2', is related to the standstill induced emf, E_2, by

$$E_2' = sE_2 \tag{23}$$

With polyphase currents in the rotor conductors, a rotor mmf is produced that rotates at a speed sN_s relative to the rotor surface in the same direction as the rotor is turning. However, the rotor is revolving at a speed of $(1 - s)N_s$ with

respect to the stator surface. This means that the rotor mmf is traveling at the same speed as the stator mmf and that there is no relative motion between them. Because of this, the analysis of the performance of a polyphase induction motor is similar to that used for the transformer. As such, on a per-phase basis, the vector diagram of a polyphase induction motor is shown in Figure 6. Subscripts 1 and 2 refer to the stator and rotor quantities, respectively.

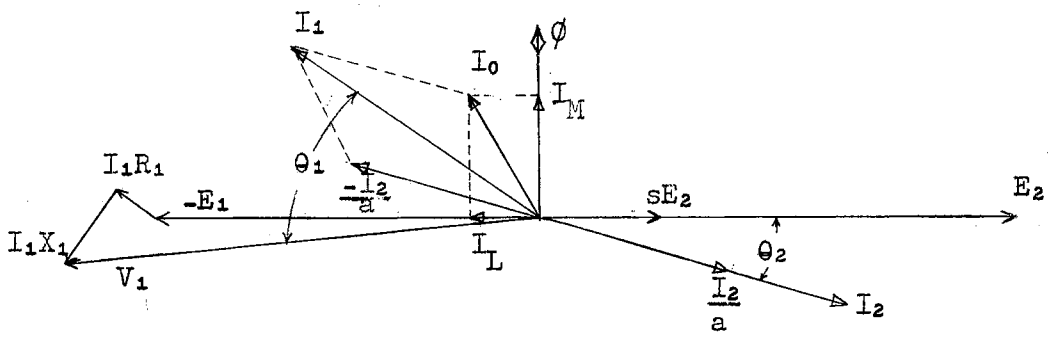

Figure 6. Vector diagram of the relations in one phase of a polyphase induction motor.

Here E_2, the rotor emf at standstill corresponding to a given flux ϕ, has been chosen as the reference vector. The flux vector is drawn 90° ahead of E_2 so as to give an "open" type vector diagram; the magnitude of their instantaneous values are related by $|e_2| = |N_2\, d\phi/dt|$, where N_2 is the effective number of turns per phase of the rotor winding.

When the motor is running with a slip s, for a given value of ϕ, the rotor emf is sE_2. This emf is in phase with E_2 as shown. The corresponding rotor current is

$$I_2 = \frac{sE_2}{\sqrt{R_2^2 + (sX_2)^2}} \qquad (24)$$

where

R_2 = the effective rotor resistance per phase in ohms

X_2 = the rotor leakage inductive reactance per phase in ohms at standstill

Because the rotor frequency varies with the slip, the reactance varies with the slip also and at a slip s is sX_2 ohms. The rotor current lags sE_2 by the angle $\Theta_2 = \tan^{-1} sX_2/R_2$.

The flux ϕ produces the emf E_1 in the stator winding. E_1 and E_2 are related in the open type diagram by $-E_1 = aE_2$ where a is the transformation ratio from the stator to the rotor. A magnetizing current of I_M amperes in required to produce the flux ϕ. The two are in phase.

When running, an induction motor has a friction and windage loss that does not exist in a transformer. Another slight difference between the induction motor and the transformer is that in a transformer the core loss is nearly independent of the load for a given applied voltage and frequency. In an induction motor, the stator core loss is likewise nearly independent of the load; however, the rotor core loss varies with the load because the rotor frequency varies with the load. Within the speed limits of normal motor operation, the

change in the rotor core loss is quite small; hence, it may be treated as a constant. Also, in the induction motor, the friction and windage losses cause a retarding torque on the rotor that must be balanced by a torque produced by currents in the rotor. However, as in the case of the rotor core loss, under usual running conditions, this loss may also be treated as a constant. The rotor core loss and the friction and windage losses are treated as stator losses and are added to the stator core loss. The sum of the three is represented by a nearly constant component of current, I_L, in the stator winding which is considered as supplying them. This current is shown in phase with $-E_1$. Its magnitude is equal to the loss per phase divided by E_1. The vector sum of I_M and I_L is the exciting current, I_o. The magnetizing component of I_o, namely, I_M, is considerably greater than in an ordinary transformer because of the presence of the air gap in the magnetic circuit. Another component of stator current has been denoted as I_2/a. It is in phase with I_2 and is related to it by the equivalent turns ratio a. The total stator current, I_1, in the open type diagram, is the vector sum of $-I_2/a$ and I_o. This current causes a resistance drop I_1R_1 and a leakage reactance drop I_1X_1 in the stator winding. The stator applied voltage per phase, V_1, is equal to the vector sum of $-E_1$, I_1R_1, and I_1X_1. The angle between V_1 and I_1 is the stator power-factor angle.

THE "EXACT" EQUIVALENT CIRCUIT

The practical identity of the vector diagram of Figure 6 with the corresponding vector diagram of the stationary transformer indicates that just as there is an equivalent circuit for the transformer there should be a similar one for the induction motor.

In Equation (24) it was shown that

$$I_2 = \frac{sE_2}{\sqrt{R_2^2 + (sX_2)^2}} \tag{24}$$

where E_2, R_2, and X_2 are considered as constants. This equation agrees with the physical fact that the rotor current, I_2, is produced by an emf that is proportional to the slip, acting on a circuit of constant resistance and variable reactance.

Dividing the numerator and denominator of Equation (24) by s, one obtains

$$I_2 = \frac{E_2}{\sqrt{\left(\frac{R_2}{s}\right)^2 + X_2^2}} \tag{25}$$

The secondary current is thus expressed in terms of the secondary standstill reactance and an equivalent value of resistance that varies inversely as the slip. Interpreting this equation, one can say that the relations in the rotor circuit are the same as if a constant emf were applied to a circuit of variable resistance and constant reactance. An increase in load, which results in an increase in the slip, is equivalent to reducing the resistance in the secondary

circuit. As s varies from a value of 1 (standstill) to s = 0 (synchronism) the value of the total secondary resistance varies from R_2 to an infinite value.

Recalling transformer equivalent circuits and vector diagrams, together with Figure 6 and Equation (25), an equivalent circuit can be drawn as shown in Figure 7 for one phase of a polyphase induction motor. Figure 7 is drawn in stator terms, with a as the ratio of the equivalent number of stator turns per phase to the equivalent number of rotor turns per phase. As expressed in Equation (25), the whole effect of the rotor resistance per phase and the motor load per phase is represented by the variable resistance R_2/s. This value must be multiplied by a^2 in order to refer it to the stator.

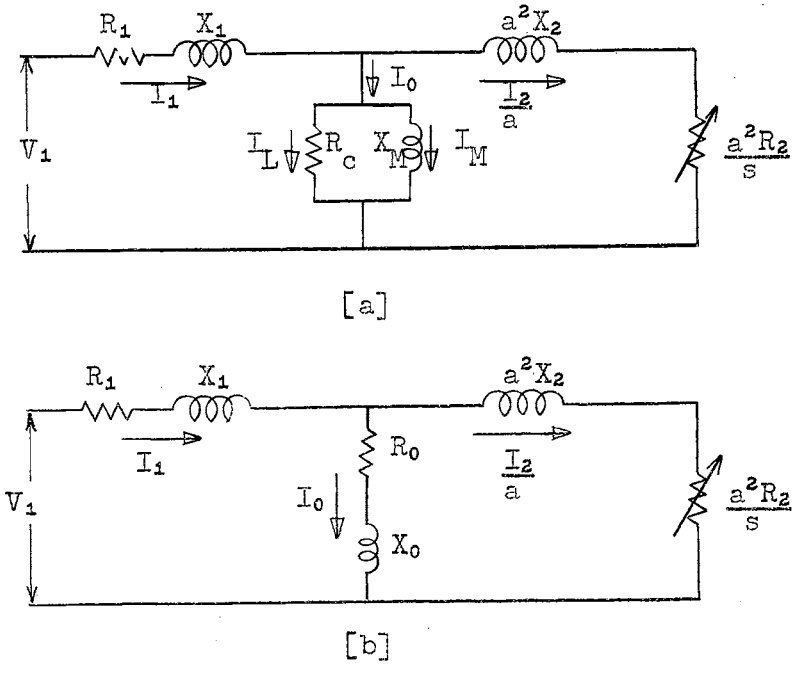

Figure 7. Alternative forms of the "exact" equivalent circuit of a polyphase induction motor.

The actual secondary winding resistance per phase is R_2; however, the total effective resistance in the secondary as expressed by Equation (25) is R_2/s. Then the resistance added to the secondary circuit is

$$R_s/s - R_2 = \left(\frac{1 - s}{s}\right) R_2 \qquad (26)$$

which is the true representation of the mechanical load. The equivalent circuit is redrawn in Figure 8.

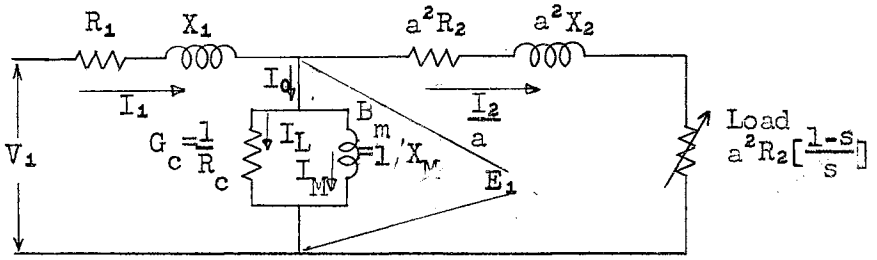

Figure 8. An "exact" equivalent circuit for one phase of a polyphase induction motor.

A complete vector diagram applying to both Figures 7 and 8 is given in Figure 9. To avoid crowding, this is drawn as an open type diagram.

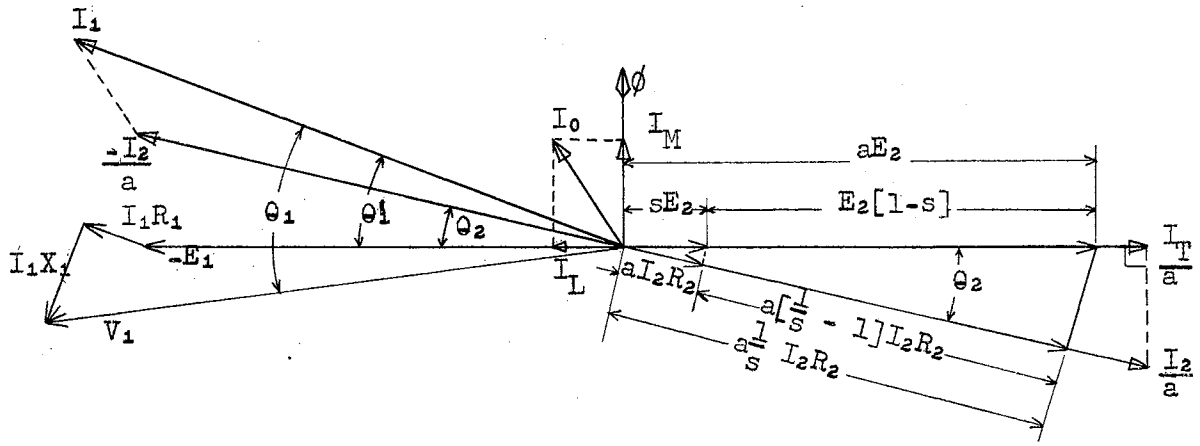

Figure 9. Vector diagram for an induction motor.

THE APPROXIMATE EQUIVALENT CIRCUIT

In general, the impedance drop in the primary resistance and reactance, $I_1(R_1 + jX_1)$, is a small percentage (about 2 per cent in large motors) of the impressed voltage, V_1, so there is little error involved in treating E_1 as substantially equal to V_1 in magnitude. This is equivalent to transferring the exciting branch from the position shown in Figure 8 to a new position directly across the input terminals as shown in Figure 10. This means that the stator impedance drop caused by the no-load current is neglected. In most motors (excepting, say, fractional horsepower sizes or those with a large primary drop) the error introduced by this assumption is very small.

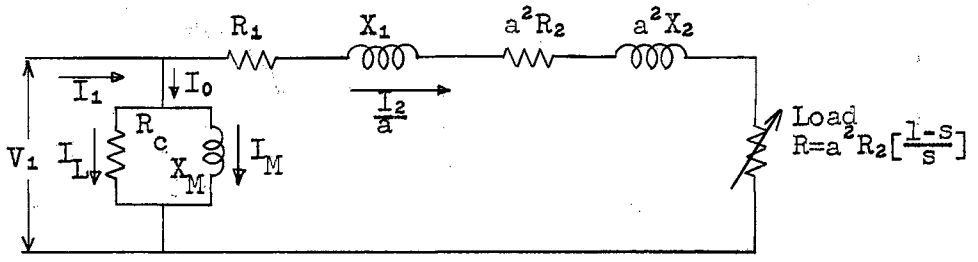

Figure 10. An approximate equivalent circuit for an induction motor.

The resistances R_1 and a^2R_2 and the reactances X_1 and a^2X_2 can be combined into an equivalent resistance and reactance, R_e and X_e. However, they are usually kept separate

because the individual values are used in computing the performance of the motor.

The advantage of the approximate equivalent circuit is the ease with which the performance characteristics of the motor can be calculated from it. The usual method of making use of such a circuit, after the constants are known, is to assume a value of slip and solve the circuit for the performance items desired. Then another value of slip is assumed and other points obtained. An analysis of the approximate equivalent circuit shows the following relations apply at any value of slip, s. These relations are on a per-phase basis.

The power input = $V_1 I_1 \cos \theta$ watts per phase. (27)

The power output = $(\frac{I_2}{a})^2 a^2 R_2 (\frac{1 - s}{s})$ watts per phase. (28)

The current $I_2/a = \frac{V_1}{\sqrt{[R_1 + a^2R_2 + a^2R_2(\frac{1-s}{s})]^2 + X_e^2}}$ amperes, where (29)

$$X_e = X_1 + a^2X_2 \tag{30}$$

The loss in the rotor winding = $(\frac{I_2}{a})^2 a^2R_2$ watts per phase. (31)

The power into the rotor = $(\frac{I_2}{a})^2 \frac{a^2R_2}{s}$ watts per phase. (32)

The efficiency of the rotor winding = 1 - s. (33)

The torque = $\frac{7.04 (\frac{I_2}{a})^2 a^2 R_2/s}{N_s}$ lb at 1 ft radius per phase. (34)

The starting torque = $\frac{7.04\ V_1^2\ a^2\ R_2}{N_s\ Z_e^2}$ lb at 1 ft radius per phase, where (35)

$$Z_e = \sqrt{R_e^2 + X_e^2} \tag{36}$$

$$R_e = R_1 + a^2 R_2 \tag{37}$$

The slip at maximum torque = $s_{mT} = \frac{a^2\ R_2}{\sqrt{R_1^2 + X_e^2}}$. (38)

The maximum torque = $\frac{3.52\ \ V_1^2}{N_s\left[R_1 + \sqrt{R_1^2 + X_e^2}\right]}$ lb at 1 ft radius per phase. (39)

Slip at maximum power output = $s_{mp} = \frac{a^2\ R_2}{a^2\ R_2 + Z_e}$. (40)

These relations can be expressed in many different forms. The particular forms given are the ones the author has found most convenient.

The constants of the approximate or the exact equivalent circuit can be computed from either design data or test data. Using design data, the value of each circuit element can be determined. The test data required are (1) the no-load readings (similar to the open-circuit test on a transformer), (2) the blocked-rotor readings (as in the short-circuit test of a transformer), (3) the ratio of turns, and (4) resistance measurements.

THE CIRCLE DIAGRAM

A graphical solution of the approximate equivalent circuit per phase of an induction motor is known as the circle diagram. Although the operating characteristics can be computed from

the equivalent circuit, it is simpler and more convenient to use the circle diagram.

In Figure 11a, the current drawn from the supply, I_1, is equal to the sum of I_o and I_2/a. The current I_o will be constant for a constant value of supply voltage. It is plotted in Figure 11b lagging the voltage V_1 by the angle θ_o.

The stator load component of current, $\frac{I_2}{a}$, was given in Equation (29) as

$$I_2/a = \frac{V_1}{\sqrt{(R_1 + \frac{a^2R_2}{s})^2 + (X_1 + a^2X_2)^2}} \tag{41}$$

This current lags V_1 by the angle θ_2, where

$$\sin \theta_2 = \frac{X_1 + a^2X_2}{\sqrt{(R_1 + \frac{a^2R_2}{s})^2 + (X_1 + a^2X_2)^2}} \tag{42}$$

By combining Equations (41) and (42),

$$I_2/a = \frac{V_1}{X_1 + a^2X_2} \sin \theta_2 \tag{43}$$

Since $X_1 + a^2X_2$, the standstill reactance, is constant, Equation (43) is the polar equation of a circle with a diameter AB = $V_1/(X_1 + a^2X_2)$. If V_1 is drawn vertically, the diameter AB is horizontal as in Figure 11c. This circle represents the stator load current. A change in load on the motor causes a change in the slip s. This causes a change in θ_2 and also in I_2; thus AP represents the stator load current for a particular value of slip.

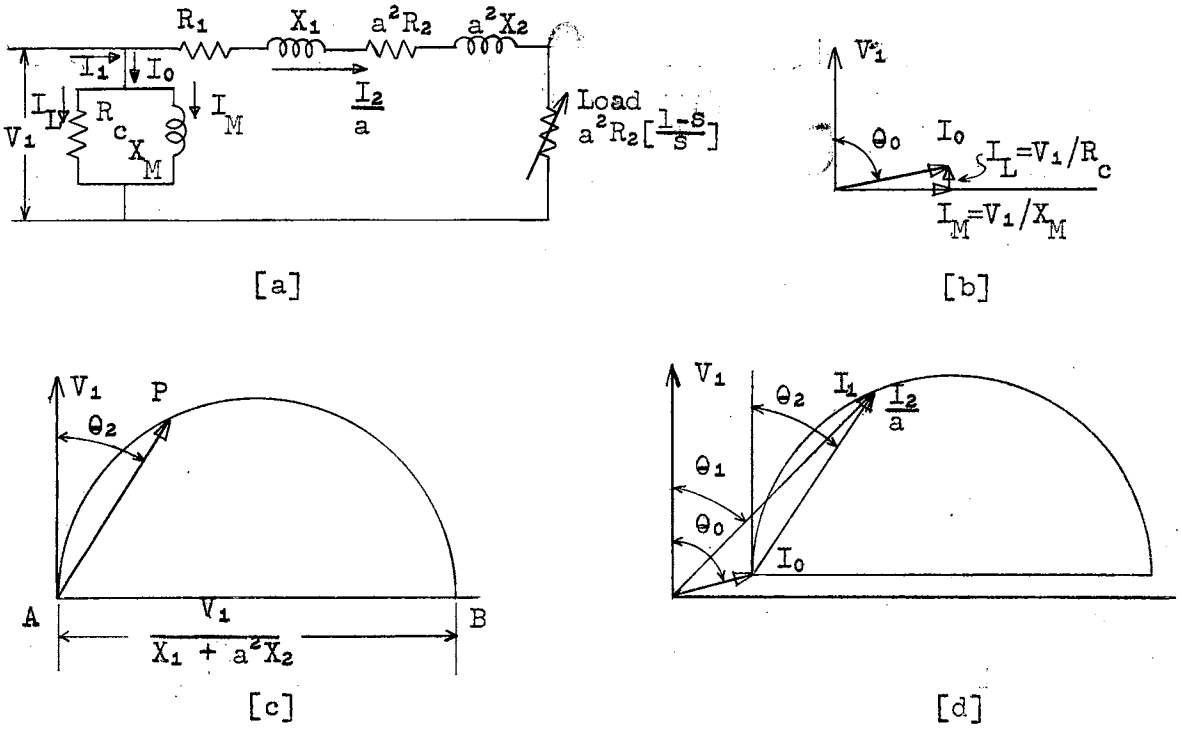

Figure 11. Current relations in the approximate equivalent circuit.

The two vector diagrams of Figures 11b and 11c can now be combined since, as stated previously, the line current, I_1, is the vector sum of I_o and I_2/a. Hence the locus of the end of the vector I_1 is the semicircle shown in Figure 11d. For any given load, the power-factor angle of the entire motor is θ_1.

CONSTRUCTION OF THE CIRCLE DIAGRAM

Data for the construction of this diagram are obtained from a no-load (open-circuit) test, a blocked (short-circuit) test, and resistance measurements as is done with the transformer. Of course, it can also be computed from design data. Because all the losses depend upon the temperature of the

machine, it is preferable to make these tests immediately after a heat run, since all parts of the machine will then be at normal temperature. If these tests are made at other than normal temperature, appropriate corrections must be applied.

No-Load Test. The motor is run at rated voltage without load, and the line voltage, V, the line current, I, and the total power input in watts, P, are measured. The no-load power-factor angle, θ_o, can then be determined. ($\cos \theta_o = P/\sqrt{3}VI$ for a three-phase motor). The voltage per phase, V_1, is laid off vertically in Figure 12, and the no-load current per phase, I_o, is laid off at an angle θ_o from

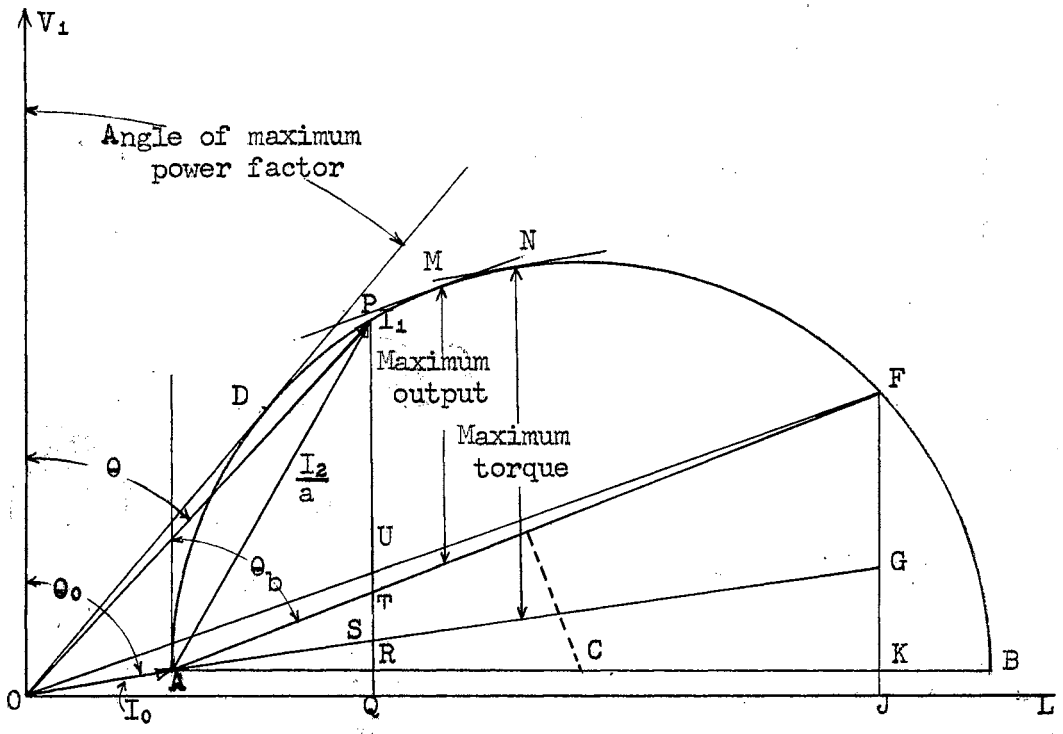

Figure 12. Circle diagram of a polyphase induction motor.

V_1 and lagging. This corresponds to Figure 11b, since at no-load the slip is so small it is assumed to be zero. In the equivalent circuit with zero slip, the resistance representing the load is infinite and I_2/a is zero; hence, the only current drawn from the source is the exciting current, I_o. For the sake of clearness, the exciting current vector in Figure 12 is drawn longer than it would be in the diagram of an actual machine.

Blocked-Rotor Test. The rotor of the machine is locked so that it cannot rotate. In order that the current may be kept within reasonable limits, a reduced voltage, V', must be applied to each phase. The reduced voltage should be of such a value as to give a short-circuit current equal to rated value or higher. One must be careful not to overheat the motor. The phase current, I_b', the total power, P', and the phase voltage, V', are measured. The current is then prorated to rated voltage by $I_b = I_b' \ V_1/V'$, where V_1 is the rated phase voltage. The current lags the voltage by an angle $\theta_b = P'/nI_b' \ V'$. Since the slip is zero under these conditions, the resistance representing the load in the equivalent circuit is equal to zero. Also, since the test with locked rotor is usually made with a greatly reduced voltage, the losses in the iron are very small and may be neglected. The approximate equivalent circuit then reduces to that shown in Figure 13. The current I_b corresponds to I_2/a of Figure 11a. On the circle diagram, Figure 12, to the chosen scale,

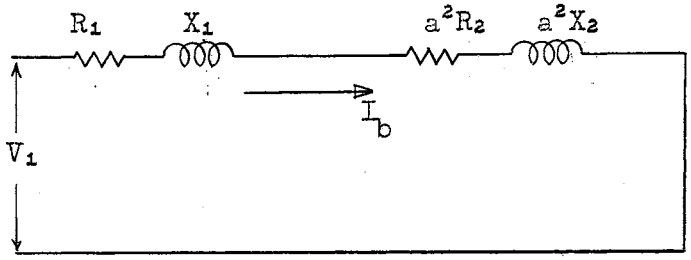

Figure 13. Equivalent circuit, blocked-rotor test.

from the point A, at the tip of I_o, lay off I_b lagging V_1 by θ_b as AF. Some writers prefer to lay this current off from O to F; however, the author believes it should appear as laid off due to the reduced voltage impressed. With this reduced voltage, the losses represented by the shunt exciting branch in the equivalent circuit are very small. The current taken by the exciting branch is such a small percentage of the other branch current that it can be considered as non-existant during the blocked-rotor test, giving the circuit of Figure 13 and a location of the blocked current from A to F in Figure 12 after prorating. This would not be true if the losses were large, but, in that case, the approximate equivalent circuit, on which the circle diagram is based, should not be used since it is based on the assumption that the exciting branch can be moved to a location across the input terminals rather than as located in the exact equivalent circuit. If the losses are large, the exact

equivalent circuit must be used. Arguments can be found in the literature for both locations of I_b.

Draw a line in the direction of AB parallel to the horizontal axis. The points A and B are on the desired circle. The center of the circle is located by constructing a perpendicular bisector of the line AF. The bisector and the horizontal line intersect at C. Using C as the center, the semicircle AFB can be drawn. A perpendicular FJ is then dropped from F to OL. The line FK is divided at G into two segments, such that

$$\frac{KG}{GF} = \frac{\text{stator resistance}}{\text{rotor resistance in stator terms}} = \frac{R_1}{a^2 R_2} \qquad (44)$$

Line AG is then drawn.

PERFORMANCE FROM THE CIRCLE DIAGRAM

After the circle diagram has been drawn, the performance for any given stator current can easily be computed. Assume that the performance at the current I_1 is to be computed.

At any load current such as I_1, I_2/a (equal to AP) is the secondary current in stator terms, being equal to $I_1 - I_o$ vectorially. PQ is the energy component of the current I_1, and, therefore, the total power input per phase is

$$P_{in} = (PQ) \times V_1 \text{ watts per phase} \qquad (45)$$

The core, friction, and windage losses

$$P_L = (RQ) \times V_1 \text{ watts per phase} \qquad (46)$$

The primary copper loss

$$I_1^2 R_1 = (RS) \times V_1 \text{ watts per phase} \qquad (47)$$

The secondary copper loss

$$(I_2/a)^2R_2 = (ST) \times V_1 \text{ watts per phase} \qquad (48)$$

The power output

$$P_{out} = (PT) \times V_1 \text{ watts per phase} \qquad (49)$$

The efficiency

$$\eta = PT/PQ \qquad (50)$$

The torque

$$T = 7.04\ V_1\ (PS)/N_s \text{ lb-ft} \qquad (51)$$

The slip

$$s = ST/SP \qquad (52)$$

The power factor

$$\cos \theta = PQ/I_1 \qquad (53)$$

The maximum power factor point is D, located by drawing a tangent to the circle from O. The maximum output and maximum torque points are similarly located at M and N by tangent lines parallel to AF and AG, respectively.

The above diagram is drawn for but one phase of the motor. The values of power, losses, and torque must be multiplied by n if the motor has n phases.

The circle diagram presented here is the one that is most frequently found in American textbooks. It is a result of the work of A. S. McAllister and is occasionally referred to as the McAllister circle diagram. In addition to the McAllister diagram, many others are available, embodying various refinements based on other equivalent networks. A very

interesting historical background of many types of circle diagrams is given by Behrend.[1]

The principle disadvantage of determining the performance of an induction motor from the circle diagram and Equations (45)-(53) is that it must be drawn to a very large scale to obtain a reasonable degree of accuracy. A much faster and more accurate method is to use one of the many analytical solutions of the circle diagram that have been worked out. The simplest, fastest, and easiest of these is the method developed by Cameron.[2]

COMPARISON OF THE APPROXIMATE AND THE EXACT EQUIVALENT CIRCUITS AND THE CIRCLE DIAGRAM

The derivation of the circle diagram given is based upon the approximate equivalent circuit. The circular locus is not a result of the approximations. The so-called "exact" equivalent circuit shown in Figure 8 likewise yields a circular locus.

In presenting the arguments for the approximate equivalent circuit, one begins to question its accuracy and the accuracy of the resultant circle diagram because of the many approximations made. Although the discussion is rather long, it would be well to look at the views of a noted

---

[1] B. A. Behrend, The Induction Motor and Other Alternating Current Motors (New York, 1921).

[2] Unpublished calculation sheet by Professor C. F. Cameron, Oklahoma Agriclutural and Mechanical College.

authority in the field of alternating-current machinery.

In discussing the exact circle diagram, Langsdorf states:[3]

> But before entering upon this analysis, [the analysis of the exact circle diagram], it is desirable to point out certain limitations of the so-called exact equivalent circuit which make it at best only a close approach to actual truth, and not a mathematically exact representation of physical reality.
>
> One of these limitations had already been mentioned; it arises from the fact that the exciting admittance, [see Figure 8], made up of the exciting conductance G_c and the exciting susceptance B_m, is not strictly constant, but changes somewhat with the load because of varying friction, windage, and core loss. In addition to this it must be remembered that R_1, X_1, a^2R_2, and a^2X_2 are themselves subject to variation with the load. The resistances, for example, that must be used in the computations are not the pure ohmic resistances that would be measured by a Wheatstone bridge or by the drop-of-potential method, but they are the effective resistances, which are always greater than the simple ohmic resistances because of the actual nonuniform distribution of the current in the cross section of the conductor. The nonuniform current distribution is a manifestation of skin effect and is caused by crowding of the current toward the surface layers due to the magnetic field; this effect is especially pronounced in the rotor under standstill conditions, that is, at starting, for the secondary is then subject to the inductive effect of a magnetic field alternating at line frequency, as contrasted with conditions near synchronism when the secondary frequency is greatly reduced. As a matter of fact, the change of effective rotor resistance between standstill and full speed can be so exaggerated by appropriate design as to make the starting torque considerably greater than it would otherwise be, without at the same time impairing efficiency and speed regulation under normal running conditions.
>
> In like manner, the primary and secondary leakage reactances, X_1 and X_2, are functions of the magnitude and distribution of the leakage paths. Changing load conditions cause changes in current and therefore of the permeability of the teeth and neighboring iron, thus affecting the reactances.
>
> In spite of all these disturbing effects, the assumption that the so-called "constants" of the equivalent circuit (G_c, B_m, R_1, X_1, a^2R_2, a^2X_2) remain invariant yields remarkably

---

[3] Alexander S. Langsdorf, Theory of Alternating-Current Machinery (New York, 1937), pp. 592-593.

accurate results--accurate, that is, when compared with actual measurements. This close agreement is due to several reasons: In the first place, the variation in the "constants" are of the second order of magnitude, and those which change the most (as R_2) are themselves so small in comparison with others that the effect is largely masked under normal running conditions; in the second place, normal running conditions comprise such a small part of the entire range between standstill and synchronism as still further to reduce the discrepancies; and in the third place, actual observations must be made with instruments which are themselves not absolutely accurate, and the readings are in addition subject to personal errors of observation. In short, the difference between absolute truth (if there is such a thing) and observed facts is not sharply defined, and the more or less hazy zone of uncertainty between them includes the effect of simplifying assumptions and of errors of observation.

It must not be assumed, therefore, that an analysis based upon the so-called exact equivalent circuit is rigorous in the mathematical sense; the word "exact" is really a misnomer, but it has been generally used to distinguish this case from that of the confessedly approximate circuits. It is to be expected that it will yield results very nearly the same as those already derived from the approximate circuit. The chief value of the more complete analysis therefore derives not from increased accuracy but from certain principles and procedures that have wide application and intrinsic importance of their own.

After deriving the circular locus for the exact equivalent circuit, Langsdorf takes typical values for a commercial motor and determines the characteristics of the motor from circle diagrams of the exact and the approximate equivalent circuits. The two circles are superimposed to show their relationship, along with data in regard to their radius and coordinates of the center of the circle. In conclusion, Langsdorf makes the following remarks:[4]

Within the working range from no load to full load it is practically impossible to distinguish between the two circles

---

[4] Ibid., p. 607.

unless they are drawn very accurately to a large scale. Beyond full load the departure between them increases, but with the constants used in this example it is at no point very great. It is apparent, therefore, that the error due to the use of the approximate equivalent circuit and the circle diagram dependent upon it is within the tolerance limit for practical purposes, and it may safely be used for all ordinary purposes.

It will be recalled that in the case of the transformer one moves the exciting branch to a new position directly across the input terminals, as is done here to arrive at the approximate equivalent circuit for the induction motor. In the case of the transformer, this simplification is in order because the leakage impedances in the transformer without an air gap are small quantities and the induced emf has nearly the same value as the impressed voltage. In the case of the induction motor, the leakage impedances are much larger and the exciting current much greater, because of the air gap and other constructional features. Besides the points already stated in regard to the nature of the induction motor parameters, there is an additional point that should be noted, namely, that measurements on the input and the output of a transformer are all made by electrical methods while measurements on a motor are partly electrical and partly mechanical. Since electrical measurements have a higher degree of accuracy than mechanical ones, the predetermination of the performance of a motor by computation will not be supported by as accurate experimental observations as in the case of the transformer. This further justifies the use of the approximate equivalent circuit in the study of the performance of all but small induction motors.

PERFORMANCE SPECIFICATIONS

Before leaving the subject of the circle diagram, it should be noted that performance specifications cannot be laid down wholly at random. Through the geometry of the circle diagram, all of the operating characteristics of the motor are interrelated. An elementary theorem of geometry states that a circle is completely fixed when any three points on it are determined; hence the specifications must fix three points, and only three. Inconsistencies would result from any additional specifications chosen at random.

CHAPTER IV

MAGNETIZING AND LEAKAGE REACTANCE

The two most important constants of the induction motor equivalent circuit are the magnetizing reactance, X_M, and the total leakage reactance, $X_1 + a^2X_2$.

The magnetizing reactance, X_M, is the reactance due to the fundamental sine-wave, or useful, air-gap flux.

The total leakage reactance, $X_1 + a^2X_2$, is a measure of all the nonuseful magnetic flux produced by a current in either the stator or rotor winding; that is, all flux producing no fundamental-frequency voltage in the other winding.

The importance of these two reactances can be seen in Figure 11. The magnetizing reactance, as shown in Figure 11b, determines the amount of shift of the circle to the right in the circle diagram. In Figure 11c and Equation (43), it was shown that the diameter of the circle in the circle diagram is inversely proportional to the total leakage reactance. In other words, these two values of reactance are of great importance in locating and determining the diameter of the circle diagram and hence directly affect all of the operating characteristics read therefrom.

CALCULATION OF THE MAGNETIZING CURRENT AND MAGNETIZING REACTANCE

In order to calculate the amount of current required in the stator winding to establish a given flux or flux density, one must first decide on a method to use to take into account fringing of the flux at the edges of the teeth. At present, two different methods are in use. One method is to increase the width of the actual tooth; the greater tooth width is intended to correct for the spreading of the flux lines. The other method is to calculate an equivalent air gap. The equivalent air gap is the length of air gap between stator and rotor which would cause the same exciting ampere-turns to establish the same amount of flux in the gap if the slotted surfaces of both stator and rotor were replaced by smooth surfaces. Many formulas appear in the literature for either method of treating the effect of fringing. The author considers the first method of taking tooth fringing into account more basic and prefers to use it.

The method of calculating the magnetizing current and the magnetizing reactance presented here is credited to Adams.[1]

Fringing. Referring to Figure 14, consider a strip of gap section one-inch wide parallel to the shaft (perpendicular

---

[1] Comfort A. Adams, "Design of Induction Motors," Transactions of the American Institute of Electrical Engineers, XXIV (June, 1905), 654-659.

to the plane of the paper), and divide this strip into three parts:

1. The part immediately under the tooth.

2. The part extending outward from the edge of the tooth tip a distance equal to the radial depth of the air gap.

3. The part from this last point to a point halfway across the slot opening. In this third part, the paths of the flux lines are considered to be circular.

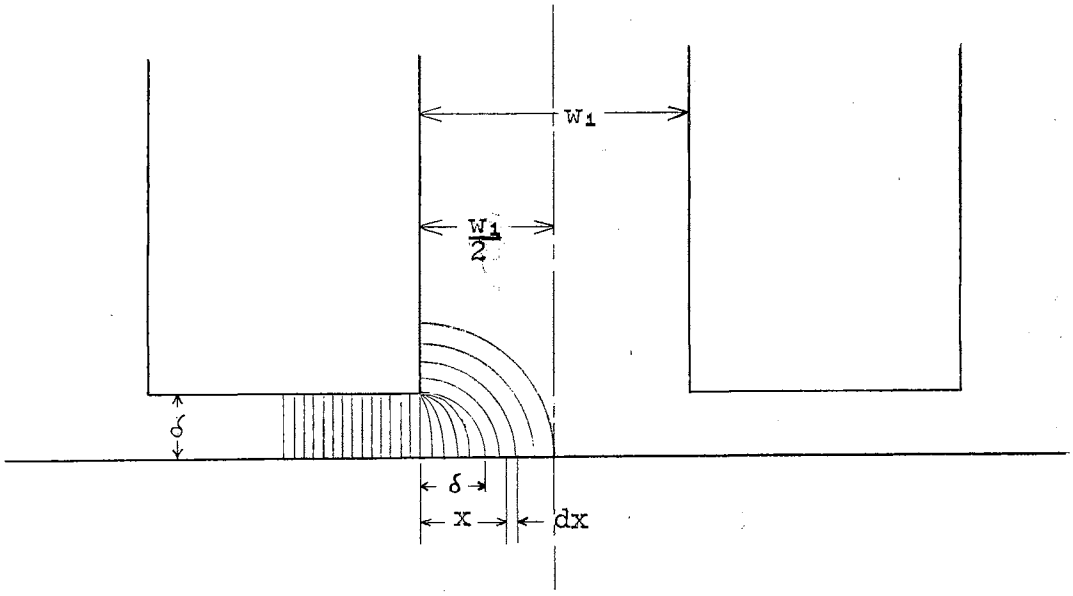

Figure 14. Tooth flux fringing.

In this method, an equivalent increase in the width of the tooth tip produced by the fringing flux, part 2 and 3 above, is found in terms of the radial air-gap depth, δ.

The permeance of the second part does not lend itself to calculation. The equivalent average width of this portion is taken as $0.6\,\delta$; the permeance as 0.6.

The permeance of the third part can be found by integration. The permeance is

$$\frac{2}{\pi}\int_{x=\delta}^{x=\frac{w_1}{2}} \frac{dx}{x} = \frac{2}{\pi} \ln \frac{w_1}{2\delta} = 1.47 \log \frac{w_1}{2\delta} \qquad (54)$$

The total fringing permeance is the sum of these two parts, or

$$F = 0.6 + 1.47 \log \frac{w_1}{2\delta} \qquad (55)$$

and is called the tooth fringing constant. It is plotted in Figure 15. When w_1 is less than 2δ, Equation (55) is not satisfactory. This is allowed for in Figure 15 by continuing the curve from $w_1 = 2\delta$ to the origin in a straight line.

The effect of fringing is equivalent to increasing the width of the tooth tip by $F\delta$ on each side of the tooth, so if the width of the actual tooth is t_t inches, the width of the equivalent tooth tip is

$$t = t_t + 2F\delta \quad \text{inches} \qquad (56)$$

All calculations of gap reluctance are made on the basis of this equivalent tooth-tip width.

The particular shape of the slot under consideration has some effect on the fringing permeance. If the slots have straight sides, the fringing flux will not follow circular paths as assumed but will extend farther back on the side of the tooth and the fringing permeance will be slightly greater than that indicated by Equation (55). If the tooth tips

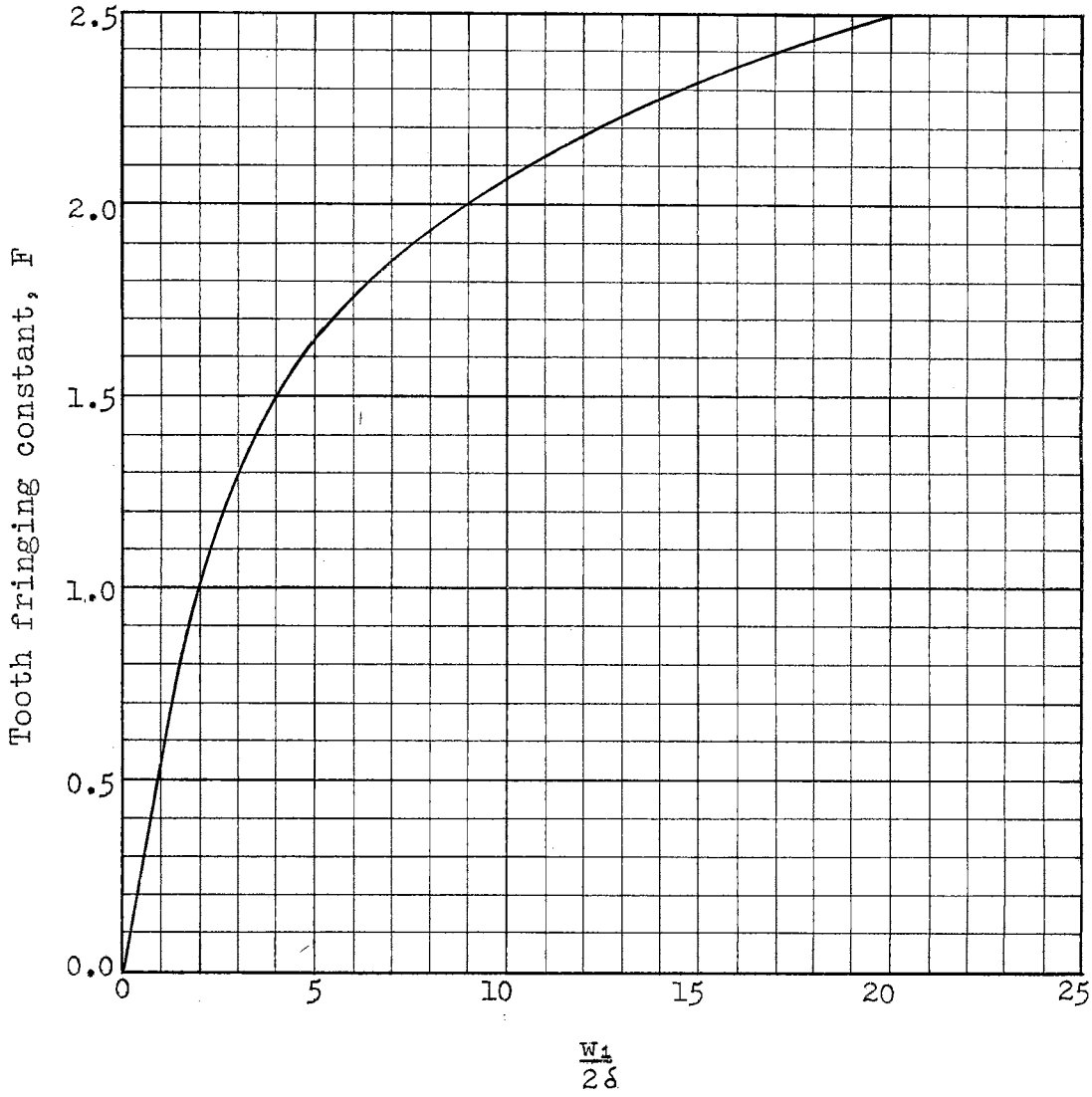

Figure 15. Tooth fringing constant.

spread out, or if there are slot openings on both sides of the gap, the fringing permeance will be slightly less than that given by Equation (55).

A slightly modified method of treating the effect of fringing, which is in a more convenient form to use, is shown in Table V. The width of the equivalent tooth tip is

$$t = t_t + G \tag{57}$$

Values of G are given in the table in terms of the slot opening and the radial air-gap length. Note that w_1' and w_1'' are the respective stator and rotor slot openings.

TABLE V[2]

EFFECTIVE TOOTH FACE FROM FRINGING (VALUES OF G)

Slot opening w_1' or w_1''	Radial air-gap length in inches					
	0.010"	0.015"	0.020"	0.025"	0.030"	0.040"
0.04	0.021	0.024	0.026	0.027	0.028	0.029
0.05	0.023	0.028	0.031	0.032	0.033	0.035
0.06	0.026	0.031	0.035	0.037	0.039	0.041
0.07	0.028	0.034	0.038	0.041	0.043	0.046
0.08	0.030	0.036	0.041	0.045	0.048	0.051
0.09	0.031	0.039	0.044	0.049	0.053	0.057
0.10	0.032	0.041	0.047	0.052	0.056	0.062
0.11	0.034	0.043	0.049	0.055	0.059	0.066
0.12	0.035	0.044	0.052	0.058	0.062	0.070
0.13	0.036	0.046	0.054	0.060	0.065	0.073

[2]Harold Pender and William A. Del Mar, Electrical Engineers' Handbook--Electric Power (New York, 1949), p. 9.75.

There is also a fringing of the flux at the ends of the core and at the ventilating ducts. Generally it is neglected, but it may be taken as an increase in length equal to the radial air-gap depth at each discontinuity.

Magnetizing Current and Magnetizing Reactance Calculations.

With slots on both stator and rotor, one must determine an average or effective gap section. In Figure 16, let t_1 and t_2 represent the equivalent tooth tips including fringing, and λ_1 and λ_2 the corresponding tooth pitches, all expressed in inches. As before, a length along the shaft of one inch will be taken.

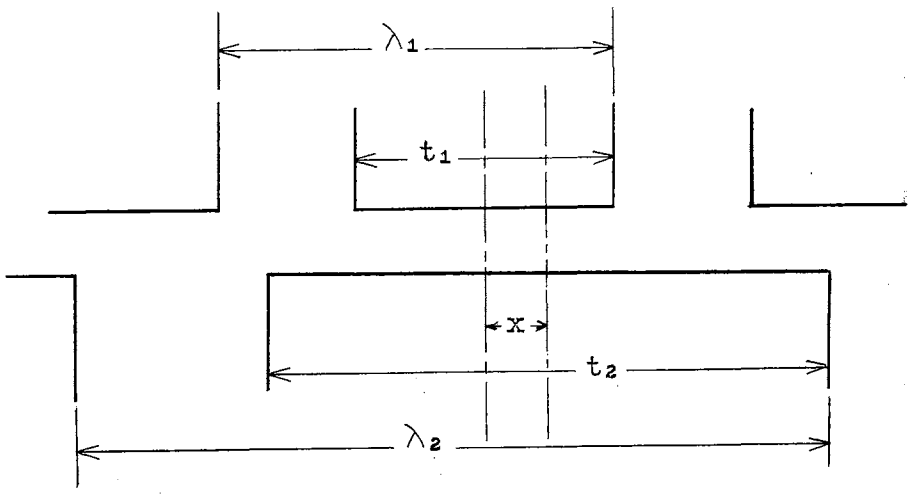

Figure 16. Tooth relations in a motor.

Consider the average overlapping area per tooth of smaller pitch during a movement equal to one-half of the larger pitch. The effective gap section can be found from the slot relations during this movement. The overlap is made up of three parts:

1. From $x = 0$ to $x = 1/2(t_2 - t_1)$

   Overlap $= t_1$

2. From $x = 1/2(t_2 - t_1)$ to $x = \lambda_2 - 1/2(t_2 + t_1)$

   Overlap $= 1/2(t_2 + t_1) - x$

3. From $x = \lambda_2 - 1/2(t_2 + t_1)$ to $x = 1/2(\lambda_2)$

   Overlap $= (t_1 + t_2) - \lambda_2$

Integrating each of these parts yields

1. $$\int_{x=0}^{x=1/2(t_2 - t_1)} t_1 \, dx = \frac{t_1}{2}(t_2 - t_1) \tag{58}$$

2. $$\int_{x=1/2(t_2 - t_1)}^{x=\lambda_2 - 1/2(t_2 + t_1)} \left[1/2(t_2 + t_1) - x\right] dx = (\lambda_2 - t_2)\left(t_1 - \frac{\lambda_2 - t_2}{2}\right) \tag{59}$$

3. $$\int_{x=\lambda_2 - 1/2(t_2 + t_1)}^{x=1/2\,\lambda_2} \left[(t_1 + t_2) - \lambda_2\right] dx = \left[(t_1 + t_2) - \lambda_2\right] 1/2 \left[(t_1 + t_2) - \lambda_2\right]$$

$$= 1/2\left[(t_1 + t_2)^2 + \lambda_2^2 - 2\lambda_2(t_1 + t_2)\right] \tag{60}$$

The sum is

$$\text{Part 1} + \text{Part 2} + \text{Part 3} = \frac{t_1 t_2}{2} \tag{61}$$

The average overlap is then

$$\frac{\frac{t_1 t_2}{2}}{\lambda_2/2} = \frac{t_1 t_2}{\lambda_2} \tag{62}$$

and the average per cent overlap is

$$\frac{t_1 t_2}{\lambda_1 \lambda_2} = a_1 a_2 = K_1 \tag{63}$$

where

$a_1 = t_1/\lambda_1$

$a_2 = t_2/\lambda_2$

K_1 = the gap-section constant

Thus, $K_1 = a_1 a_2$ is the ratio of the effective gap section to the superficial or apparent gap section. The gross length of the core minus the space for air ducts is used in calculating the superficial gap section.

With these constants, one can easily calculate the magnetizing current and the magnetizing reactance.

Let

NI_g = the ampere-turns necessary for a single air gap at the point of maximum flux density

q_m = the peripheral magnetizing current density (ampere-conductors per inch of periphery due to the magnetizing current)

B_g = the superficial maximum gap flux density

Then

B_g/K_1 = the actual maximum gap flux density

and

$$NI_g = 0.313\, B_g/K_1\, \delta \qquad (64)$$

also

$$2NI_g = (1/1.11)\, q_m \tau \qquad (65)$$

assuming sinusoidal distribution of the peripheral magnetizing current density.

Solving Equations (64) and (65) for q_m gives

$$q_m = \frac{0.695\ B_g\ \delta}{K_1\ \tau} \tag{66}$$

The ampere-turns necessary to pass the flux through the iron can be taken into account by introducing another constant, K_2, called the iron constant, and writing Equation (66) as

$$q_m = \frac{0.695\ B_g\ \delta}{K_1\ K_2\ \tau} \tag{67}$$

The constant K_2 varies from 0.85 to 0.95 for 60-cycle motors.

If C' is the number of stator conductors per inch of periphery, Equation (67) reduces to

$$q_m/C' = \frac{0.695\ B_g\ \delta}{K_1\ K_2\ C'\ \tau} = I_M \tag{68}$$

the actual magnetizing current in amperes.

Equation (68) is correct if the motor has a full-pitch winding. In the case of fractional pitch, a higher flux density is required in the gap in order to produce the same resultant electromotive force, because the electromotive forces in the two sides of a given coil differ in phase. Not only is the magnetizing current higher because of the increased gap density, but it is still further increased because of the overlapping of currents of differing phase and the consequent reduction in effectiveness for magnetomotive force production. Adams[3] has

---

[3] C. A. Adams, W. K. Cabot, and G. A. Irving, Jr., "Fractional Pitch Windings for Induction Motors," Transactions of the American Institute of Electrical Engineers, XXVI (June, 1907), 1485-1503.

shown that for the general winding of either full or fractional pitch Equation (68) must be divided by a correction factor, k_m. Equation (68) then becomes

$$I_M = \frac{0.695\ B_g\ \delta}{K_1\ K_2\ k_m\ C'\ \tau} \tag{69}$$

Values of the magnetizing-reactance correction factor are given in Figure 17 as a function of the pitch expressed as a decimal fraction of full pitch.

If

v'' = the synchronous peripheral velocity in inches per second

and

ω_f = the angular velocity of the revolving field in radians per second

then

$$v'' = \omega_f\left(\frac{D}{2}\right) = \frac{2\pi f}{\frac{p}{2}}\ \left(\frac{D}{2}\right) = 2f\ \left(\frac{\pi D}{p}\right) = 2f\tau \tag{70}$$

By dividing Equation (70) by 12 and rearranging, one obtains

$$\frac{f}{v} = \frac{6}{\tau} \tag{71}$$

where

v = the synchronous peripheral velocity in feet per second

Using Equation (71) and introducing the magnetizing-reactance correction factor, Equation (67) can be written as

$$q_m = \frac{0.116\ B_g\ \delta\ f}{K_1\ K_2\ k_m\ v} \tag{72}$$

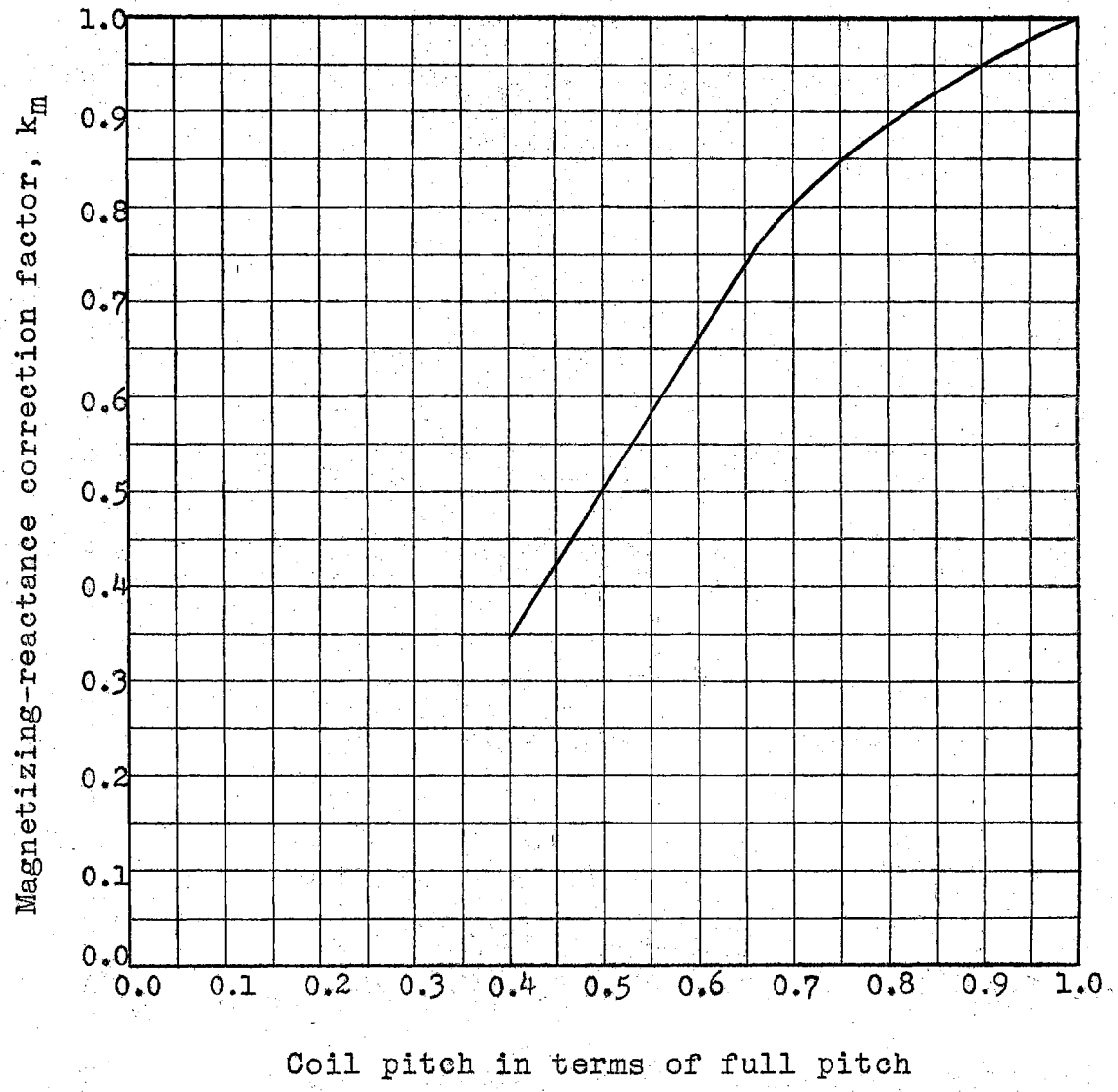

Figure 17.[4] The Adams' magnetizing-reactance correction factor as a function of pitch.

Letting q_T denote the ampere-conductors per inch of air-gap periphery due to the full-load torque current, I_T/a, in

[4] Ibid., p. 1491.

stator terms, the magnetizing current can be expressed in terms of the full-load torque current as

$$b_m = \frac{q_m}{q_T} = \frac{0.116 \ B_g \ \delta \ f}{K_1 K_2 k_m \ q_T \ v} \qquad (72)$$

The torque current is shown in Figure 9. It is the horizontal projection, or the component of the current I_2/a, in phase with the voltage aE_2.

The magnetizing reactance can be found from the known voltage and the expression for the magnetizing current given in Equation (69).

PHYSICAL CONCEPTS OF LEAKAGE REACTANCE

There is only a single magnetic field in a motor. However, in the analysis of leakage reactance the concept of separate leakage fluxes is used. In general, the leakage reactance of the stator is considered to be due to that part of the total flux produced by the stator magnetomotive force, considered to be acting alone, which fails to link with the rotor winding; and the rotor leakage reactance is attributed to that part of the total flux produced by the rotor magnetomotive force, also assuming to be acting alone, which fails to link with the stator winding. Actually the stator and rotor magnetomotive forces do not produce separate fluxes, but combine to form a resultant magnetomotive force which in turn produces a single magnetic field. The several elements of leakage flux are elements of the main flux diverted from their normal path. The principle of superposition enables one to consider them as separate independent

quantities if saturation is neglected. Saturation can be neglected in normal operation; however, in calculating starting performance a correction must be applied since the high current drawn by the motor during the starting period produces saturation in the tooth tips which has the effect of reducing the total leakage reactance.

A common method of analysis is to divide the leakage flux into components based upon the path followed. The resulting leakage reactance is considered to be composed of six distinct components:

1. The stator-slot reactance
2. The rotor-slot reactance
3. The zigzag reactance
4. The skew reactance
5. The belt leakage reactance
6. The coil-end leakage reactance

Some of the leakage flux paths are indicated in Figure 18. The flux represented by the solid line which crosses the air gap and interlinks with the rotor winding is the useful flux. This flux produces the useful output of the motor. It is produced by the resultant mmf of the three phases (in a three-phase machine). The stator flux crossing the slots, ϕ_s, is called the slot leakage flux. The stator flux crossing the air gap and completing its path through the tips of the rotor teeth is called the tooth-tip or zigzag leakage flux and is indicated as ϕ_z. The name zigzag is used because it

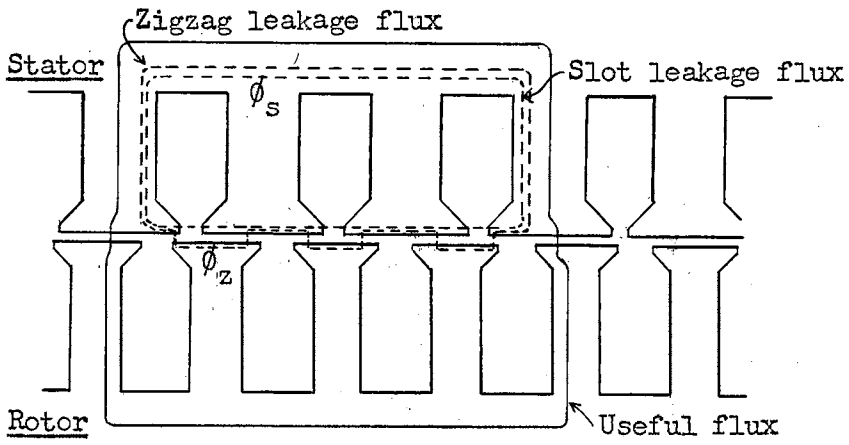

Figure 18. Some of the leakage flux paths in an induction motor.

designates the path the tooth-tip leakage flux may follow for a stator with more than one slot per pole per phase, i.e., flux considered to be due to the magnetizing action of a belt of conductors occupying consecutive slots. There is also a flux surrounding the coil-end connections, in other words, that portion of the coil which lies outside of the core. Flux taking this path is called the coil-end leakage flux. Similar leakage flux paths exist for the rotor.

Sometimes the slots of either the rotor or stator are twisted or skewed rather than arranged parallel to the shaft. The variation in flux density caused by the skewed slots results in a reduction in the total flux linkages. This result is an effect equivalent to a leakage flux and appears as an increase in the zigzag reactance. It is convenient to add it as an extra term to the formula for zigzag reactance. In practice, skewing adds very little to the standstill reactance

at rated voltage because it is limited by magnetic saturation of the rotor and stator teeth. At low currents it does cause an increase in the reactance. In this analysis the increased reactance due to skewing will be omitted; if desired, it can easily be taken into account through an increase in the zig-zag reactance.

Another leakage is present in the wound-rotor induction motor. The windings of the stator and rotor have distribution. The rotor can assume positions where the phase belts of the two windings do not coincide. Because of the displacement of the two windings, the field is different for any given position of the rotor and will result in positive and negative flux loops in the air gap of a pole face. The resultant flux linkages with the rotor winding produce voltages that cancel out in the rotor. In the stator, however, because of the relative position of the winding and the flux distribution, only partial neutralization occurs, resulting in a net voltage. In other words, the resultant flux, through linking both windings, acts as though it were a leakage flux in that it induces a resultant voltage in one winding and not in the other. This effect may be treated as a true leakage flux and is referred to as the belt leakage flux, or, as named by some investigators, the differential leakage flux. The belt leakage reactance is equal to zero for motors with squirrel-cage rotor windings since a squirrel-cage winding has no phase belts.

CALCULATION OF LEAKAGE REACTANCE

Many methods have been proposed for calculating the components of leakage reactance. Certain of the leakage flux components can be computed accurately from the various dimensions and other data of a given machine; the other components are found from empirical formulas. The method of calculation will more than likely differ from one design office to another, but, in general, the results are in close agreement.

Lloyd, Giusti, and Chang[5] have compared six of the existing methods of calculating the slot, zigzag, and coil-end leakage reactances for a sample motor. The results are summarized in Table VI.

The comparison in Table VI is for only one sample motor. The author has used some of these methods and others concluding that Adams' Method gives the best results. This might possibly be concluded from examining the numerical values in Table VI since Adams' Method gives near average values; however, more information would have to be known and more sample motors studied before drawing a definite conclusion. Since Adams' Method has been found to give good results by the author, it will be used here for all leakage reactance calculations.

To better acquaint the reader with Adams' Method, a detailed analysis of his scheme for calculating the leakage

---

[5]T. C. Lloyd, V. F. Giusti, and S. S. L. Chang, "Reactances of Squirrel-Cage Induction Motors," Transactions of the American Institute of Electrical Engineers, LXVI (1947), 1349-1355.

TABLE VI[6]

LEAKAGE REACTANCE OF SAMPLE MOTOR BY VARIOUS METHODS

	R.&M.	Adams	Kuhlmann	Gray	Arnold	Punga Raydt
X Slot	1.400	1.233	1.180	1.238	Stator 0.845 Rotor 0.335	1.178
Pitch Correction	0.863	0.860	0.835	0.884	0.86	none given
Final	1.21	1.06	0.985	1.094	1.06	1.178
X Zigzag	1.31	1.278	1.047	1.15	* ** 1.046 0.988 0.574 0.474	1.100
Pitch Correction	0.822	0.845	none given	0.884	0.845	none given
Final	1.08	1.08	1.047	1.018	1.460 1.309	1.100
X End	1.365	1.21	1.06	1.465	1.156	0.592
Pitch Correction	0.725	0.71	0.835	0.889	none given	none given
Final	0.99	0.861	0.880	1.295	1.156	0.592
X (total)	3.28	3.001	2.920	3.407	3.676 3.525	2.870

*Arnold's exact method is multiplied by 2 as per Punga.
**Arnold's approximate method.

reactance is given below. The basis of this analysis is three articles[7,8,9] in which Adams originally presented his method

[6]Ibid., p. 1352.

[7]C. A. Adams, "The Leakage Reactance of Induction Motors," Transactions of the International Electrical Congress, St. Louis, 1904, I (1905), 706-728.

[8]Adams, "Design of Induction Motors," pp. 660-670.

[9]Adams, Cabot, and Irving, pp. 1485-1503.

and additional information from articles by Alger[10] and Lloyd.[11]

Slot Reactance. A unit length of stator slot will be used in calculating the stator-slot reactance.

Referring to Figure 19, and assuming that the slot leakage flux passes straight across the slot and completes its path through iron of negligible reluctance, one can see that the slot flux linkages are made up of four different parts:

1. The flux crossing the slot opening, and linking with all the conductors in the slot. This is measured by

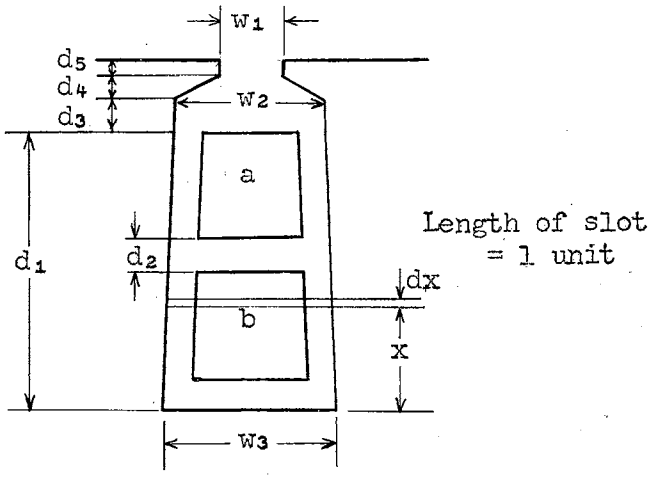

Figure 19. Slot leakage.

---

[10]Philip L. Alger, The Nature of Polyphase Induction Machines (New York, 1951), Chapt. 7.

[11]Lloyd, Giusti, and Chang, "Reactances of Squirrel-Cage Induction Motors."

the ratio of depth to width of the opening. The permeance of this path is

$$\mathcal{P}_1 = \frac{\text{area}}{\text{length}} = \frac{d_5}{w_1} \tag{73}$$

2. The flux crossing the tapered neck of the slot which also links all of the conductors in the slot. This is measured by the integral of the depth over width ratio, or

$$\mathcal{P}_2 = \int_0^{d_4} \frac{d_4\, dx}{(d_4 - x)w_2 + xw_1} = \frac{-d_4}{w_2 - w_1} \ln \left[(d_4 - x)w_2 + xw_1\right]_0^{d_4}$$

$$= \frac{d_4}{w_2 - w_1} \ln \frac{w_2}{w_1} \tag{74}$$

If x is small,

$$\ln (1 + x) = x - \frac{x^2}{2} + \ldots = \frac{x}{1 + \frac{x}{2}} + \ldots$$

Then Equation (74) can be written as

$$\mathcal{P}_2 = \frac{d_4}{w_2 - w_1} \ln \frac{w_2}{w_1} = \frac{2\, d_4}{w_2 + w_1} \tag{75}$$

approximately.

3. The flux crossing the slot above the top of the coil, linking all the conductors in the slot. The permeance is

$$\mathcal{P}_3 = \frac{d_3}{w_2} \tag{76}$$

4. The flux crossing the body of the slot, and linking only a part of the conductors. If the slot is tapered as shown in Figure 19, let $w_3 = w_2(1 + e)$. The slot width at

height x from the bottom of the slot is

$$\frac{(d_1 - x)\, w_3 + x\, w_2}{d_1} = w_2 \left[1 + \frac{(d_1 - x)\, e}{d_1}\right] \qquad (77)$$

The fraction of the total slot current below x, which establishes and is linked by the flux at this point, is

$$\frac{x\left[(2d_1 - x)\, w_3 + x\, w_2\right]}{d_1^2\,(w_2 + w_3)} = \frac{x\left[1 + \frac{(2d_1 - x)\, e}{2d_1}\right]}{d_1\,(1 + \frac{e}{2})}$$

$$= \frac{x}{d_1}\left[1 + \frac{(d_1 - x)e}{2d_1}\right] \qquad (78)$$

approximately.

The permeance corresponding to the total linkages is

$$\mathcal{P}_4 = \int_0^{d_1} \frac{x^2 \left[1 + \frac{(d_1 - x)\, e}{2d_1}\right]^2 dx}{d_1^2\, w_2 \left[1 + \frac{(d_1 - x)\, e}{d_1}\right]}$$

$$= \int_0^{d_1} \frac{x^2\, dx}{d_1^2 w_2} = \frac{d_1}{3w_2} \qquad (79)$$

approximately.

Thus, if terms of the order of e^2 and higher are neglected, the linkages of a tapered slot are just the same as those of a slot of uniform width, w_2.

The sum of the four parts; Equations (73), (75), (76), and (79); gives the total slot permeance for one unit length of slot as

$$\mathcal{P} = \mathcal{P}_1 + \mathcal{P}_2 + \mathcal{P}_3 + \mathcal{P}_4 = \frac{d_1}{3w_2} + \frac{d_3}{w_2} + \frac{2d_4}{w_1 + w_2} + \frac{d_5}{d_1} \qquad (80)$$

If d_2 is large, a corrective term, $d_2/12w_2$, should be

subtracted from Equation (80) since the flux crossing the slot between the two coil sides is produced by, and links, only half the conductors.

Ohm's law for magnetic circuits (cgs system of units) is

$$\phi = \mathcal{F}\mathcal{P} \tag{81}$$

where

ϕ = the flux in maxwells

$\mathcal{F}$ = the magnetomotive force

$\mathcal{P}$ = the permeance = $\frac{\text{area of path in cm}}{\text{length of path in cm}}$ (for air)

The magnetomotive force is

$$\mathcal{F} = 0.4\,\pi\,NI \tag{82}$$

in which

N = the number of turns

I = the current in amperes

Substitution of Equation (82) into Equation (81) yields

$$\phi = 0.4\,\pi\,NI\,\mathcal{P} \tag{83}$$

Multiplication by N gives an equation for the interlinkages,

$$\psi = N\,\phi = 0.4\,\pi\,N^2 I\,\mathcal{P} \tag{84}$$

The induction is found by dividing by $I \times 10^8$,

$$L = \frac{N\,\phi}{I \times 10^8} = 0.4\,\pi\,N^2\,\mathcal{P} \times 10^{-8} \text{ henrys} \tag{85}$$

Substituting Equation (80) into Equation (85), converting the units of measure to inches, and letting C_s equal the number of series conductors per slot, one finds that the inductance per inch of any one stator slot is

$$L'_{si} = 0.4\ \pi\ 2.54\ C_s^2\ \left(\frac{d_1}{3w_2} + \frac{d_3}{w_2} + \frac{2d_4}{w_1+w_2} + \frac{d_5}{d_1}\right) 10^{-8}$$

$$= 3.2 \times 10^{-8}\ C_s^2\ \left(\frac{d_1}{3w_2} + \frac{d_3}{w_2} + \frac{2d_4}{w_1+w_2} + \frac{d_5}{d_1}\right) \qquad (86)$$

The corresponding reactance per inch of stator slot is

$$X'_{si} = 2\pi f L_{si} = 20.1 \times 10^{-8} f\ C_s^2\ \left(\frac{d_1}{3w_2} + \frac{d_3}{w_2} + \frac{2d_4}{w_1+w_2} + \frac{d_5}{d_1}\right) \qquad (87)$$

The term in parentheses in Equations (86) and (87) is called the slot constant and is designated by K_s. It expresses the effective linkages per inch of stack per ampere. With the notation

$$K_s = \left(\frac{d_1}{3w_2} + \frac{d_3}{w_2} + \frac{2d_4}{w_1+w_2} + \frac{d_5}{d_1}\right) \qquad (88)$$

Equation (86) becomes

$$L'_{si} = 3.2 \times 10^{-8}\ C_s^2\ K_s \qquad (89)$$

and Equation (87) becomes

$$X'_{si} = 20.1 \times 10^{-8} f\ C_s^2\ K_s \qquad (90)$$

The value of the slot constant, K_s, can be calculated for all practical conditions of slot shape. The most notable work in calculating slot constants is an article by Puchstein[12] in which he derives formulas for elliptical, rectangular, and trapezoidal slots with rectangular shape or with one or both ends of semicircular shape. Flux plotting techniques may also

---

[12] A. F. Puchstein, "Calculation of Slot Constants," Transactions of the American Institute of Electrical Engineers, LXVI (1947), 1315-1322.

be used to determine the slot constant. Once a line of punchings has been standardized by a manufacturer, it would be relatively easy to fix, by flux plotting methods, the effective leakage flux lines per inch per ampere for each punching, essentially a slot constant for each punching. Designers have not made much use of flux plotting techniques, apparently preferring to rely on formulas. The reader interested in flux plotting techniques will find of value books by Moore[13] and Johnson.[14] The leakage flux paths can also be found from water-trough experiments.[15]

The above equations for inductance and reactance assume a full-pitch winding with the conductors all in series, carrying currents in the same phase relationship. If a double-layer winding of full pitch is used, the above formulas are adequate. If fractional-pitch windings are used, there is a reduction in the slot reactance. A correction, developed by Adams,[16] must be applied to Equations (89) and (90) to take into account the use of fractional-pitch windings. This correction can be read from Figure 20; it is called the slot-

---

[13]A. D. Moore, Fundamentals of Electrical Design (New York, 1927), Chapter 4 and following.

[14]Walter C. Johnson, Mathematical and Physical Principles of Engineering Analysis (New York, 1944), pp. 317-331, 335-336.

[15]John F. H. Douglas, "The Reluctance of Some Irregular Magnetic Fields," Transactions of the American Institute of Electrical Engineers, XXXIV (June, 1915), 1067-1125.

[16]Adams, Cabot, and Irving, pp. 1485-1503.

leakage pitch factor, k_{sp}. For a pitch of not less than 70 per cent, the factor $(0.625\ p_f + 0.375)$ can be used instead, where p_f is the pitch expressed as a decimal fraction.

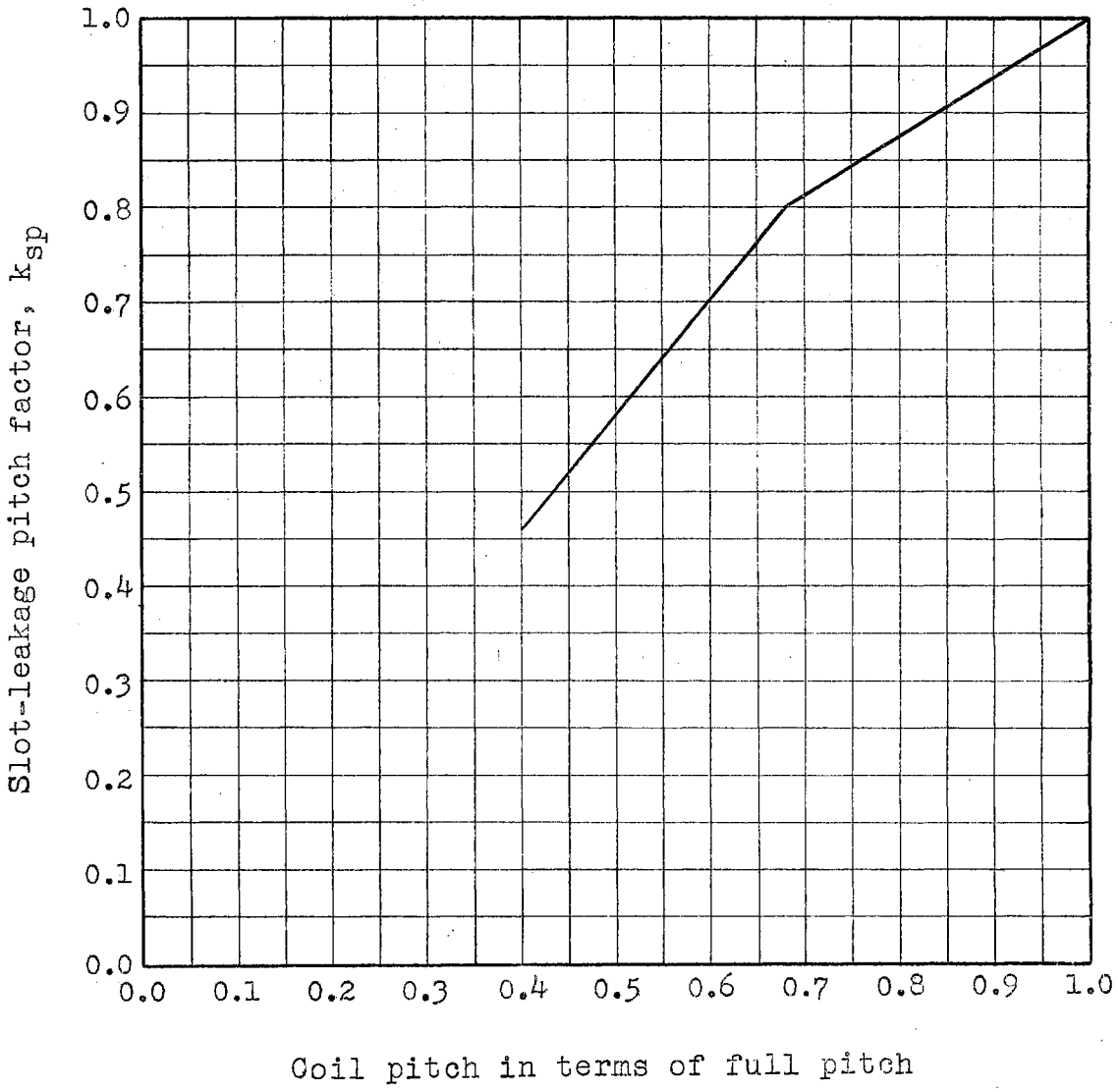

Figure 20.[17] Adams' correction for slot-leakage reactance as a function of pitch.

[17] Ibid., p. 1491.

The stator-slot leakage inductance and reactance can then be written in the more general form of

$$L'_{si} = 3.2 \times 10^{-8} C_s^2 K_s k_{sp} \qquad (91)$$

$$X'_{si} = 20.1 \times 10^{-8} f C_s^2 K_s k_{sp} \qquad (92)$$

where k_{sp} is the necessary slot correction factor, dependent on the pitch.

The equations for the stator-slot inductance and reactance are for a one-inch length of stator slot. The equations can be modified so as to express the inductance and reactance in many different ways. For example, for a total of S_1 slots, or S_1/n slots per phase on the stator, the total reactance per phase per inch of stack is

$$X'_{spi} = 2\pi f \frac{S_1}{n} (3.2 C_s^2 K_s k_{sp} \times 10^{-8}) \qquad (93)$$

If the total series conductors per phase are C, then

$$C_s = C \frac{n}{S_1} \qquad (94)$$

and the reactance of each phase winding for L inches of stack is

$$X'_{sp} = 2\pi f C^2 \frac{n}{S_1} L (3.2 K_s k_{sp} \times 10^{-8}) \qquad (95)$$

For the purpose of this investigation, it is necessary to express this reactance as a per-unit value which enables one to deal with a general rather than a specific machine. Letting C_i equal the number of conductors per inch of periphery, then the number of slots per inch of periphery is C_i/C_s, and the total slot width per inch of periphery is

$$w = \frac{C_i}{C_s} w_2 \tag{96}$$

This is also the ratio of the slot width to tooth pitch.

Since there are q_T/C_i torque-amperes per conductor, the reactance emf per inch of slot is

$$E'_{xsi} = 2 \pi f (3.2 C_s^2 K_s k_{sp} \times 10^{-8}) \frac{q_T}{C_i}$$

$$= 20.1 \times 10^{-8} f C_s^2 K_s k_{sp} \frac{q_T}{C_i} \tag{97}$$

but, from Equation (96),

$$C_i = \frac{w C_s}{w_2}$$

hence

$$E'_{xsi} = 20.1 \times 10^{-8} f C_s K_s k_{sp} \frac{w_2}{w} q_T \tag{98}$$

There will be induced in the same conductors by the gap flux an emf per inch of slot of

$$E_{1i} = \frac{12}{\sqrt{2}} \times 10^{-8} k_w v B_g C_s \tag{99}$$

From Equations (98) and (99), the reactance emf of slot leakage in terms of the induced emf (per-unit value) is

$$x'_s = \frac{E'_{xsi}}{E_{1i}} = 2.37 \frac{K_s k_{sp} w_2}{k_w w} \frac{f q_T}{v B_g} \tag{100}$$

The same procedure is followed in calculating the rotor-slot reactance. To express this reactance in stator terms, it is necessary only to multiply the permeance ratio for the rotor by the ratio of the squares of stator and rotor winding factors and by the ratio of stator to rotor slots. This relation follows from the fact that, for equal and opposite

mmfs in stator and rotor, the product of the number of slots times the effective amperes per slot must be the same on both sides, and that the actual amperes per slot are the effective amperes divided by the winding factor, k_w, for each winding.

Thus, the rotor-slot reactance in stator terms is, from Equation (95),

$$a^2X''_{sp} = 2\pi f\, C^2\, \frac{n}{S_1} L \left[3.2 \times 10^{-8} (K''_s k''_{sp}\ \frac{S_1}{S_2}\ \frac{k^2_{w1}}{k^2_{w2}})\right]$$

$$= 2\pi f\, C^2\, nL \left[3.2 \times 10^{-8}\ (\frac{K''_s k''_{sp}}{S_2}\ \frac{k^2_{w1}}{k^2_{w2}})\right] \qquad (101)$$

For a squirrel-cage winding, $k_{w2} = k_{p2}\, k_{d2} = 1$, since the pitch and distribution factors are unity, and the slot-leakage pitch factor equals one.

Then, for a squirrel-cage rotor, the slot reactance in ohms per phase in stator terms is

$$a^2X''_{sp} = 2\pi f\, C^2\, nL \left[3.2 \times 10^{-8}\, k^2_{w1}\, (\frac{K''_s}{S_2})\right] \qquad (102)$$

In this equation, note the absence of any winding factor for the rotor, because a squirrel-cage rotor has full pitch. Hence, no Adams' slot-leakage pitch factor is needed for the squirrel-cage rotor. Instead, the square of the winding factor of the stator is a fundamental part of the derivation. For convenience, it is assumed that the square of the winding factor for the stator, k^2_{w1}, is equivalent to the Adams' pitch correction.

With a squirrel-cage rotor, the expressions for the slot leakage reactance of the stator and rotor can be combined to give the total equivalent slot reactance in ohms per phase (in stator terms) as

$$X_{se} = X'_{sp} + a^2 X''_{sp}$$

$$= 2 \pi f C_s^2 n L \left[3.2 \times 10^{-8} \left(\frac{K'_s}{S_1} + \frac{K''_s}{S_2}\right) k'_{sp}\right] \quad (103)$$

where the single-primed values concern the stator and the double-primed values concern the rotor.

A comparison of Equations (103) and (100) shows that the total slot reactance as a per-unit value can be written as

$$x_s = 2.37 \left(\frac{K'_s k'_{sp}}{k'_w} \frac{w'^2_2}{w'} + \frac{K''_s k'_{sp}}{k'_w} \frac{w''^2_2}{w''}\right) \frac{f q_T}{v B_g} \quad (104)$$

If the motor has a wound rotor, the second term within the parentheses must be divided by the square of the winding factor of the rotor and multiplied by the rotor slot-leakage pitch factor. As mentioned above, for convenience, the square of the winding factor is generally taken as the Adams' pitch correction. If this is done, then Equation (104) also applies to a wound-rotor induction motor.

Zigzag Reactance. Leakage flux, such as ϕ_t in Figure 21, which crosses the air gap and completes its path through the opposite tooth tip which bridges the slot in question, is called the tooth-tip or zigzag leakage. As pointed out previously, the origin of the latter designation is the zigzag path,

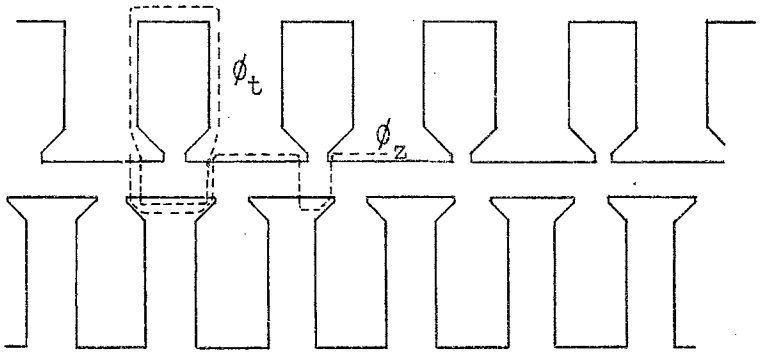

Figure 21. Partial diagram of tooth-tip or zigzag leakage paths.

ϕ_z, that may be followed by flux considered to be due to the magnetizing action of a belt of conductors occupying consecutive slots. The permeance of this path varies with the relative position of the stator and rotor teeth, and can be readily calculated for any and all positions of the rotor. This leakage, like the slot leakage, is purely a distortional flux.

Referring to Figure 22, assume that the stator and rotor have the same tooth pitch, λ , t_1 is the width of the stator tooth tip plus an allowance for fringing of the flux, and t_2 is the same for the rotor. At the instant represented, x represents the displacement of the center of a rotor tooth from the center of a stator slot opening. Consider the series reluctance from t_1 to t_2 and back to the next stator tooth

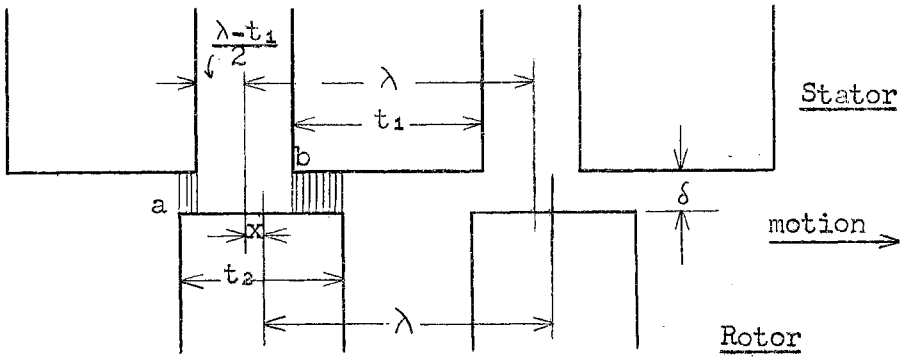

Figure 22. Zigzag leakage flux.

tip, neglecting the reluctance of the iron part of the magnetic circuit. The series reluctance takes account of the total tooth-tip or zigzag leakage, primary and secondary. Taking the flux paths as straight across the gap, the reluctance in the air gap will be the sum of two parts, corresponding to the two overlapping portions shown in the figure.

The overlap on the left is

$$\frac{t_2}{2} - \frac{\lambda-t_1}{2} - x = \lambda\left(\frac{t_1+t_2}{2\lambda} - \frac{1}{2}\right) - x = m - x \qquad (105)$$

The overlap on the right is

$$m + x \qquad (106)$$

If all dimensions are in centimeters, the total reluctance per centimeter length of core is

$$\mathcal{R} = \frac{\delta}{m-x} + \frac{\delta}{m+x} = \frac{2\,m\,\delta}{m^2-x^2} \qquad (107)$$

and the permeance is then

$$\mathcal{P} = \frac{1}{\mathcal{R}} = \frac{m^2 - x^2}{2m\,\delta} \tag{108}$$

Converting the units of measure to inches, one obtains

$$\mathcal{P} = 2.54\ \frac{m^2 - x^2}{2m\,\delta} \tag{109}$$

Considering the permeance as a function of x, it is seen that the permeance falls from $\mathcal{P} = m/2\delta$ when $x = 0$, to $\mathcal{P} = 0$ when $x = m$; thereafter the permeance remains at a value of zero until the point a (Figure 22) is aligned with point b, then a new rotor tooth to the left of a comes into play and the function repeats itself in reverse order until a complete tooth pitch has been included. The mean value of the permeance for a one-inch length of stator slot is therefore

$$\mathcal{P}_{zi} = \frac{1}{\lambda/2}\int_{x=0}^{x=m} 2.54\ \frac{m^2 - x^2}{2m\,\delta}\,dx = 1.693\ \frac{m^2}{\lambda\delta} \tag{110}$$

This derivation assumes that the tooth pitches of both stator and rotor are the same. If they are not the same, and in most designs they are not equal, their average value may be substituted for λ.

From Equation (110), one can compute the zigzag flux linking the conductors in a slot and the linkages for the winding as a whole.

Since the permeance of the path is known, the zigzag inductance per inch of slot (conductors in series) can be found by substituting Equation (110) into Equation (85), giving

$$L_{zi} = \frac{0.4\pi C_s^2}{10^8} \rho_{zi} = 2.13 \frac{m^2}{\lambda} C_s^2 \times 10^{-8} \qquad (111)$$

From Equation (105),

$$m = \lambda\left(\frac{t_1 + t_2}{2\lambda} - \frac{1}{2}\right) \qquad (112)$$

Substituting for t_1/λ and t_2/λ [see Equation (63)] gives

$$m = \lambda\left(\frac{a_1 + a_2}{2} - \frac{1}{2}\right) \qquad (113)$$

Equation (111) can then be written as

$$L_{zi} = 2.13 \frac{\lambda}{\delta} C_s^2 \left(\frac{a_1 + a_2}{2} - \frac{1}{2}\right)^2 \times 10^{-8} = \frac{\lambda}{\delta} C_s^2 A \times 10^{-8} \qquad (114)$$

where

$$A = 2.13\left(\frac{a_1 + a_2}{2} - \frac{1}{2}\right)^2 \qquad (115)$$

The quantity A, called the gap constant, is plotted against $(a_1 + a_2)/2$ in Figure 23.

The corresponding zigzag reactance per inch of slot is

$$X_{zi} = 2\pi f L_{zi} = 2\pi f \frac{\lambda}{\delta} C_s^2 A \times 10^{-8} \qquad (116)$$

The zigzag reactance emf per inch of slot due to the full-load torque current is

$$I_T X_{zi} = \frac{2\pi f q_T C_s^2 \lambda A}{10^8 C_i \delta} \qquad (116)$$

Since

$$\frac{C_i}{C_s} = \frac{1}{\lambda} \qquad (118)$$

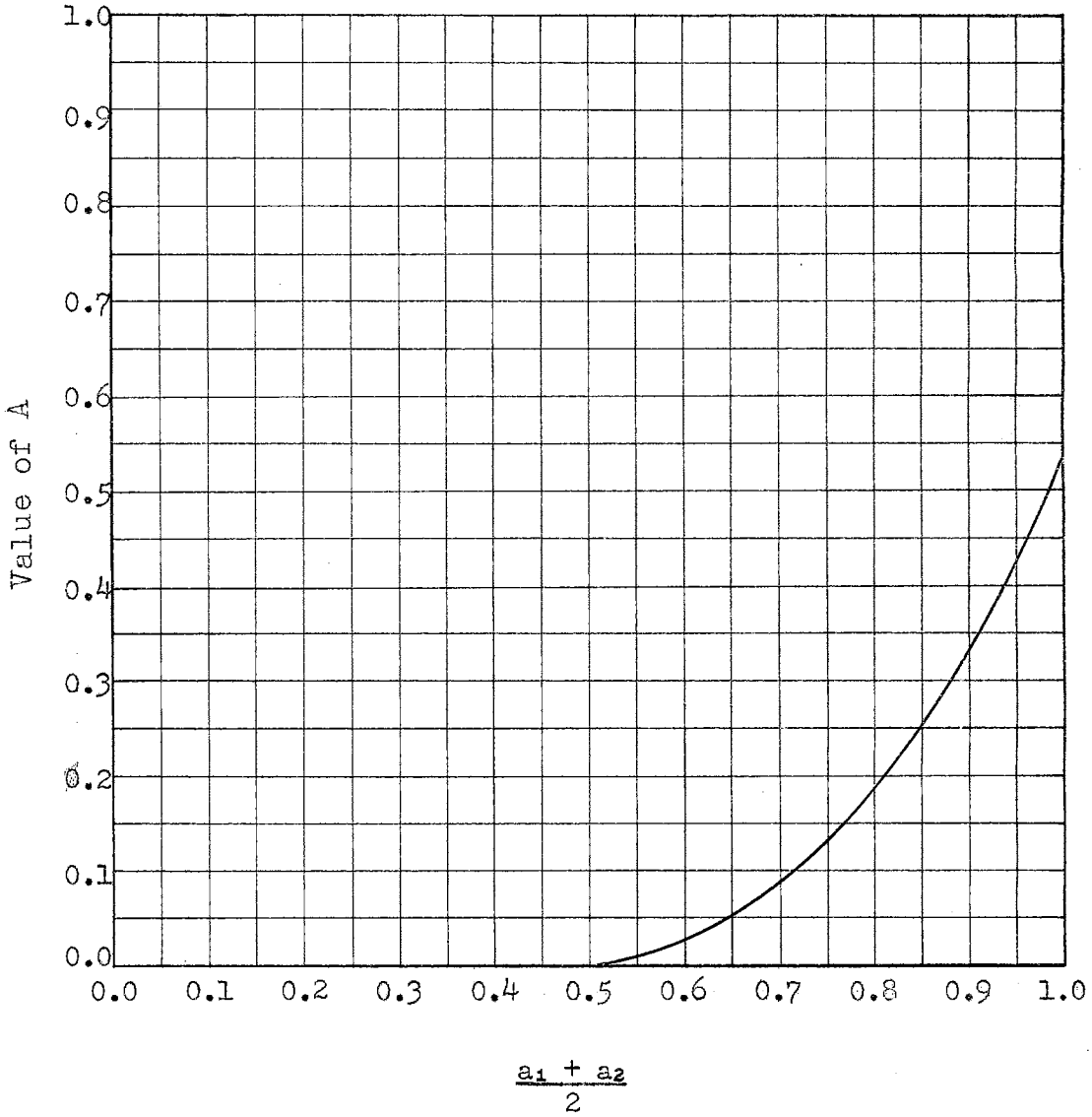

Figure 23. Gap constant, A.

Equation (117) can be written as

$$I_T X_{Zi} = \frac{2\pi f \, q_T \, C_s^2 \, \lambda^2 \, A}{10^8 \, \delta} \qquad (119)$$

From Equation (99), the emf per inch of slot induced by the useful flux is

$$E_{li} = \frac{l2}{\sqrt{2}} k_w \, v \, B_g \, C_s \times 10^{-8} \tag{99}$$

When Equation (119) is divided by (99), the per-unit value of zigzag reactance is found to be

$$x_z = \frac{I_T X_{zi}}{E_{li}} = 0.74 \, \frac{q_T \, f \, \lambda^2 \, A}{k_w \, \delta \, v \, B_g} \tag{120}$$

If S_p is the number of slots per pole,

$$\lambda = \frac{6v}{fS_p} \tag{121}$$

and Equation (120) can be written as

$$x_z = 26.7 \, \frac{q_T \, v \, A}{k_w \, B_g \, f \, \delta \, S_p^2} \tag{122}$$

It is necessary to apply a correction to Equation (122) if the winding is of fractional pitch. This correction, k_{zp}, developed by Adams, can be obtained from Figure 24, or, for a pitch of not less than 70 per cent, the factor $(0.8p_f + 0.2)$ can be used instead. With this correction, Equation (122) becomes

$$x_z = 26.7 \, \frac{q_T \, v \quad A}{k_w \, B_g \, f \, \delta \, S_p^2} \, k_{zp} \tag{123}$$

where

k_{zp} = the zigzag-leakage pitch factor

As noted previously, this equation takes into account the total zigzag leakage for both stator and rotor.

For a wound-rotor motor, the number of slots per pole in this equation should be taken as the average of the values for the stator and the rotor.

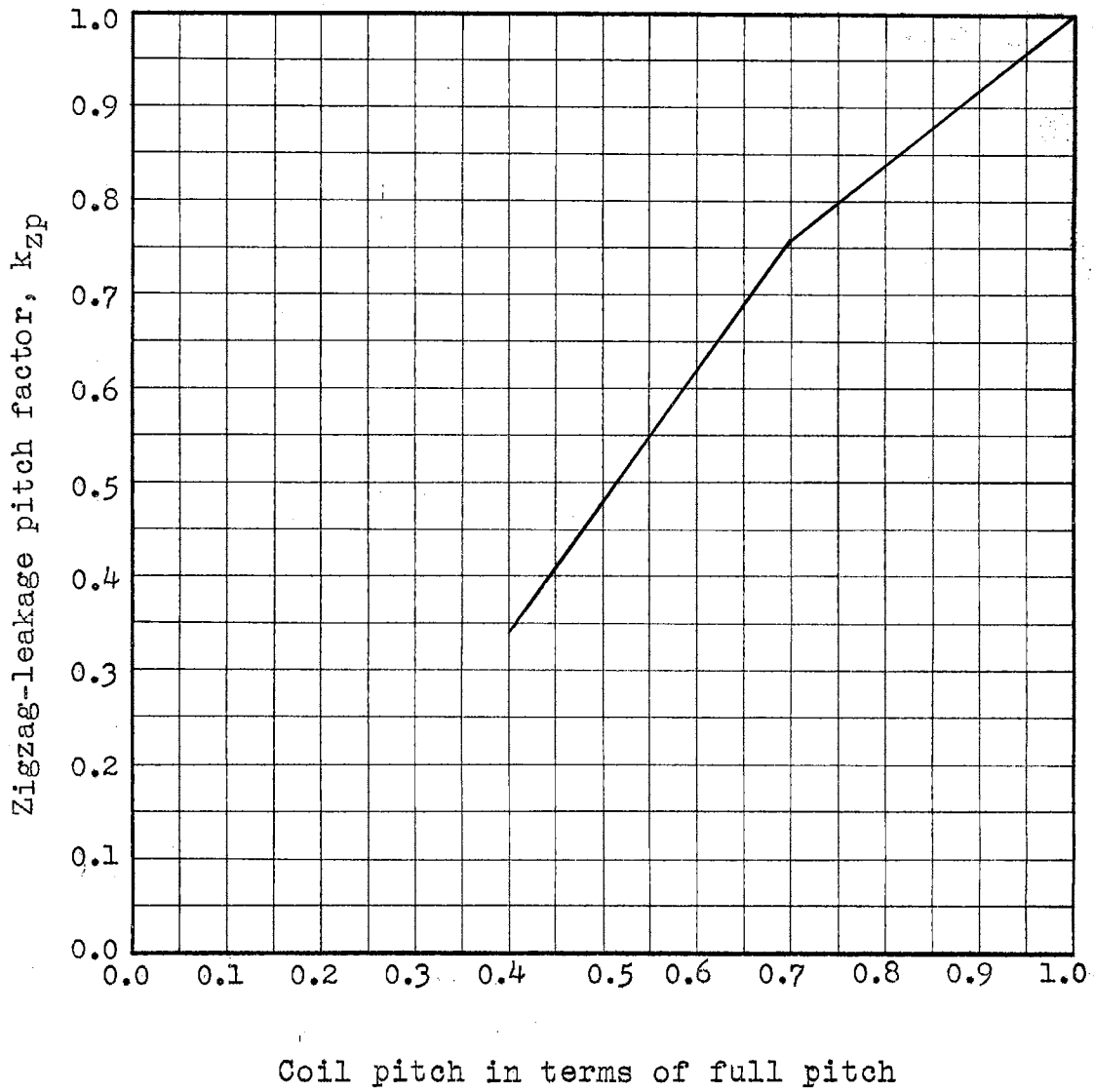

Figure 24.[18] Adams' correction for zigzag leakage reactance as a function of pitch.

Coil-End Leakage Reactance. The leakage around the coil ends is the most difficult element to calculate. These

[18] Ibid., p. 1491.

fluxes are caused by the mmf of the end turns of the winding, acting principally on air paths. In linking the end-turn conductors, reactance voltages are generated which are reflected as ohmic reactance in the stator and rotor windings. Because the end-turn leakage flux paths are almost all, if not totally, in air, it is unaffected by magnetic saturation, and the inductance of the end turn is practically constant for wide ranges of machine excitation. In some cases, magnetic structures, such as the machine frame and air deflecting baffles, are close to the coil ends and cause an increase in the end-turn leakage flux.

The geometry of the coil cross-section will affect the flux linking the coil for a given current flowing in it. The shape of the end portions of the coils will also affect its reactance. On most windings, the coil extends straight out of the core for a short distance before it is bent at an angle to proceed to the next pole. The flux linkages of this straight portion will be different from those elsewhere in the end connection.

Adams applied the work of several others toward the development of a practical end-turn reactance solution. He viewed the two end portions of a stator or rotor coil as constituting a circular coil in air, and then applied rationally derived procedures to determine the inductance of the circular coils when they are arranged physically to simulate the coil-end pattern of the double-layer wound induction

machine stator or rotor. The method has been extended to the squirrel-cage rotor.

The flux per ampere per inch length of a circular coil, in air, with a rectangular section whose long side is not more than twice its short side and whose diagonal is not more than one-tenth of the diameter of the coil is

$$\phi_f' = 0.508 \ln \left(1.74 \frac{d_m'}{d_d'}\right) \tag{124}$$

where

d_m' = the mean diameter of the coil in inches

d_d' = the diagonal of the coil section in inches

If two similar coils, such as that described, are placed parallel to each other and at a distance apart which is small compared to their diameter, the mutual flux per ampere per inch of length is approximately

$$\phi_f = 0.482 \ln \left(1.74 \frac{d_m}{d_d}\right) \tag{125}$$

where

d_m = the common diameter in inches

d_d = the mean perpendicular distance between them in inches

When Equation (125) is applied to a motor winding to determine the equivalent flux per ampere per inch of free length of coil end, coil end is understood to include all the conductors of a phase-belt bundle, or the conductors per pole per phase. For the ordinary double-layer winding, d_m may be taken as seven-tenths of the pole pitch. Thus, for a

given shape of coil end, the flux per ampere per inch depends approximately upon the logarithm of the ratio of the pole pitch to the diagonal of the cross-section of a coil end. For a given type of winding, this ratio is fairly constant. For example, consider the rewinding of a given frame for double pole pitch and half frequency. The coil end, which includes all the conductors of one phase belt, will be twice as long and twice as broad as before, so that the ratio of pole pitch to the diagonal of the coil section, and the required logarithm, will be the same, or ϕ_f will be constant.

Let

$$c_3 = \lambda/L \tag{126}$$

and

c_f = ratio of free length (per conductor) to pole pitch (127)

Then

$c_3\, c_f$ = ratio of free length to active length (128)

Also, in a three-phase machine, there are

$$\frac{c_i \tau}{3} \text{ conductors per phase belt} \tag{129}$$

When Equations (125) and (129) are substituted into Equation (85), the inductance per free inch of belt (conductors in series) is found to be

$$L_{ci} = \phi_f \frac{c_i^2 \tau^2}{9} \times 10^{-8} \tag{130}$$

The corresponding reactance is

$$X_{ci} = 2\pi f \, \phi_f \, \frac{C_i^2 \, \tau^2}{9} \times 10^{-8} \qquad (131)$$

For every inch of active belt there are c_3 c_f inches [see Equation (128)] of free or idle belt; therefore, the reactance of the free belt per inch of active belt is

$$X_{ci} = 2\pi f \, \phi_f C_f \frac{\tau}{L} \frac{C_i^2 \, \tau^2}{9} \times 10^{-8} \qquad (132)$$

Since $I_T = q_T/C_i$ = the full-load torque-amperes per conductor, the reactance emf for the free length, per inch of active belt, is

$$I_T \, X_{ci} = 2\pi f \, \phi_f C_f \frac{\tau^3}{L} \frac{q_T C_i}{9} \times 10^{-8} \qquad (133)$$

This can be expressed as a per-unit value. The emf induced in one inch of active belt by the useful flux is

$$E_{1i} = \frac{12}{\sqrt{2}} k_w \frac{v \, B_g \, C_i \, \tau}{3} \times 10^{-8} \qquad (134)$$

hence

$$x_c = \frac{I_T X_{ci}}{E_{1i}} = 0.247 \, \phi_f C_f \frac{\tau^2 \, q_T \, f}{L \, k_w \, v \, B_g} \qquad (135)$$

For the stator and the rotor, in stator terms, Equation (135) becomes

$$x_c = 0.247 \, (\phi_f' \, C_f' + \phi_f'' \, C_f'') \frac{\tau^2}{L} \frac{q_T f}{k_w \, v \, B_g} \qquad (136)$$

If the value of ϕ_f is known for a full-pitch phase belt, the value for a fractional-pitch winding can be found by multiplying the full-pitch value by the proper correction factor, k_{cp}, given in Figure 25. This correction factor was

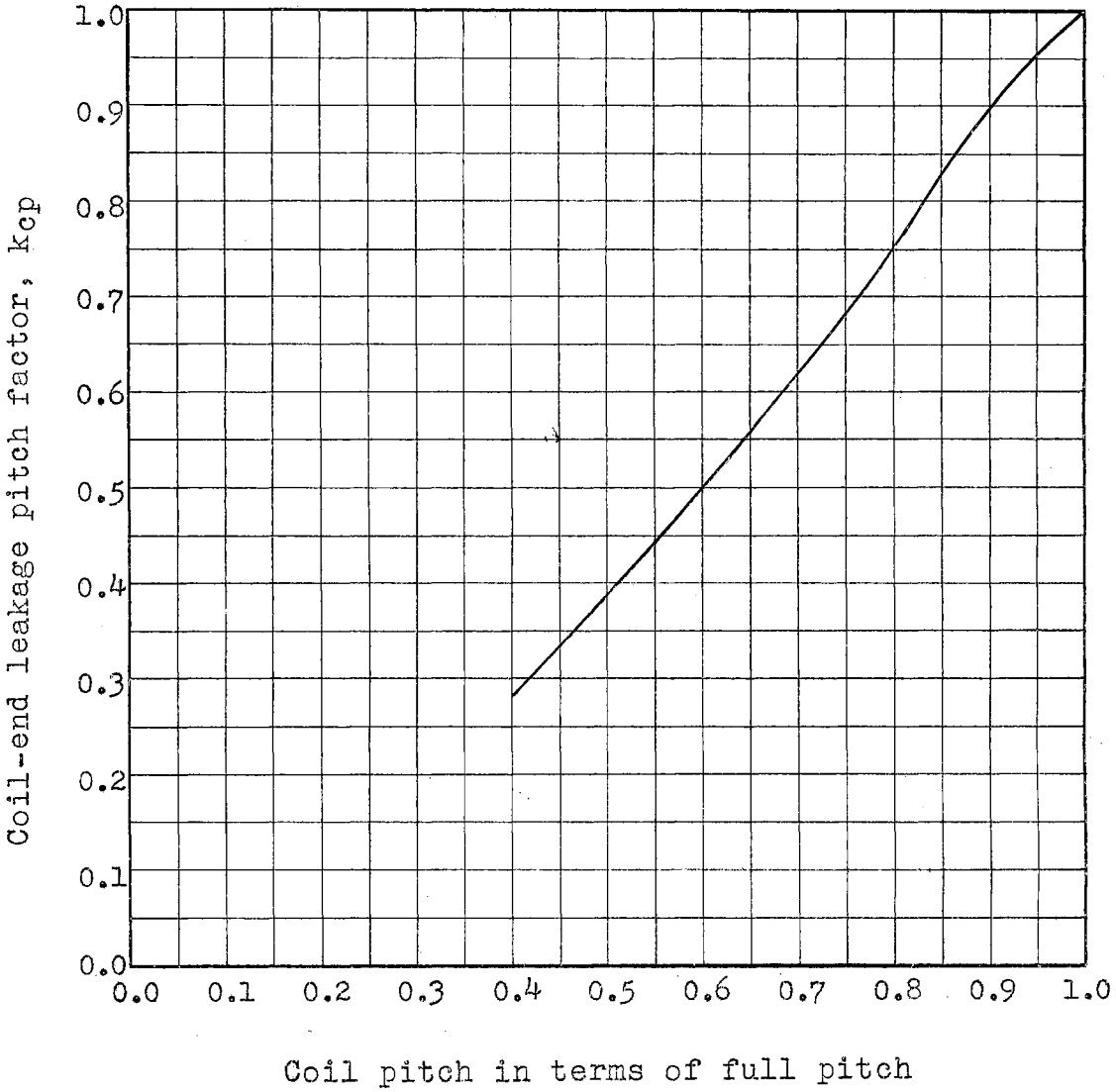

Figure 25[19] Adams' correction for the coil-end leakage reactance as a function of pitch.

developed by Adams; it is called the coil-end leakage pitch factor. With this factor, Equation (136) becomes

[19] Ibid., p. 1497.

$$x_c = 0.247\ (\phi'_f\ C'_f + \phi''_f\ C''_f)\ k_{cp}\ \frac{\tau^2}{L}\ \frac{q_T\ f}{k_w\ v\ B_g} \qquad (137)$$

Adams[20] has shown that, for the usual wound-rotor motor, the full-pitch value of ϕ_f in stator terms is about 1.14. The total value of ϕ_f in stator terms for a squirrel-cage motor with bars extending well out from the core is known to be about one or a little more, which is very close to the value for a wound-rotor motor.

Belt Leakage Reactance. To avoid repetition in the following discussion of belt leakage, consider that the rotor current frequently referred to is in stator terms.

When the stator and rotor are in the relative position shown in Figure 26a, the currents in the stator phase belts are exactly opposed by those in the rotor phase belts. Considering a three-phase motor, the starts of the windings are spaced 120 electrical degrees apart, and it may be seen from the corresponding vector diagram in Figure 26b that the currents in the three stator belts S_A, S_B, and S_C, and in the three rotor belts R_A, R_B, and R_C have 60-degree relationships.

When the stator and rotor are in the relative position indicated in Figure 26c, the currents in the stator and rotor phase belts have the phase relations shown in Figure 26d. Figure 26e is an enlargement of a portion of Figure 26c. The rotor belt R_C overlaps the stator belt S_C by a distance of mn and overlaps the stator belt S_B by a distance of np.

---

[20] Ibid., p. 1496.

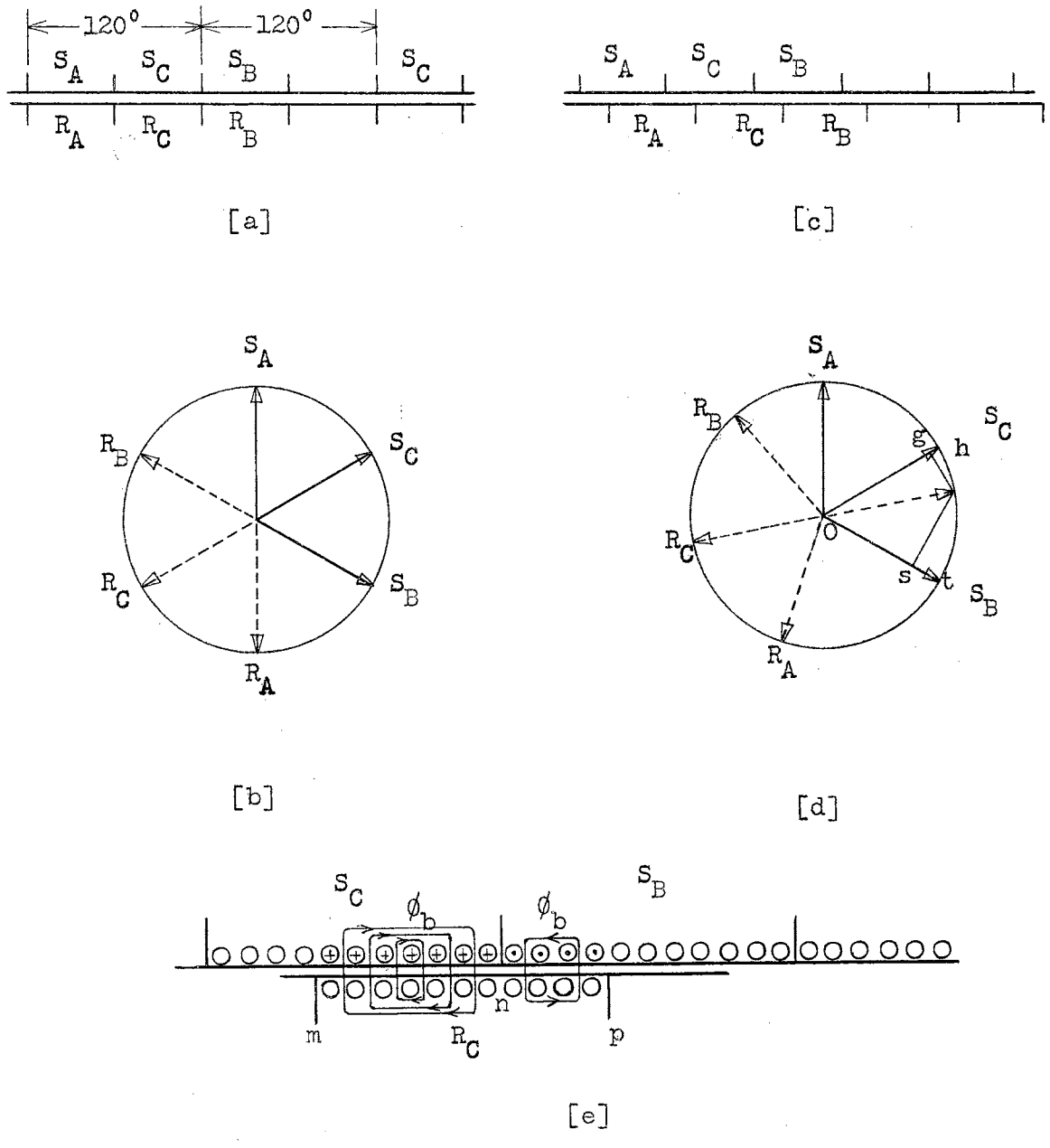

Figure 26. Belt leakage in a three-phase wound-rotor induction motor.

In the distance mn, the current in the stator conductors is S_C, Figure 26d, and that in the rotor conductors is R_C, of which the component Og opposes the stator current; the remaining part of this stator phase current, gh, is not opposed

by an equivalent rotor current and is represented by crosses in Figure 26e.

In the distance np, the current in the stator conductors is S_B, Figure 26d, and that in the rotor conductors is R_C, of which the component Os opposes the stator current; the remaining part of this stator phase current, st, is not opposed by an equivalent rotor current and is represented by dots in Figure 26e.

The currents represented by the crosses and dots in Figure 26e set up the flux ϕ_b, which is in phase with the current in the belt which it links and, therefore, produces the same effect as a leakage flux. This flux is called the belt leakage flux. This flux varies with the overlap of the phase belts, varying through one cycle while the rotor moves, relative to the stator, through the distance of one phase belt.

The belt leakage is of the same nature as the tooth-tip or zigzag leakage. The zigzag leakage takes account of the leakage over the individual slots, which does not link with any of the opposing current, while the belt leakage takes account of a similar flux which links with equal portions of both stator and rotor currents. Because the two leakage elements are of the same nature, one would expect to follow a similar procedure in calculating the belt leakage as is used in calculating the zigzag leakage. Since the procedure is the same and since the belt leakage is zero in a squirrel-cage motor and only of minor importance in the wound-rotor

motor, the mathematical derivation will be omitted. The reader is referred to Adams'[21] analysis for the derivation.

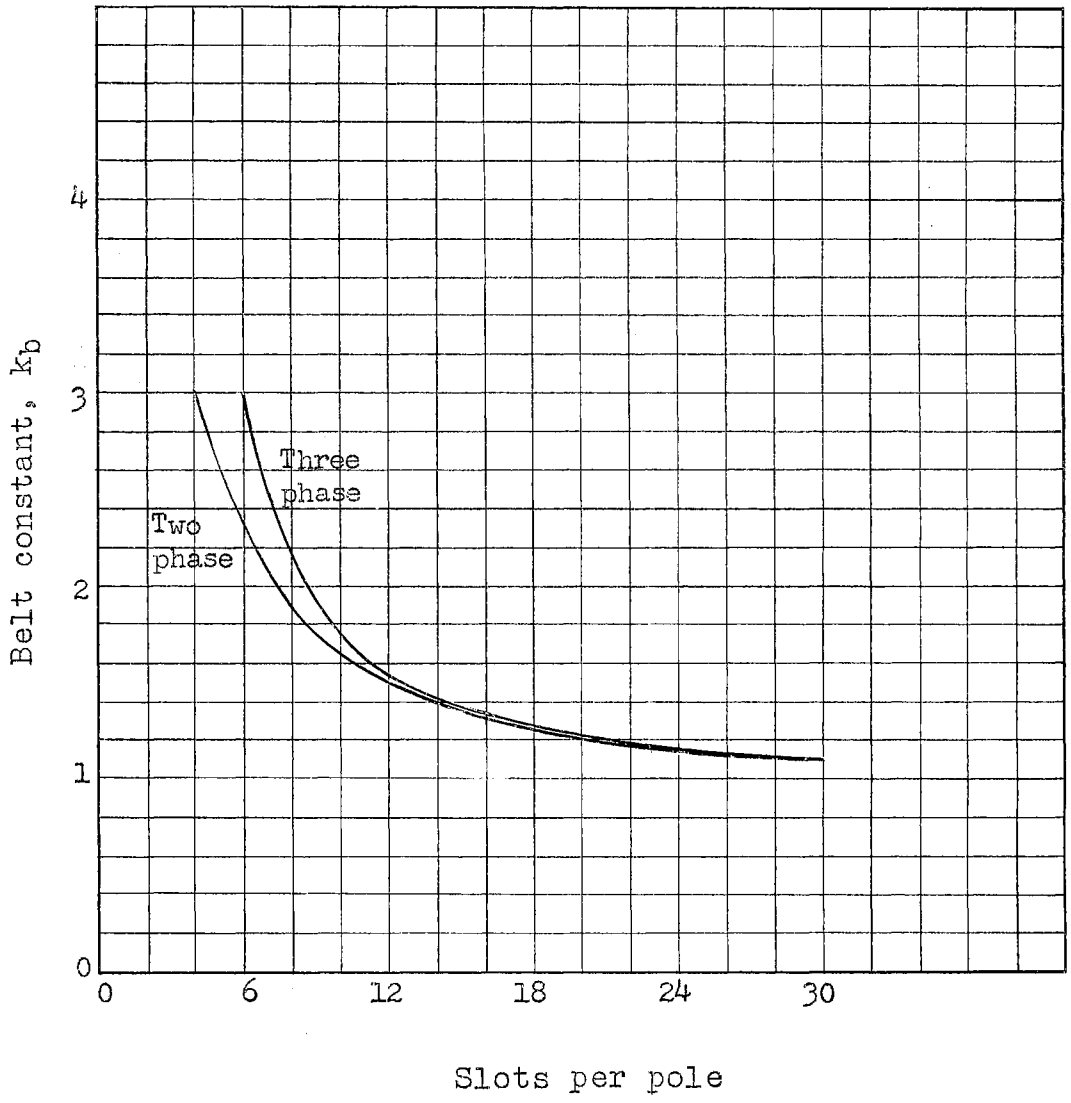

Figure 27.[22] Belt constant.

---

[21] Adams, "The Leakage Reactance of Induction Motors," pp. 711-715.

[22] I. E. Hanssen, "Leakage Reactance of Induction Motors," Electrical World, XLIX (March 30, 1907), 637.

His result, converted to a per-unit value, is

$$x_b = \frac{I_T X_{bi}}{E_{1i}} = 0.03 k_b K_1 K_2 \frac{q_T v}{\delta f B_g} \qquad (138)$$

where

k_b = a constant, called the belt constant, which depends upon the number of slots per pole

Values of the belt constant for two- and three-phase wound-rotor induction motors are given in Figure 27.

This equation includes the total belt leakage, stator and rotor.

CHAPTER V

SEPARATING THE COMPONENTS OF THE D^2L EQUATION FOR OPTIMUM MAXIMUM POWER FACTOR

From the quotations in Chapter II and other sources, it may be taken as axiomatic that a high maximum power factor is the first desideratum in polyphase induction motor design, and, secondly, that the cost shall be reasonable. This chapter is concerned with the subject of maximum power factor; the subject of cost will be considered in Chapter VI.

THE LEAKAGE COEFFICIENT

The maximum power factor of a polyphase induction motor can be related to the dimensions of the motor through the circle diagram.

Consider a circle of radius r with center at G as shown in Figure 28. Construct auxiliary lines as shown with HG parallel to OX.

From the geometry of the figure,

$$\measuredangle FHG = \measuredangle FOA \tag{139}$$

and

$$\measuredangle FGH = \measuredangle FOY \tag{140}$$

since angle FGH and angle FOY are complements of the same angle ($\measuredangle FOA$).

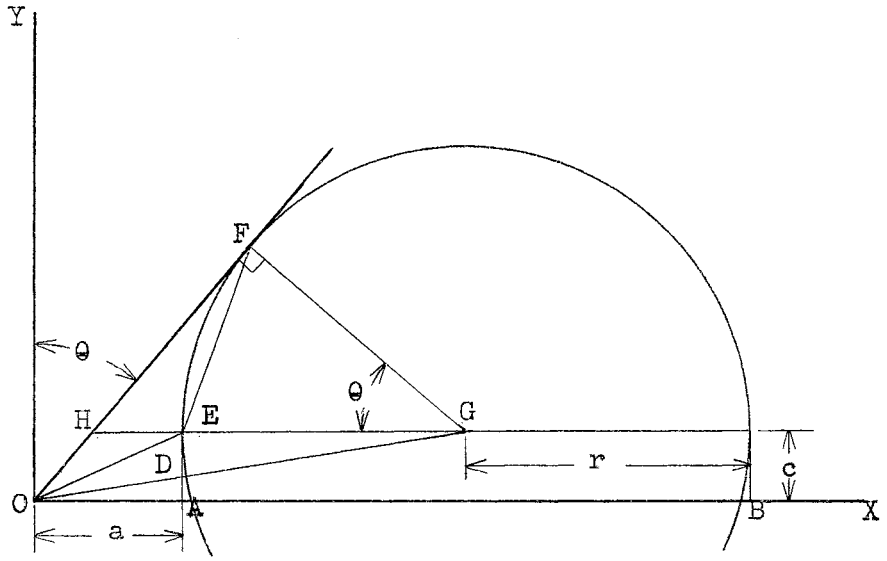

Figure 28. Circle for calculating maximum power factor.

The equation of the line segment OG is

$$\frac{y}{x} = \frac{c}{a + r} \tag{141}$$

This line intersects line EA at

$$D = (a, \frac{ac}{a + r}) \tag{142}$$

Therefore, the length

$$ED = c - ac/(a + r) = cr/(a + r) \tag{143}$$

In triangle EDG,

$$ED = cr/(a + r) \tag{143}$$

$$EG = r \tag{144}$$

$$DG = \frac{r}{a + r}\sqrt{(a + r)^2 + c^2} \tag{145}$$

In triangle FOG,

$$OG = \sqrt{(a + r)^2 + c^2} \tag{146}$$

$$FG = r \tag{147}$$

$$OF = \sqrt{(a + r)^2 + c^2 - r^2} \tag{148}$$

From Figure 28,

$$\theta = \measuredangle FGO - \measuredangle EGD \tag{149}$$

The trigonometric relation for the difference of two angles in terms of the angles involved in Equation (149) is

$$\cos \theta = \cos(\measuredangle FGO)\cos(\measuredangle EGD) + \sin(\measuredangle FGO)\sin(\measuredangle EGD) \tag{150}$$

Substituting Equations (143)-(148) for the necessary sines and cosines in Equation (150), one obtains

$$\cos \theta = \frac{r(a + r) + c\sqrt{(a + r)^2 + c^2 - r^2}}{(a + r)^2 + c^2} \tag{151}$$

If Figure 28 is the circle diagram of a polyphase induction motor, then Equation (151) expresses the maximum power factor of the motor. The maximum power factor is a function of the radius of the circle and the location of its center.

In an actual induction-motor circle diagram, the distance c is very small. Gray[1] has shown that, for a reasonably good motor, the diameter of the circle, 2r, is not less than eighteen times the distance OE. A survey of several lines of commercially available motors shows that a conservative minimum value for the no-load power-factor angle is 75 degrees. Therefore, the distance c does not exceed one-seventieth of the circle diameter. Hence, little error will be introduced if the distance c is neglected.

---

[1]Alexander Gray, Electrical Machine Design (New York, 1926), p. 395.

If one neglects the distance c, the maximum power factor as given by Equation (151) reduces to

$$\cos \theta_{max} = \frac{r}{a + r} \tag{152}$$

or

$$\cos \theta_{max} = \frac{1}{\frac{a}{r} + 1} \tag{153}$$

Equation (153) can be rewritten in terms of the distances between the indicated points in Figure 28 as

$$\cos \theta_{max} = \frac{1}{\frac{OA}{\frac{AB}{2}} + 1} = \frac{1}{2\frac{OA}{AB} + 1} = \frac{1}{2\sigma + 1} \tag{154}$$

where σ is the ratio of the magnetizing current to the circle diameter; it is called the leakage coefficient since it is the ratio of the leakage or nonuseful flux, to the useful flux. [See Equation (159)]. The relation expressed in Equation (154) is shown graphically in Figure 29. One should note that the value of the maximum power factor is dependent on the leakage coefficient. If one knows the leakage coefficient, the maximum power factor can be found from Equation (154) or Figure 29. A high value of maximum power factor requires a small leakage coefficient. In addition, Gray[2] shows that a motor having a leakage coefficient of 0.06 or less will have approximately the following minimum values: a full-load power factor of 90 per cent, a starting torque of about 1.5 times full-load torque, a maximum torque of about 2.7 times full-load torque, and a maximum

---

[2] Ibid., p. 395.

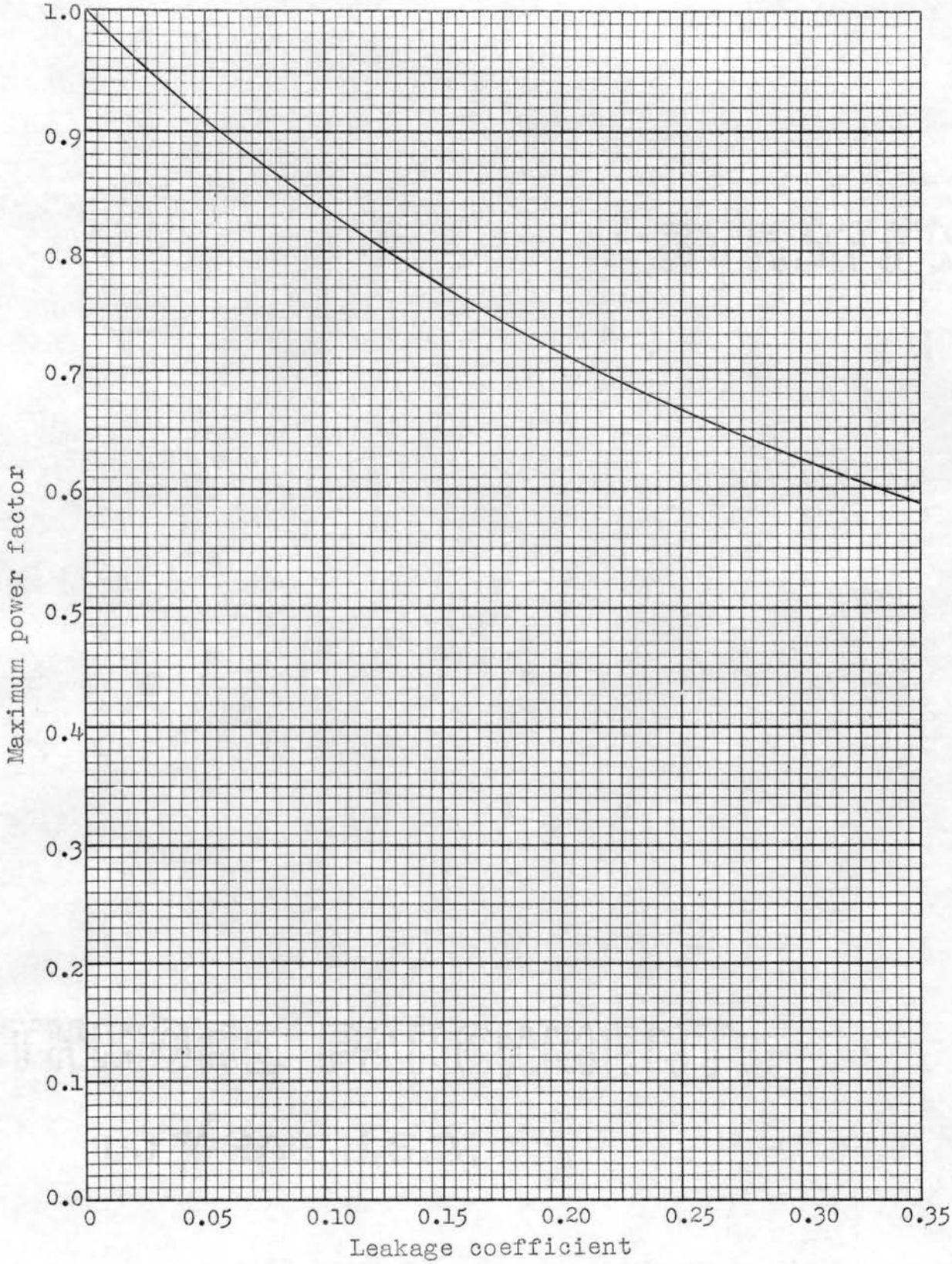

Figure 29. Relation of maximum power factor to the leakage coefficient.

output of about 2.2 times full-load output. These values indicate the great importance of the leakage coefficient.

The effect of neglecting the distance c is to move the center of the circle to the base line as shown in Figure 30. How does the maximum power factor obtained from Figure 29 compare to that of a real motor? This question can best

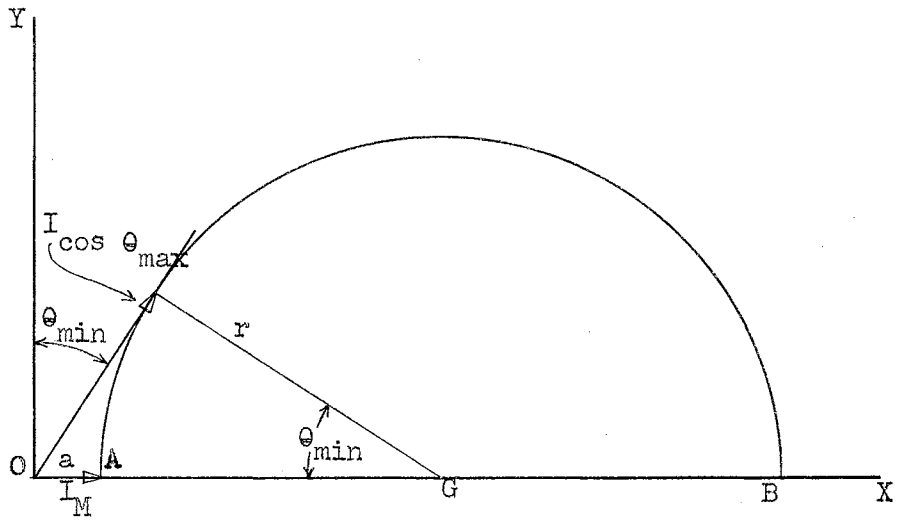

Figure 30. Simplified circle diagram.

be answered by observing Figure 31. In Figure 31, two circles are drawn, the solid-line circle has its center on the base line, the dashed-line circle has its center located above the base line a distance c which, for the purpose of illustration, is greatly exaggerated over what it would be in an actual induction-motor circle diagram. It is obvious that neglecting the distance c leads to a value of maximum power factor which is lower than will be

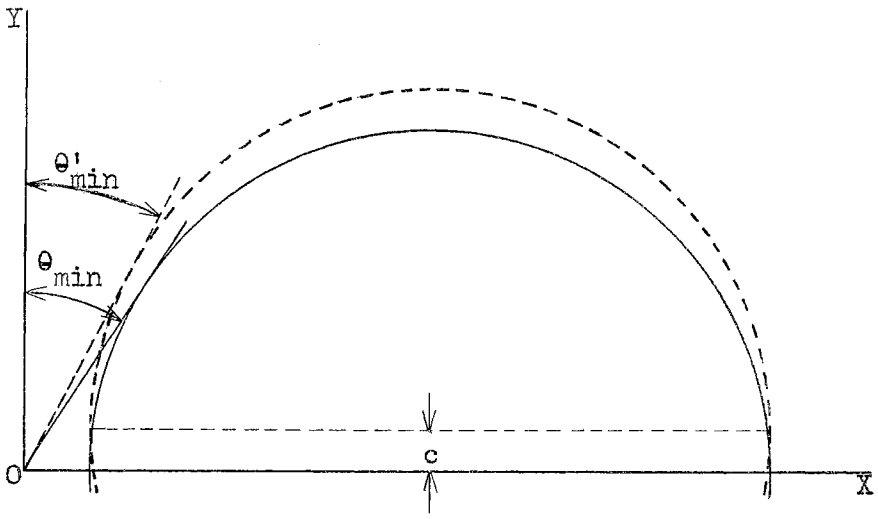

Figure 31. The effect of neglecting the distance c on the maximum power factor.

found in a real motor. Hence, the error introduced is definately on the conservative side. By comparing the values of Figure 29 with several lines of commercial motors, the author finds that the values indicated in Figure 29 are low by 1/2 to 3/4 per cent for large motors and by 1 to 2 per cent for small motors.

Another relationship of interest is the current at which the maximum power factor occurs. From Figure 30,

$$I_{\cos\theta_{max}} = \sqrt{(OG)^2 - r^2} = \sqrt{(a + r)^2 - r^2} = \sqrt{a^2 + a(2r)} \quad (155)$$

but

$$2r = AB = \frac{OA}{9} \quad (156)$$

and

$$a = OA = I_M \quad (157)$$

hence

$$I\cos\theta_{max} = \sqrt{(OA)^2 + (OA)\frac{OA}{\sigma}} = I_M\sqrt{1 + \frac{1}{\sigma}} \qquad (158)$$

THE RELATIONSHIP BETWEEN THE LEAKAGE COEFFICIENT AND THE MOTOR REACTANCES

The leakage coefficient is the ratio of the distances OA to AB on the circle diagram. In Figure 11b, it was shown that

$$OA = V_1/X_M \qquad (159)$$

and

$$AB = V_1/(X_1 + a^2X_2) = V_1/X_e \qquad (160)$$

By substituting Equations (159) and (160) into the expression for the leakage coefficient, one obtains

$$\sigma = \frac{OA}{AB} = \frac{X_e}{X_M} \qquad (161)$$

The leakage coefficient may then be defined in terms of the reactances of the induction motor as the ratio of the total leakage reactance to the magnetizing reactance.

The total leakage reactance per inch of slot, as a per-unit value, is the sum of its per-unit components of slot leakage reactance, zigzag reactance, coil-end leakage reactance, and belt reactance, or

$$x_e = x_s + x_z + x_c + x_b \qquad (162)$$

The total leakage reactance in ohms per inch of slot can be obtained from the per-unit value and the base used here. It is

$$X_e = x_e E_{1i}/I_T \qquad (163)$$

In the vector diagram of Figure 9, the magnetizing reactance per inch of slot is

$$X_M = E_{1i}/I_M \tag{164}$$

From Equation (72),

$$I_M = b_m I_T \tag{165}$$

consequently,

$$X_M = E_{1i}/b_m I_T \tag{166}$$

From the substitution of Equations (163) and (166) into Equation (161), the leakage coefficient is found to be

$$\sigma = \frac{X_e}{X_M} = \frac{x_e\ E_{1i}}{I_T}\ \frac{b_m\ I_T}{E_{1i}} = x_e\ b_m \tag{167}$$

An expression for the total leakage reactance per inch of slot as a per-unit value can be obtained by adding its per-unit components, that is, by substituting Equations (104), (123), (137), and (138) into Equation (162), giving

$$x_e = 2.37\ \left(\frac{K_s'\ k_{sp}'}{k_w'}\ \frac{w_2'}{w'} + \frac{K_s''\ k_{sp}'}{k_w'}\ \frac{w_2''}{w''}\right) \frac{f\ q_T}{v\ B_g}$$

$$+ 26.7\ \frac{q_T\ v\ A\ k_{zp}}{k_w\ B_g f\ S_p^2\ \delta} + 0.247\ (\phi_f'\ C_f' + \phi_f''\ C_f'')\ \frac{q_T\ f\ k_{cp}\ \tau^2}{k_w\ v\ B_g\ L}$$

$$+ 0.03\ k_b\ K_1\ K_2\ \frac{q_T\ v}{\delta\ f\ B_g} \tag{168}$$

Substituting Equations (72) and (168) into Equation (167) and letting

$$M = \left(K_s'\ k_{sp}'\ \frac{w_2'}{w'} + K_s''\ k_{sp}'\ \frac{w_2''}{w''}\right) \tag{169}$$

and

$$W = \left(\phi_f'\ C_f' + \phi_f''\ C_f''\right) \tag{170}$$

one can express the leakage coefficient as

$$\sigma = \frac{0.275\ M}{K_1\ K_2\ k_m k_w}\ \delta\ \frac{f^2}{v^2} + \frac{3.1\ A\ k_{zp}}{K_1\ K_2\ k_m\ k_w\ S_p^2}$$

$$+ \frac{0.2865\ W\ k_{cp}}{K_1\ K_2\ k_m\ k_w}\ \frac{\delta}{L}\ \frac{\tau^2\ f^2}{v^2} + 0.0035\ \frac{k_b}{k_m} \qquad (171)$$

The first and third terms on the right-hand side of Equation (171) contain the factor v^2 which can be eliminated by the substitution of the square of Equation (71),

$$\frac{f^2}{v^2} = \frac{36}{\tau^2} \qquad (172)$$

The leakage coefficient then reduces to

$$\sigma = 9.9\ \frac{M\ \delta}{K_1\ K_2\ k_m\ k_w\ \tau^2} + 3.1\ \frac{Ak_{zp}}{K_1\ K_2\ k_m\ k_w S_p^2} + 1.031\ Wk_{cp}\frac{\delta}{L}$$

$$+ 0.0035\ \frac{k_b}{k_m} \qquad (173)$$

The leakage coefficient can be calculated with great accuracy from the dimensions of the motor and the winding data by using Equation (173). Note that under the condition of no magnetic saturation the leakage coefficient is independent of voltage and current. As soon as the type of slots, the length, the winding, and the diameter are determined, the leakage coefficient is fixed. All running characteristics of the motor are improved by decreasing the leakage coefficient.

The relationship expressed by Equation (173) is of great importance. Each factor should be carefully examined. The slot constants, as the name implies, are constants for any given type of slot. The approximate range of the slot

constants is from 0.9 to 2.4 depending on whether the slots are open or nearly closed. The ratio w_2/w is also a constant for any given type of slot varying from 0.35 to 0.6 depending upon the type of slot. Hence, M is a constant for given types of stator and rotor slots. The factor W is also a constant which varies little from a value of three for induction motors. Once the type of slots is chosen and the type of winding is determined, so that the D^2L equation can be evaluated, the factors k_w, k_{zp}, k_{cp}, k_m, k_b, and S_p are constants. For 60-cycle motors, K_2 is approximately constant at 0.90. The factors A and K_1 are small and likewise may be considered as constants. The radial depth of the air gap, δ, is empirically related to the diameter and the length, but for small variations in the diameter and length it need not change and may be considered a constant.

SEPARATING THE COMPONENTS OF THE D^2L EQUATION FOR OPTIMUM MAXIMUM POWER FACTOR

Equation (173) allows one to investigate the relationship between the leakage coefficient, the motor diameter at the air gap, and the core length. As stated previously, it is feasible to build a series of motors, some with large diameters and short core lengths and some with small diameters and long cores, all having the same value of D^2L. These motors will certainly have different characteristics. The one with the smallest leakage coefficient will have the best overall performance characteristics.

In the preliminary design of a polyphase induction motor, the necessary factors of the right-hand side of the D^2L equation, Equation (8), are evaluated as illustrated in the example of Chapter I. The value of D^2L for a given design is then considered to be a constant which will be called H, or

$$D^2L = H \tag{174}$$

Solving for D, one obtains

$$D = \sqrt{H/L} \tag{175}$$

The pole pitch is

$$\tau = \pi D/p \tag{176}$$

Substituting Equation (175) into Equation (176), one can express the pole pitch as

$$\tau = \frac{\pi}{p}\sqrt{\frac{H}{L}} \tag{177}$$

and

$$\tau^2 = \frac{\pi^2}{p^2}\,\frac{H}{L} \tag{178}$$

If Equation (178) is substituted into Equation (173), one obtains an expression for the leakage coefficient in terms of the length L and numerous quantities which are constants for a given type of winding and a given type of slots. The result is

$$\sigma = \frac{1}{K_1 K_2 k_m k_w}\left(9.9\, M \frac{\delta p^2 L}{\pi^2 H} + 3.1\, A\, k_{zp} \frac{1}{S_p^2}\right.$$

$$\left. + 1.031\, W\, k_{cp} \frac{\delta}{L}\right) + 0.0035\, \frac{k_b}{k_m} \tag{179}$$

Taking the first derivative of Equation (179) with respect to L and setting $d\sigma/dL$ equal to zero give the conditions necessary for minimum leakage coefficient or highest maximum power factor as

$$\frac{d\sigma}{dL} = 9.9\ M \frac{p^2}{\pi^2 H} - 1.031\ W\ k_{cp}\ \frac{1}{L^2} = 0 \qquad (180)$$

The leakage coefficient will be at its minimum value when the total slot leakage reactance is equal to the total coil-end leakage reactance. For a high value of maximum power factor, the zigzag-leakage and the belt-leakage components of the leakage coefficient should be kept as low as possible.

Solving Equation (180) for L, one obtains an expression for the value of core length corresponding to a minimum leakage coefficient. The value of L is

$$L = \frac{1.015}{p} \sqrt{\frac{W\ k_{cp}\ H}{M}} \qquad (181)$$

After one determines L, the corresponding value of D is easily found from Equation (175).

Equations (181), (175), and (179) and Figure 29 can be used directly in the preliminary design of a squirrel-cage or a wound-rotor induction motor. They also serve as an easy comparison in determining the most advantageous frame size in which to build a motor.

AN EXAMPLE

In the discussion of Gray's Method of separating the components of the output equation in Chapter II, an example was cited in which Gray carried out the design of a particular

motor by selecting five different diameters, roughly determining the performance of each, and then selecting the one he thought was best.

The equations of the previous section will be applied to this same example to show the enormous amount of time saved through eliminating the need of designing a series of machines and then deciding which would be the best.

The machine under consideration is a three-phase, 75-hp, 440-volt, 60-cycle, squirrel-cage, general-purpose induction motor.[3] It is to have a synchronous speed of 900 rpm. Gray used typical values of full-load power factor, efficiency, ampere-conductors, and gap flux density of 89%, 89%, 820, and 25,000, respectively. The winding is to be a double-layer winding with 12 slots per pole of 9/12 pitch. The stator slots are to be open and the rotor is to have partially closed rectangular slots.

Using this information, the output equation can be evaluated, giving

$$D^2L = H = 2180 \text{ cubic inches}$$

Also,

$p = 8$	$k_m = 0.83$
$W = 3$	$K_2 = 0.9$
$M = 1.507$	$k_{cp} = 0.68$
$k_w = 0.885$	$k_{sp} = 0.85$
$S_p = 12$	$k_{zp} = 0.82$

---

[3] Ibid., pp. 396-400.

The belt leakage reactance is zero since this is a squirrel-cage induction motor.

Applying Equation (181), one finds the leakage coefficient will be a minimum when

$$L = \frac{1.015}{p}\sqrt{\frac{W\, k_{cp}\, H}{M}} = \frac{1.015}{8}\sqrt{\frac{3(0.68)2180}{1.507}} = 6.9 \text{ inches}$$

The corresponding value of D is

$$D = \sqrt{\frac{H}{L}} = \sqrt{\frac{2180}{6.9}} = 17.8 \text{ inches}$$

Hence, the values of D and L are determined without the necessity of designing several different machines and selecting one of these for the final design. Gray chose a machine having a diameter of 19 inches as the final machine. In working out the preliminary designs, he selected only odd numbers of inches for the diameter. A complete reworking of his preliminary design procedure shows a machine having a diameter of 17.8 inches has better characteristics than the 19-inch machine. Gray's decision is based on performance and cost. This example will be continued in the next chapter to show the influence of cost data on the selection. For a machine of this particular size, there is little difference in performance in machines having diameters in the range of 17 to 19 inches. This can be seen from Figure 32, where one can observe that the minimum value reached by the leakage coefficient is not sharply defined since the curve of the total leakage coefficient changes slope very slowly near the minimum. The influence of the diameter on the leakage coefficient is greater for machines having large

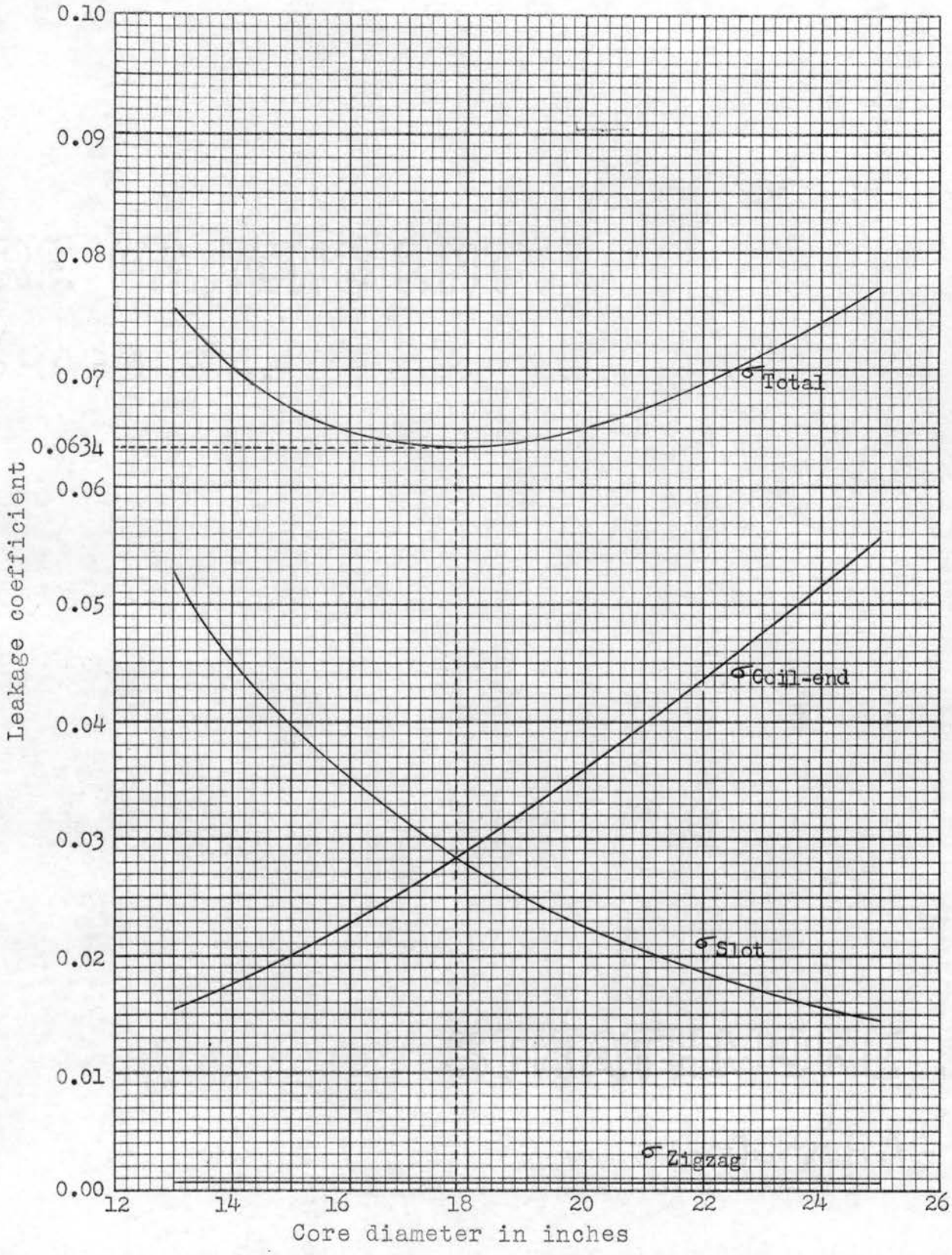

Figure 32. Variation of leakage coefficient with core diameter for a sample motor.

leakage coefficients. In other words, machines with a low power factor, which corresponds to a large leakage coefficient, will be more sensitive to changes in diameter and length than those with small leakage coefficients and high power factors. Motors with a large number of poles generally have low power factors, making it important that the diameter and length be selected as close to the best value as possible.

Having determined the diameter and length, one can calculate the radial length of the air gap by whichever empirical relation he wishes to use. In this example, consider the length of the air gap to be 0.033 inch, in conformance with Gray. For diameters within the range of 15 to 21 inches, there certainly would be no need to change the gap length. If the machine were built with smaller or larger diameters than this range, a change in the gap length might be necessary. Assuming a gap of 0.033 inch, one can plot the components of the leakage coefficient by using Equation (179). This plot, Figure 32, clearly shows the influence a change in diameter has on the leakage coefficient and, therefore, the maximum power factor. The minimum leakage coefficient for this machine is 6.34%, corresponding to a maximum power factor of 88.7%. The actual maximum power factor will be about 3/4% greater than this value, or about 89.5%.

CHAPTER VI

SEPARATING THE COMPONENTS OF THE D^2L EQUATION FOR MINIMUM COST

It is very doubtful if anyone could obtain sufficient cost information to make a complete study of the variation of the total cost of a motor as the dimensions are changed. In order to make a complete study, all shop conditions, production levels, accounting procedures, and many other items would need to be accurately known. Since many of these costs are continually changing, a detailed investigation would be nearly impossible. However, a general consideration of costs for use in the preliminary design of an induction motor can be made.

COSTS AND HORSEPOWER RATINGS

It is reasonable to assume that if the production costs of a particular class of motors are plotted against the horsepower ratings, the resulting curves will be loci of minimum cost points. That is, the highly competitive motor market that exists in this country will force the manufacturers to produce these machines at, or very near, minimum cost. Such a set of curves, representing present-day production costs of several manufacturers, is shown in Figure 33. These curves are for open, N. E. M. A. design B, three-phase, 60-cycle, $40^{\circ}C$, squirrel-cage induction motors of 208-220-440-550 volts.

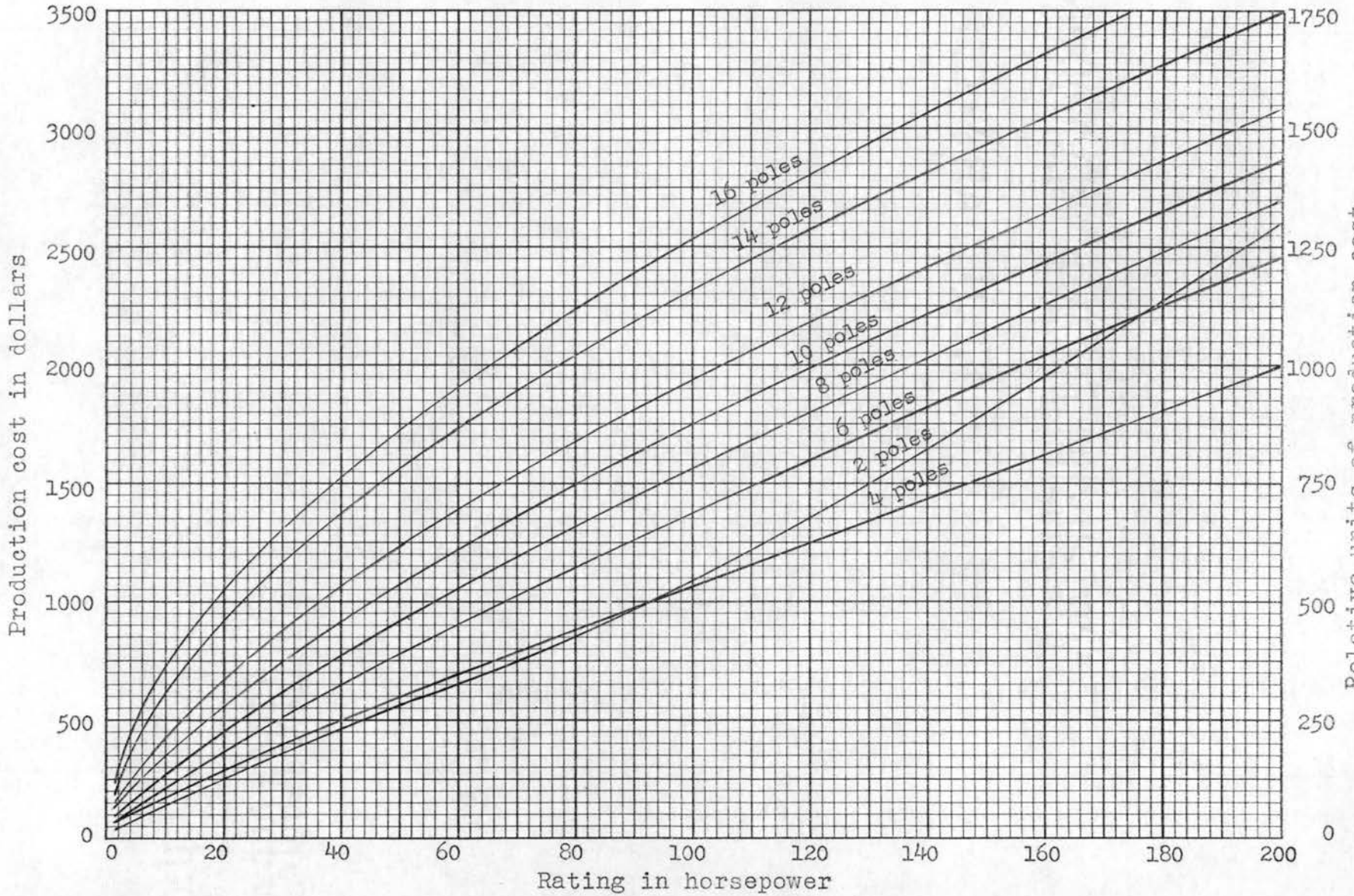

Figure 33. Production costs for sample lines of squirrel-cage induction motors.

The curves of Figure 33 also apply to 60-cycle, two-phase, $40^{\circ}C$ motors and 50-cycle, three-phase, $50^{\circ}C$ motors of the same type and design having the same number of poles.

The author has found that over a period of several years, the changes in production costs of this class of motors are reflected as a shift of these curves up or down, the general shape remaining the same. These changes can be eliminated from this discussion by putting the costs on a relative basis. For convenience, the cost of a 200-horsepower, 4-pole motor is arbitrarily chosen as a reference value of 1000 units of cost.

SEPARATING THE COMPONENTS OF THE D^2L EQUATION FOR MINIMUM COST

Suppose all machines cost a definite amount per square inch of equivalent cylindrical surface at the air gap. Then one could write

$$P.C. = K_c D (L + a\tau) \qquad (182)$$

where

P.C. = relative units of production cost

K_c = relative cost coefficient

a = equivalent surface coefficient

Under these conditions, the cost coefficient would be a constant. The factor $D(L + a\tau)$ is not an arbitrary quantity, as one might think at first sight. This product is proportional to the cylindrical surface of the machine at the air

gap measured from end to end of the winding. If a winding employs end connections lying in an extension of the cylindrical surface of the slot portion of the winding, the length over end connections is equal to $(L + a\tau)$, where a is a function of the shape of the coil ends.

From the D^2L equation, as expressed in Equation (174),

$$L = H/D^2 \tag{183}$$

Also, in Equation (176),

$$\tau = \pi D/p \tag{176}$$

Substitution of Equation (183) and (176) into Equation (182) gives

$$P.C. = K_c \left(\frac{H}{D} + \frac{a\pi D^2}{p}\right) \tag{184}$$

Setting the first derivative of Equation (184) equal to zero yields

$$\frac{d\ P.C.}{dD} = -\frac{H}{D^2} + 2a\ \frac{\pi}{p} = 0 \tag{185}$$

The right-hand sides of Equation (183) and (176) are factors involved in Equation (185), and, when these equations are substituted into Equation (185), one finds that the motor core length corresponding to minimum production cost is

$$L = 2\ a\ \tau \tag{186}$$

In order to obtain an expression in terms of the diameter, Equation (186) can be substituted into the D^2L equation, resulting in

$$D^2L = H = D^2(2a\tau) = D^3\left(\frac{2a\pi}{p}\right)$$

or

$$D = \sqrt[3]{\frac{pH}{2a\pi}} \tag{187}$$

This is the core diameter that results in minimum production cost. The corresponding value of length can then be found. The influence of the components L and D on the relative production cost may be investigated by using Equation (182).

In practice, the cost coefficient for a particular class of motors is not a true constant as supposed, but fairly constant values, particularly for large motors, can be assigned. The same is true for the equivalent surface coefficient; however, the equivalent surface coefficient does not necessarily retain its physical significance. The author has calculated values of the cost coefficient and the equivalent surface coefficient for the type of motors mentioned in the last section. The two coefficients were calculated from the dimensions of motors ranging from 3 to 200 horsepower. The resulting values of a and K_c are plotted in Figures 34 and 35, respectively. Figures 34 and 35 are confirmed only through a range of 3 to 200 horsepower. Since a similar rate of rise is known to exist for direct- and alternating-current generators up to 500 kw and possibly much higher, it is not unjustifiable to conclude that curves such as those of Figures 34 and 35 can be projected to much higher values.

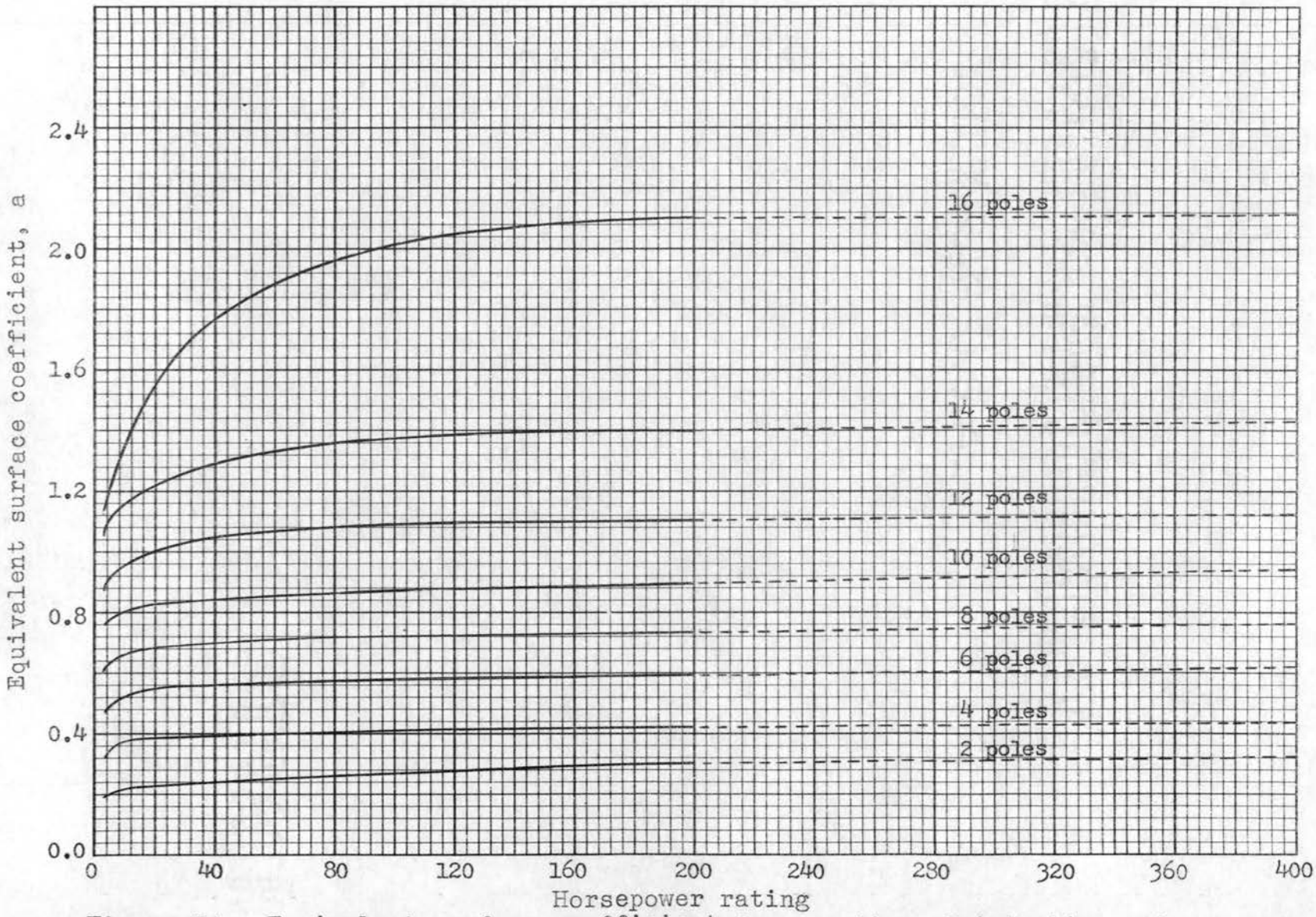

Figure 34. Equivalent surface coefficient for one line of induction motors.

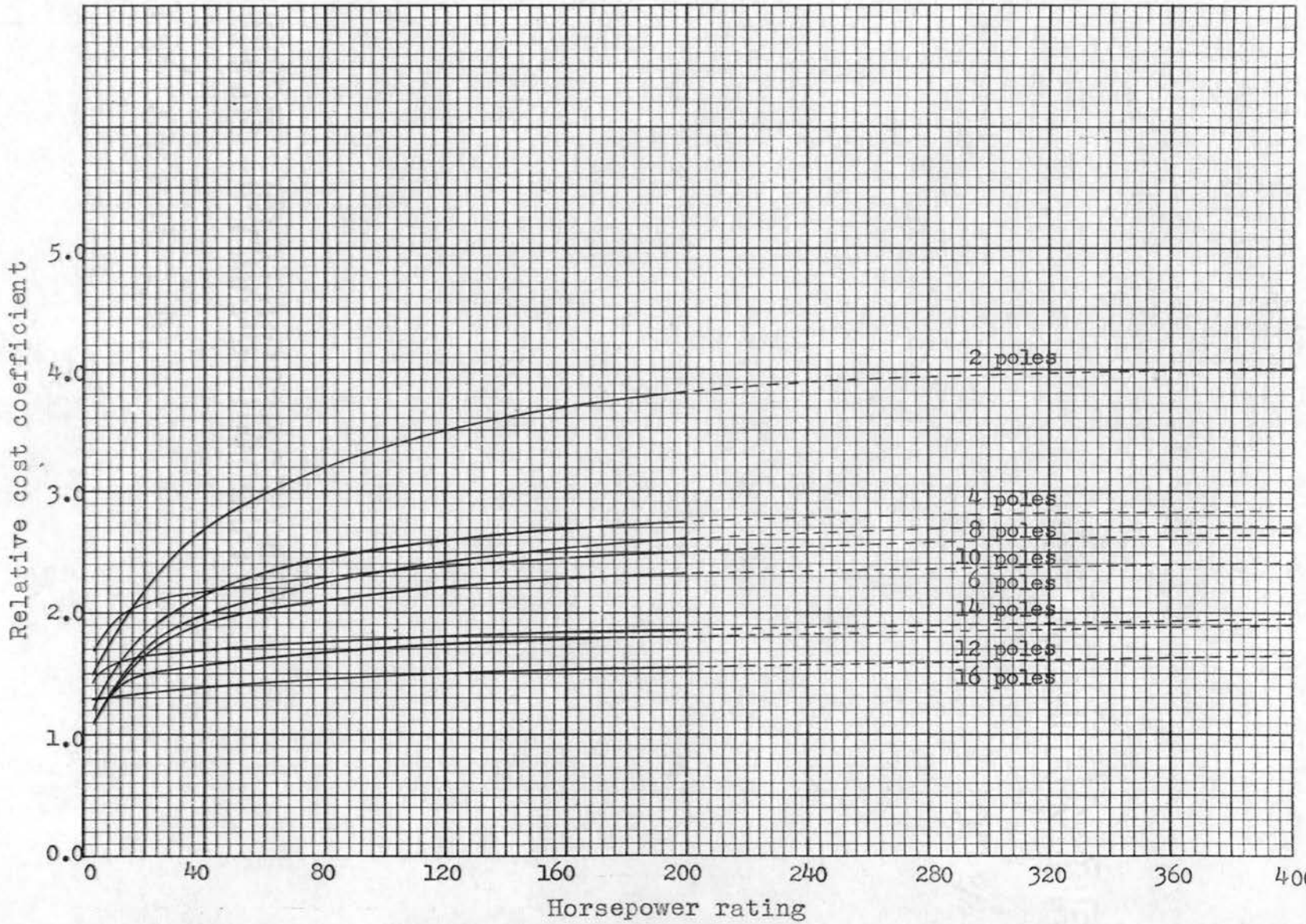

Figure 35. Relative cost coefficient for one line of induction motors.

AN EXAMPLE

This method of separating the components of the D^2L equation will now be applied to the example of the last chapter. The machine is to be a three-phase, design B, open, squirrel-cage induction motor having a synchronous speed of 900 rpm and $D^2L = H = 2180$.

Using Equation (187) and Figure 34, one finds the diameter for minimum production cost to be

$$D = \sqrt[3]{\frac{pH}{2a\pi}} = \sqrt[3]{\frac{8(2180)}{2(0.705)\pi}} = 15.8 \text{ inches}$$

The corresponding value of L is

$$L = \frac{H}{D^2} = \frac{2180}{(15.8)^2} = 8.72 \text{ inches}$$

This result is not in agreement with Gray's statement that the 19-inch diameter motor is the cheapest. One would not expect present-day cost data to apply to the time when Gray worked out his design. However, it may be of interest to the reader that the author has found these costs, on a relative basis, to extend back a period of at least ten years. This particular motor design is referred to for purposes of illustration only. Assuming a and K_c to be constant at the corresponding values indicated in Figures 34 and 35, it is interesting to observe how the cost would vary with a change in diameter. Figure 36 shows this variation. The minimum cost is indicated as 100 per cent. One would expect a very slow change from minimum for this curve. A variation in the

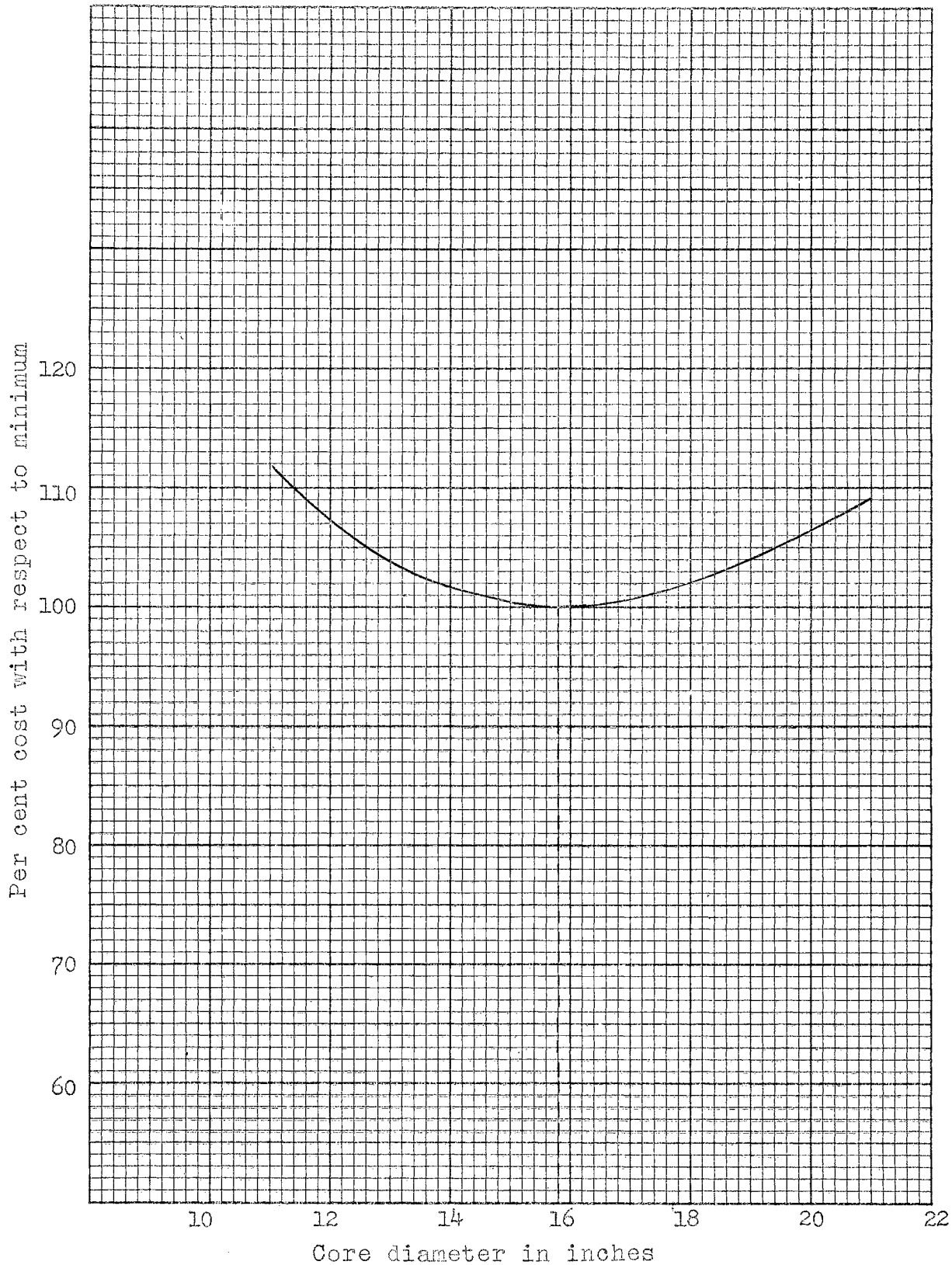

Figure 36. Percentage variation of cost as a function of core diameter for a sample motor design.

diameter of plus or minus one inch from the minimum-cost value results in a cost variation of less than 3/4 of 1 per cent. A machine built with a diameter greater than that giving minimum cost results in an increased cost due to the yoke, spider, and housing. A machine of smaller diameter would result in increased costs for assembling the windings and cores.

This analysis of costs is only an approximate solution, but it is valuable in preliminary designs.

CHAPTER VII

THE AIR GAP

The power factor at which an induction motor operates is determined by the ratio of the in-phase component of the stator current to the total stator current. The latter is equal to the square root of the sum of the squares of the in-phase and reactive components. The power factor therefore is larger when the reactive component of the current is reduced. It has been shown in the foregoing that the reactive component consists of two parts; one part is the reactive magnetizing current necessary to sustain the main flux, and the other part is due to the leakage fluxes. The reactive magnetizing current depends on the length of the air gap and on the saturation of the iron. A small air gap, low saturation, and low leakage reactances increase the operating power factor.

The maximum torque which can be developed by an induction motor is its "breakdown" torque, that is, the torque at which it will become unstable with increasing slip. The maximum torque and the slip at which that torque occurs depend upon the stator and rotor leakage reactances. Both decrease with increasing reactance [see equations (38) and (39)]. It is, therefore, obviously impossible to have a large breakdown torque associated with small slip. In order to have a large breakdown torque, the leakage reactance of an induction motor

must be small. Since the leakage reactance of an induction motor, like that of a transformer with an air gap between its primary and secondary windings, increases with the length of the air gap, the necessity for small reactances requires the use of a small air gap. Hence, it is seen that a large air gap not only decreases the maximum torque but also decreases the operating power factor. Moreover, the leakage coefficient, Equation (171), is increased by using a large air gap. In order to reduce the reactive current drawn from the power supply, induction motors are built with smaller air gaps than synchronous machines which get their excitation from a direct-current source through the rotor. Also, direct-current machines have larger air gaps than induction motors.

In addition, the length of the air gap has an important bearing on the noise produced by the motor when running. The main cause of this noise is the variations in the zigzag leakage flux across the tips of the stator and rotor teeth, and, since the magnitude of this flux is inversely proportional to the air gap as shown in Equation (123), it follows that one condition for silent running is that the gap not be too small. For quiet operation, it is also desirable that the number of rotor slots shall not be within 20 per cent of the number of stator slots. Reduced gaps may also increase the tooth-face losses.

Thus, the requirements of good power factor and of noiseless operation and low tooth-face losses are conflicting in so far as they are influenced by the length of the air gap.

USUAL METHODS OF CALCULATING THE AIR-GAP LENGTH

The air gap in an induction motor is usually made as small as mechanical construction will permit. Obviously, a stiff shaft and rigid framework are required when the air gap is reduced to a mere mechanical clearance. Great length axially should be avoided so that the bearings shall not be too far apart. The bearings must be of a type which does not wear appreciably, and the stator and rotor must be circular and concentric.

Very few design engineers agree on the relationship to be used in calculating the air-gap length. Since these relationships are based on mechanical considerations, the formulas for calculating the minimum gap are empirical. A few of the many empirical relations used are given below.

Gray[1] relates the air gap to the stator internal diameter, the gross frame length, and the peripheral velocity by

$$\delta = 0.005 + 0.00035\, D_a + 0.001\, L_g + 0.003\, V \qquad (188)$$

where

δ = the air-gap clearance in inches

---

[1]Alexander Gray, Electrical Machine Design (New York, 1926), p. 394.

D_a = the stator internal diameter in inches

L_g = the gross iron in the frame length in inches

V = the peripheral velocity of the rotor in thousands of feet per minute

For induction motors of normal design with usual peripheral velocities, Still and Siskind[2] suggest

$$\delta = \frac{15 + D}{1000} \tag{189}$$

Kuhlmann[3] uses

$$\delta = 0.125 - 10.17/(D + 90) \tag{190}$$

Lloyd[4] suggests

$$\delta = 0.0016\ D + 0.0072 + 0.001\ L \tag{191}$$

Cotton[5] uses

$$\delta_c = \frac{240\ D_c + 1.5\ D_c^2}{(6 - \frac{L_c}{\tau_c})\ \frac{p}{2}} \times 10^{-4} \tag{192}$$

where all dimensions are in centimeters.

Aston[6] prefers to use a curve to determine the length of the air gap. This curve is shown in Figure 37.

---

[2]Alfred Still and Charles S. Siskind, Elements of Electrical Machine Design (New York, 1954), p. 309.

[3]John H. Kuhlmann, Design of Electrical Apparatus (New York, 1950), p. 316.

[4]T. C. Lloyd and Howard B. Stone, "Some Aspects of Polyphase Motor Design--The Design and Properties of the Magnetic Circuit," Transactions of the American Institute of Electrical Engineers, LXV (December, 1946), 815.

[5]H. Cotton, Design of Electrical Machinery (London, 1934), p. 343.

[6]Kenneth Aston, Design of Alternating-Current Machines London, 1934), p. 318.

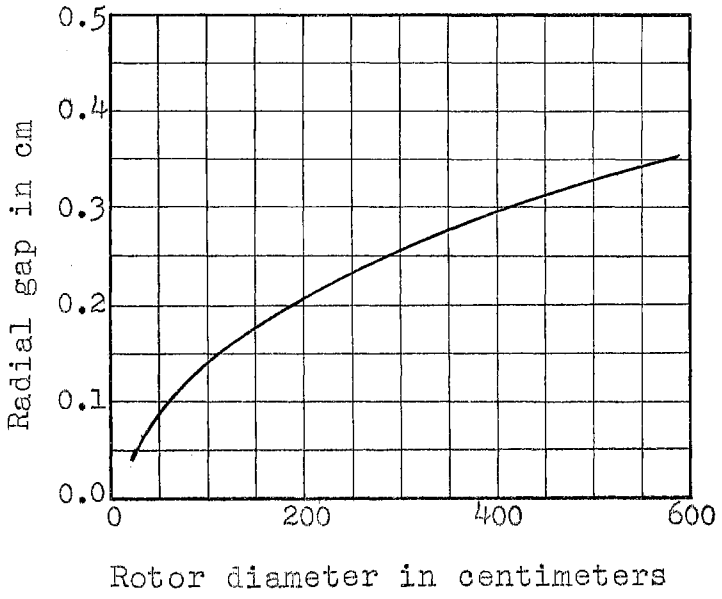

Figure 37. Induction motor air gaps (More than 4 poles).

It is interesting to observe how the values obtained from these different empirical relations compare for a given

TABLE VII

RADIAL AIR-GAP LENGTH FOR A SAMPLE MOTOR

Method of calculation	Air-gap length, δ, in inches
Gray	0.0324
Still and Siskind	0.035
Kuhlmann	0.0325
Lloyd	0.0302
Cotton	0.0355
Aston	0.0352

motor. The results are tabulated in Table VII for a 60-cycle, three-phase motor having 8 poles, a core diameter of 20 inches, and a core length of 6 inches.

POWER FACTOR OF A POLYPHASE INDUCTION MOTOR

In order to study the effect of the air gap on the power factor at any load, it is first necessary to see how they are related. The vector diagram of the exact equivalent circuit will be used to establish this relationship. For the purpose of this derivation, the vector diagram of the exact equivalent circuit, in one of its common forms, is drawn in Figure 38. If E_1 and the other primary voltage and current vectors are rotated counterclockwise through 180°, this diagram will be the same as that of Figure 9. All secondary quantities in Figure 38 are expressed in primary terms.

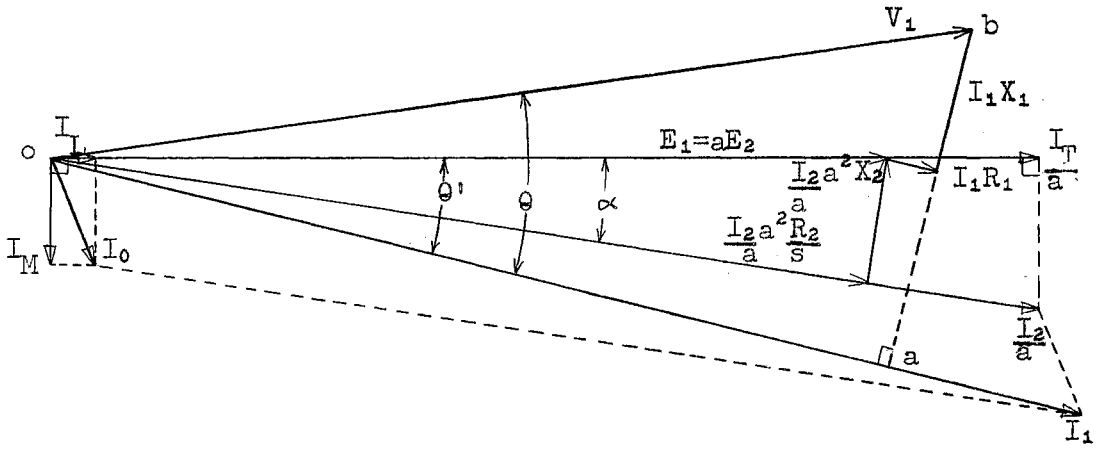

Figure 38. Vector diagram of the exact equivalent circuit.

Referring to Figure 38, one can write

$$\cos \theta' = \frac{I_T + I_L}{I_1} \tag{193}$$

$$\tan \alpha = \frac{\frac{I_2}{a} a^2 X_2}{\frac{I_2}{a} a^2 \frac{R_2}{s}} = \frac{\frac{X_2}{R_2}}{s} = \frac{\frac{I_2}{a} a^2 X_2}{\sqrt{E_1^2 - (\frac{I_2}{a} a^2 X_2)^2}}$$

$$= \frac{\frac{I_2}{a} a^2 X_2}{E_1} \frac{1}{\sqrt{1 - \left(\frac{\frac{I_2}{a} a^2 X_2}{E_1}\right)^2}} \tag{194}$$

$$\tan \theta' = \frac{I_M + I_T \tan \alpha}{I_T + I_L} = \frac{\frac{I_M}{I_T} + \tan \alpha}{1 + \frac{I_L}{I_T}} \tag{195}$$

Let

$$\frac{I_M}{I_T} = u_m \tag{196}$$

$$\frac{I_L}{I_T} = u_c \tag{197}$$

$$\frac{\frac{I_2}{a} a^2 X_2}{E_1} = u_{x2} \tag{198}$$

Then

$$\tan \alpha = \frac{u_{x2}}{\sqrt{1 - u_{x2}^2}} \tag{199}$$

and

$$\tan \theta' = \frac{u_m + \frac{u_{x2}}{\sqrt{1 - u_{x2}^2}}}{1 + u_c} = u' \tag{200}$$

The vector I_1X_1 in Figure 38 is extended to intersect the I_1 vector. Since I_1X_1 is a reactive voltage drop due to the current I_1, this extension will be perpendicular to

I_1. The power factor of the motor, cos θ, can be found from the sides of the right triangle oab. It is

$$\cos\theta = \frac{1}{\sqrt{1 + \left(\frac{ab}{oa}\right)^2}} = \frac{1}{\sqrt{1 + \tan^2\theta}}$$

$$= \frac{1}{\sqrt{1 + \left(\frac{I_1 X_1 + E_1 \sin\theta'}{I_1 R_1 + E_1 \cos\theta'}\right)^2}}$$

$$= \frac{1}{\sqrt{1 + \left(\frac{\frac{I_1 X_1}{E_1}\ \frac{1}{\cos\theta'} + \tan\theta'}{\frac{I_1 R_1}{E_1}\ \frac{1}{\cos\theta'} + 1}\right)^2}}$$

$$= \frac{1}{\sqrt{1 + \left(\frac{\frac{I_1 X_1}{E_1}\sqrt{1 + u'^2} + u'}{\frac{I_1 R_1}{E_1}\sqrt{1 + u'^2} + 1}\right)^2}} \qquad (201)$$

Let

$$\frac{I_1 X_1}{E_1} = u_{x1} \qquad (202)$$

and

$$\frac{I_1 R_1}{E_1} = u_{R1} \qquad (203)$$

Then Equation (201) becomes

$$\cos\theta = \frac{1}{\sqrt{1 + \left(\frac{u' + u_{xi}\sqrt{1 + u'^2}}{1 + u_{R1}\sqrt{1 + u'^2}}\right)^2}} \qquad (204)$$

THE RELATIONSHIP BETWEEN THE POWER FACTOR AND THE MOTOR CONSTANTS

Equation (204) gives exact results for the power factor; however, the operation is somewhat tedious. If Equation (204) is expanded in terms of the currents, voltages, and impedances involved, one can readily see several approximations that can safely be made, such as

$$\cos \theta = \frac{1}{\sqrt{1 + \left(\frac{u_{x1} + \frac{u_{x2} + u_m}{1 + u_c}}{1 + u_{R1}} \right)^2}} \tag{205}$$

$$\cos \theta = \frac{1}{\sqrt{1 + \left(\frac{u_{x1} + u_{x2} + u_m}{1 + u_c} \right)^2}} \tag{206}$$

$$\cos \theta = \frac{1}{\sqrt{1 + (u_{x1} + u_{x2} + u_m)^2}} \tag{207}$$

Equation (205) gives results that are too high by about 0.2 per cent to 0.3 per cent in a good motor. Equation (206) gives closer results, and Equation (207) gives results that are too low by about 0.5 per cent to 1 per cent.

It will be remembered that u_{x1} and u_{x2} of Equation (207) rely on the total stator and rotor currents, respectively. These currents vary with the load on the motor. At full load u_{x1} and u_{x2} would be determined from the respective full-load currents. In Equation (168), an expression is given for x_e which refers to the full-load torque current. Since the torque current is slightly less than the total primary or secondary

current, the substitution of x_e of Equation (168) for $u_{x1} + u_{x2}$ in Equation (207) will give a larger value of full-load power factor which will a little more than neutralize the error due to the approximation of Equation (207). An expression for the full-load value of u_m is given in Equation (72). One can then write a very close approximation to the full-load power factor as

$$\cos \theta = \frac{1}{\sqrt{1 + (b_m + x_e)^2}} \tag{208}$$

The expressions for b_m and x_e use full-load torque current as a base in determining the per-unit values. These same expressions will apply in Equation (208) not only for full load, but for any load if the torque current is altered accordingly. To avoid confusion between a torque current varying with load and full-load torque current, b_m and x_e will be used to denote full-load values and u_m and u_x to denote values changing with load. A general power-factor expression for any load is then

$$\cos \theta = \frac{1}{\sqrt{1 + (u_m + u_x)^2}} \tag{209}$$

where u_m and u_x are given by Equations (72) and (168), respectively, with the torque current, I_T or q_T, varying in accordance with the load on the motor and symbolized by $I_{\dot{T}}$ and $q_{\dot{T}}$.

Inspection of Equation (209) shows the power factor is inversely related to $u_m + u_x$. An expression for $u_m + u_x$ can be obtained by adding Equations (72) and (168), giving

$$u_m + u_x = 0.116 \frac{B_g \quad f \quad \delta}{K_1 \quad K_2 \quad k_m \; q_T' \quad v} + 2.37 \; M \frac{f \; q_T'}{k_w \; v \; B_g}$$

$$+ 26.7 \frac{q_T' \; v \; A \; k_{zp}}{k_w \; B_g \; f \; \delta \; S_p^2} + 0.247 \; W \frac{k_{cp} \; \tau^2 \; q_T' \; f}{k_w \; v \; L \; B_g}$$

$$+ 0.03 \; k_b \; K_1 \; K_2 \; \frac{q_T' \; v}{\delta \; f \; B_g} \qquad (210)$$

Since

$$\frac{v}{f} = \frac{\tau}{6} = \frac{\pi D}{6 \; p} \qquad (211)$$

Equation (210) can be written as

$$u_x + u_m = 0.116 \frac{B_g \; \delta \; 6p}{K_1 \; K_2 \; k_m \; q_T' \; \pi D} + 2.37 \; M \frac{q_T' \quad 6p}{k_w \; B_g \; \pi D}$$

$$+ 26.7 \frac{q_T' \quad A \; k_{zp} \quad \pi \; D}{k_w \; B_g \; \delta \; S_p^2 6 \; p} + 0.247 \; W \frac{q_T' \; k_{cp} \; 6 \; \pi \; D}{k_w \; B_g \; L \; p}$$

$$+ 0.03 \; k_b \; K_1 \; K_2 \; \frac{q_T' \quad \pi \quad D}{B_g \; \delta \; 6 \; p} \qquad (212)$$

THE BEST VALUE OF AIR-GAP LENGTH

Equation (212) contains many interesting relations. Any change in the design values which causes a net decrease of the right-hand side of Equation (212) will increase the operating power factor of the motor. There is evidently a particular value for many of the components which will make $u_m + u_x$ a minimum and, hence, the operating power factor a maximum. The variation of $u_x + u_m$ with the length of the air gap is of special interest.

Assuming all the quantities involved in Equation (212) remain constant as the air gap is changed, the best value of air-gap length will be when

$$\frac{d(u_m + u_x)}{d\delta} = 0 = 0.116 \frac{B_g\ 6\ p}{K_1\ K_2\ k_m\ q_T'\ \pi D}$$

$$- 26.7 \frac{q_T'\ A\ k_{zp}\ \pi D}{k_w\ B_g\ S_p^2\ 6\ p\ \delta^2} - 0.03\ k_b\ K_1\ K_2 \frac{q_T'\ \pi\ D}{B_g\ 6\ p\ \delta^2} \qquad (213)$$

or

$$\delta = \sqrt{\frac{K_1\ K_2\ k_m}{0.116} \left(\frac{26.7\ A\ k_{zp}}{k_w\ S_p^2} + 0.03\ k_b\ K_1\ K_2 \right) \frac{q_T'}{B_g} \left(\frac{\pi D}{6p}\right)} \qquad (214)$$

Generally, the value of air-gap length indicated by Equation (214) is lower than the mechanical limitations will allow; however, this is not always true. The following examples will point out the importance of selecting the right air-gap length.

EXAMPLES

Equations (212) and (214) permit one to investigate the effect of the air gap on the power factor. For the example of Chapter V,

$p = 8$	$k_w = 0.885$	$k_{sp} = 0.85$
$D = 17.8$	$K_1 = 0.54$	$k_{zp} = 0.82$
$L = 6.9$	$K_2 = 0.9$	$W = 3$
$B_g = 25{,}000$	$K_m = 0.83$	$A = 0.14$
$S_p = 12$	$k_{cp} = 0.68$	$M = 1.507$

q_T' = approximately 700 at full load

Figure 39 shows the variation of the full-load power factor and $(u_m + u_x)$ as a function of air-gap length. The components are numbered to correspond to the terms of Equation (212). The fifth term in Equation (212) is equal to zero since this is a squirrel-cage induction motor. In practice, terms 3 will not increase as rapidly for small air gaps, as indicated. Tooth saturation will limit the rate of increase. However, the curves do indicate general trends.

Figure 39 illustrates a very important relation. An air-gap length larger than the best value has less effect on the operating power factor than does an air gap smaller than the best value. One could not build this machine with the indicated best value of air-gap length of 0.0095 inch; mechanical considerations dictate that the air-gap length must be about 0.033 inch. The importance of the air gap can be seen from the fact that a change from 0.035 to 0.030 inch, only 5 mils, changes the full-load power factor by 1 per cent.

If Equation (211) is substituted into Equation (214), one obtains

$$\delta = \sqrt{\frac{K_1 K_2 k_m}{0.116}\left(\frac{26.7 A k_{zp}}{k_w S_p} + 0.03 k_b K_1 K_2\right)}\ \frac{q_T' v}{B_g f} \qquad (215)$$

Observing Equations (214) and (215), one can readily see that with high power frequencies and a large number of poles the best value of air-gap length is probably below the mechanical limit, but with low power frequencies or a small number of poles the empirical relations for calculating the

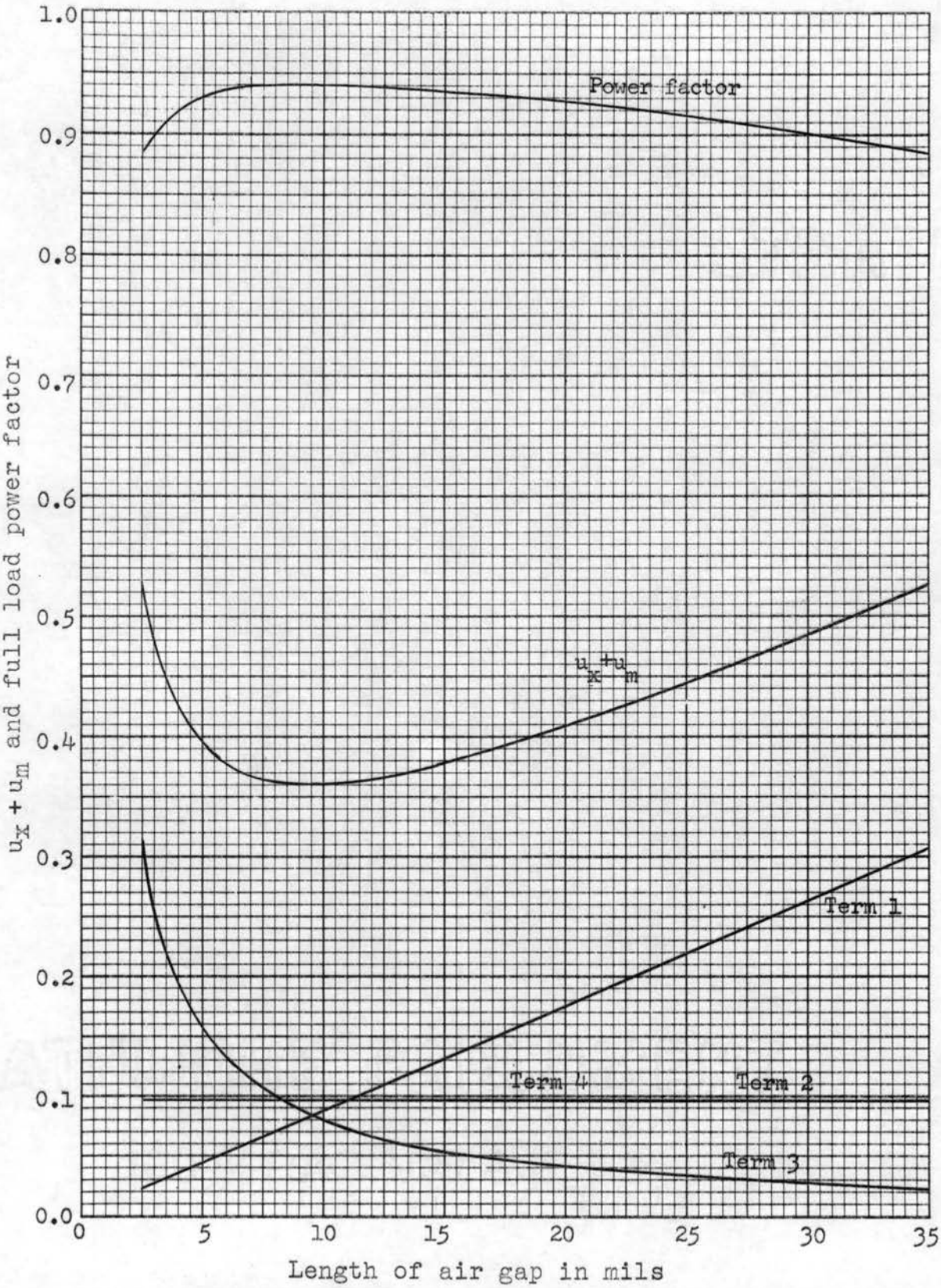

Figure 39. Variation of power factor with air-gap length for a sample motor.

length of the air gap may give results below the best value, which would certainly be detrimental to the motor's performance. For example, consider a three-phase squirrel-cage induction motor having partially closed slots and the following constants:

$K_1 = 0.95$	$k_{zp} = 1$
$K_2 = 0.9$	$B_g = 25{,}000$
$A = 0.48$	$f = 25$
$k_w = 1$	$v = 50$
$k_m = 1$	$S_p = 9$

q_T' = approximately 600 at full load

Using Equation (215), one finds that the best value of air-gap length for this load is

$$\delta = \sqrt{\frac{(0.95)(0.9)}{0.116}\left[\frac{(26.7)(0.48)}{81}\right]\frac{600}{25{,}000}\,\frac{50}{25}} = 0.052 \text{ inch}$$

This value of air-gap length is over twice that dictated by mechanical considerations; if the machine were a wound-rotor induction motor the empirical formulas would give results about three times the best value. It is true that this is an extreme example but nevertheless it is a case that could be encountered in practice. The lower regions of Figure 39 show clearly what the effect would be if one insisted on using the empirical formulas.

Equations (214) and (215) indicate that the best value of air gap is proportional to the ampere-conductors per inch

due to the torque current. One must be extremely cautious in selecting the air-gap length in machines having a combination of (1) high values of ampere-conductors due to the torque current and (2) low frequencies or a small number of poles. Extensive tests and studies have been conducted since 1942 on the use of silicone insulation in electrical machinery; a thorough engineering and economic evaluation has yet to be achieved. An indication of the potential value of silicone resins used in conjunction with fiberglass and mica is given by the recommended hot-spot temperature of 180°C which has been approved by the American Institute of Electrical Engineers for a period of trial use. Hence, use of silicone resins will result in a high value for the best air-gap length. However, high values of ampere-conductors per inch due to the torque current will result in increased noise, but many of the applications of motors using silicone resins place little, if any, limitations on noise. With these materials, the best value of air-gap length as given by Equation (207) must be given due consideration.

CHAPTER VIII

SUMMARY AND CONCLUSIONS

The first step in designing a polyphase induction motor is to evaluate the product D^2L by using what is known as the D^2L or output equation. The D^2L product is considered to be a constant; this is based upon the supposition that the flux density and the number of ampere-conductors per inch of periphery are independent of the diameter of the rotor. While it might be advantageous to change these quantities slightly as the diameter of the rotor is changed, the assumption is nearly exact.

The next step in the design is to separate the product D^2L into its two components. It is obvious that the motor may be built with a large core diameter and short core length or with great length and small diameter, with either combination satisfying the D^2L equation. The selection of the most appropriate dimensions is of great importance.

One of the procedures used at the present time for separating the components is to assume different values of D and L and work out the performance for each set of values and then pick out the set that gives good performance at reasonable cost. Another procedure is to rely on judgement and past experience from which empirical relations can be obtained and used in selecting the dimensions of the motor.

In this thesis, a method of separating the components of the D^2L equation is derived which is based on a minimum leakage coefficient. The value of length for minimum leakage coefficient is given in Equation (181), Chapter V. The corresponding value of core diameter can be found from the D^2L equation. The leakage coefficient will be at a minimum when the total slot leakage reactance is equal to the total coil-end leakage reactance. Why has this derivation been successful while others that have tried apparently failed? Perhaps the use of per-unit values has been the greatest contributing factor. When the parameters of an induction motor, such as impedances, voltage drops, and losses, are expressed in ohms, volts, and watts, they apply only to a specific motor having fixed speed, fixed output, fixed voltage, and all other quantities fixed. It is possible to express the parameters so that they become general, that is, applicable to a wide range of induction motors differing in such things as size, speed, and voltage. The quantities so expressed are then referred to as resistances, reactances, voltage drops, and so on, on a per-unit basis.

The author can cite two other attempts that have been made in trying to determine a relation for separating the components of the D^2L equation through use of the leakage coefficient. Neither of these is of much value. Bailey[1]

---

[1]Benjamin F. Bailey, The Induction Motor (New York, 1911), pp. 131-133.

derived a relationship for separating the components which was based on Behrend's empirical formula for the leakage coefficient of

$$\sigma = C\frac{\delta}{\tau} \tag{216}$$

where

C = a constant for a given set of dimensions

δ = depth of the air gap

τ = pole pitch

A glance at Equation (171) will show that one can say Bailey's attempt was fruitless. Another attempt has been made by Vickers.[2] His result was that the core diameter should be related to the length by

$$D = 1.35\ p\ \sqrt{L} \tag{217}$$

This result is of little value. It is easy to show that for a given number of poles, D and $\sqrt{L}$ do not bear a constant relation as indicated.

The leakage coefficient is a term that should be used more widely in referring to induction motors. It gives complete information in regard to power factor and overload capacity. A reasonably good motor has a magnetizing current not exceeding 1/3 of the full-load current and an ideal short-circuit current of not less than 6 times full-load current. This corresponds to a leakage coefficient of 0.06 or less, and the motor will have approximately the following

---

[2]Herbert Vickers, The Induction Motor (London, 1925), pp. 218-224.

minimum values: a full-load power factor of 90 per cent, a starting torque of about 1.5 times full-load torque, a maximum torque of 2.7 times full-load torque, and a maximum output of about 2.2 times full load. This shows the importance of the leakage coefficient. One can see how various factors affect the leakage coefficient by referring to Equation (179).

A motor must be produced at a reasonable cost. Chapter VI is devoted to a general study of costs. It is not intended to be an exact treatment. Equation (187) gives a quick estimate as to how to separate the components of the D^2L equation for minimum cost, and Equation (182) provides an easy general method of determining how costs vary with the main dimensions. This is illustrated in Figure 36. This analysis may not apply for radical changes in motor constants.

The author has made an intensive search of the literature on the subject of the air gap and how to determine the radial length of the gap. Nowhere has he found that anyone makes a statement or indicates that a small air gap may have a detrimental effect on the power factor. Equation (214), Figure 39, and the examples at the end of Chapter VII show that it can happen. Equations (212) and (209) can be used to examine how the many factors involved affect the power factor at any load.

In conclusion, the components of the D^2L equation can be separated on a sound engineering basis, eliminating the

need of relying on judgement and cut-and-try processes. In addition, a general consideration of costs and how they are affected by D and L can be made. The air gap which has heretofore been based on mechanical clearances only may, in some cases, need to be examined to see that it is not smaller than the optimum value for the particular design.

A SELECTED BIBLIOGRAPHY

Adams, Comfort A. "The Design of Induction Motors." Transactions of the American Institute of Electrical Engineers, 24 (June, 1905), 649-684.

Adams, C. A. "The Leakage Reactance of Induction Motors." Transactions of the International Electrical Congress, St. Louis, 1904, 1 (1905), 706-724.

Adams, C. A., W. K. Cabot, and G. A. Irving, Jr. "Fractional Pitch Windings for Induction Motors." Transactions of the American Institute of Electrical Engineers, 26 (June, 1907), 1485-1503.

Alger, P. L. The Nature of Polyphase Induction Machines. New York: John Wiley and Sons, Inc., 1951.

Alger, P. L., and H. R. West. "The Air Gap Reactance of Polyphase Machines." Transactions of the American Institute of Electrical Engineers, 66 (1947), 1331-1343.

Aston, Kenneth. Design of Alternating-Current Machinery. London: Oxford University Press, 1934.

Bailey, Benjamin F. The Induction Motor. New York: McGraw-Hill Company, Inc., 1911.

Barnes, E. C. An Experimental Study of Induction Machine End-Turn Leakage Reactance. New York: American Institute of Electrical Engineers, Technical Paper 51-111, December, 1950.

Behrend, B. A. The Induction Motor and Other Alternating Current Motors. New York: McGraw-Hill Book Company, Inc., 1921.

Cameron, Charles F. Induction Motor Characteristics, Analytic Solution. Stillwater: Oklahoma Agricultural and Mechanical College, Oklahoma Engineering Experiment Station Publication 68, May, 1948.

Cotton, H. Design of Electrical Machinery. London: Oxford University Press, 1934.

Dalziel, Charles F. "The Per Unit System." Allis-Chalmers Electrical Review, 4 (June, 1939), 20-23.

Douglas, John F. H. "The Reluctance of Some Irregular Magnetic Fields." Transactions of the American Institute of Electrical Engineers, 34 (June, 1915), 1067-1125.

Fitzgerald, A. E., and Charles Kingsley, Jr. Electrical Machinery. New York: McGraw-Hill Book Company, Inc., 1952.

Gray, Alexander. Electrical Machine Design. New York: McGraw-Hill Book Company, Inc., 1926.

Hanssen, I. E. "Leakage Reactance of Induction Motors." Electrical World, 49 (March 30, 1907), 636-637.

Hellmund, R. E. "Leakage Coefficient of Induction Motors." Electrical World, 50 (November 23, 1907), 1004-1005.

Hellmund, R. E. "Zigzag Leakage of Induction Motors." Transactions of the American Institute of Electrical Engineers, 26 (June, 1907), 1505-1524.

Hobart, H. M. "A Method of Designing Induction Motors." Transactions of the International Electrical Congress, St. Louis, 1904, 1 (1905), 783-799.

-----. "Induction Motor Leakage Reactance Calculations." Electrical Engineering, 67 (May, 1948), 430-444.

Jeffrey, Fraser. "The Circle Diagram and the Induction Motor." Allis-Chalmers Electrical Review, 4 (September, 1939), 5-12.

Johnson, Walter C. Mathematical and Physical Principles of Engineering Analysis. New York: McGraw-Hill Book Company, Inc., 1944.

Knowlton, Archer E. Standard Handbook for Electrical Engineers. New York: McGraw-Hill Book Company, Inc., 1949.

Kuhlmann, John H. Design of Electrical Apparatus. New York: John Wiley and Sons, Inc., 1950.

Kuhlmann, John H. "Physical Concepts of Leakage Reactance." Electrical Engineering, 67 (February, 1948), 142-145.

Lagron, Louis. Polyphase Induction Motors. London: Blackie and Son, Ltd., 1931.

Langsdorf, Alexander S. Theory of Alternating-Current Machinery. New York: McGraw-Hill Book Company, Inc., 1937.

Lawrence, Ralph R. Principles of Alternating Current Machinery. New York: McGraw-Hill Book Company, Inc., 1921.

Liwschitz-Garik, Michael. D-C and A-C Machines. New York: D. Van Nostrand Company, Inc., 1952.

Liwschitz, M. M. "Differential Leakage of a Fractional-Slot Winding." Transactions of the American Institute of Electrical Engineers, 65 (May, 1946), 314-320.

Liwschitz, M. M., and W. H. Formhals. "Some Phases of Calculation of Leakage Reactance of Induction Motors." Transactions of the American Institute of Electrical Engineers, 66 (1947), 1409-1413.

Lloyd, T. C., "Machine Synthesis." Electrical Engineering, 69 (November, 1950), 1001-1003.

Lloyd, T. C., Victor F. Giusti, and S. S. L. Chang. "Reactances of Squirrel-Cage Induction Motors." Transactions of the American Institute of Electrical Engineers, 66 (1947), 1349-1355.

Lloyd, T. C., and Howard B. Stone. "Some Aspects of Polyphase Motor Design--The Design and Properties of the Magnetic Circuit." Transactions of the American Institute of Electrical Engineers, 65 (December, 1946), 812-818.

Moore, A. D. Fundamentals of Electrical Design. New York: McGraw-Hill Book Company, Inc., 1927.

Mueller, George V. Alternating-Current Machines. New York: McGraw-Hill Book Company, Inc., 1952.

Pender, Harold, and William A. Del Mar. Electrical Engineers' Handbook--Electric Power. New York: John Wiley and Sons, Inc., 1949.

Poliquin, A. L., and A. S. Bickham. Test Results of Motor Used for Leakage Reactance Calculations. New York: American Institute of Electrical Engineers, Miscellaneous Paper 47-213, 1947.

Poritsky, H. "Calculation of Flux Distribution with Saturation." Transactions of the American Institute of Electrical Engineers, 70 (1951), 309-319.

Puchstein, A. F. "Calculation of Slot Constants." Transactions of the American Institute of Electrical Engineers, 66 (1947), 1315-1322.

Puchstein, A. F., and T. C. Lloyd. Alternating-Current Machines. New York: John Wiley and Sons, Inc., 1947.

Punga, Franklin, and Otto Raydt. Modern Polyphase Induction Motors. Tr. from the German by Henry M. Hobart. London: Sir Isaac Pitman and Sons, Ltd., 1933.

Robinson, R. C. "The Horsepower Output of Polyphase Induction Motors." Transactions of the American Institute of Electrical Engineers, 66 (1947), 770-775.

Still, Alfred, and Charles S. Siskind. Elements of Electrical Machine Design. New York: McGraw-Hill Book Company, Inc., 1954.

Travis, Irven. "Per Unit Quantities." Supplement to the 1937 Transactions of the American Institute of Electrical Engineers, 56 (1937), 22-28.

Trickey, P. H. "Output of Induction Motor Depends on Total Active Material." Product Engineering, 17 (December, 1946), 114-116.

Tsang, N. F., and T. C. Tsao. Determination of Network Constants of Polyphase Induction Motors. New York: American Institute of Electrical Engineers, Technical Paper 53-12, October, 1952.

Vickers, Herbert. The Induction Motor. London: Sir Isaac Pitman and Sons, Ltd., 1925.

VITA

Russell Lloyd Riese
candidate for the degree of
Doctor of Philosophy

Thesis: NEW ASPECTS OF POLYPHASE INDUCTION MOTOR DESIGN

Major: Electrical Engineering

Biographical:

Born: The writer was born in Kulm, North Dakota, June 20, 1923, the son of Albert R. and Anna Riese.

Undergraduate Study: He attended grade school in Kulm and Grand Forks, North Dakota, and graduated from the Kulm Special High School in 1941. In the fall of 1941, he matriculated at North Dakota State Normal and Industrial School. In the fall of 1942, he entered the University of North Dakota and in the spring of 1943 he enrolled at the University of Washington from which he received the Bachelor of Science degree in Electrical Engineering (Cum Laude) in June, 1946.

Graduate Study: He started his graduate study the last semester in attendance at the University of Washington. In June, 1948, he enrolled in the Graduate School of the Oklahoma A. and M. College. In the fall of 1948, he entered the Graduate School of New Mexico College of A. and M. A. for one course. He returned to Oklahoma A. and M. College the summers of 1949 and 1950, from which he received the Master of Science degree, with a major in Electrical Engineering, in August, 1950. In June, 1951, he entered the Graduate School at the University of Florida, then, in June, 1952, returned to Oklahoma A. and M. College for the summer session and again in June, 1953. In June, 1954, he again entered Oklahoma A. and M. College. Requirements for the Doctor of Philosophy degree were completed in August, 1955.

Experience: The writer, after serving a two-year apprenticeship, became a licensed Special Electrican in the State of North Dakota in 1939, at which time he became manager and motion-picture technician at the Roxy Theatre, Kulm, North Dakota. In September, 1941, he accepted a position as motion-picture technician at Ellendale, North Dakota. In September, 1942, he entered Civil Service as an employee of the U. S. Army Signal Corps. In October, 1943, the writer joined the U. S. Navy, serving until February, 1946.

During his last semester at the University of Washington, the author served as an assistant for the Department of Electrical Engineering. In August, 1946, he accepted a position with the Physical Science Laboratory at New Mexico College of A. and M. A. doing research and development work on guided-missile telemetering and cut-off systems. In September, 1947, he joined the staff of the Department of Electrical Engineering at New Mexico College of A. and M. A. as an Instructor, becoming an Assistant Professor in the fall of 1950.

Membership: The writer is a member of Phi Kappa Phi, Eta Kappa Nu, Tau Beta Pi, an Associate Member of the Society of Sigma Xi, and a member of the American Institute of Electrical Engineers with grade of Member. He is a Registered Professional Engineer in the State of New Mexico.

THESIS TITLE: NEW ASPECTS OF POLYPHASE INDUCTION MOTOR DESIGN

AUTHOR: Russell Lloyd Riese

THESIS ADVISER: Professor C. F. Cameron

The content and form have been checked and approved by the author and the thesis adviser. The Graduate School Office assumes no responsibility for errors either in form or content. The copies are sent to the bindery just as they are approved by the author and faculty adviser.

TYPIST: Sara Preston